INFORMATION TO USERS

This manuscript has been reproduced from the microfilm master. UMI films the text directly from the original or copy submitted. Thus, some thesis and dissertation copies are in typewriter face, while others may be from any type of computer printer.

The quality of this reproduction is dependent upon the quality of the copy submitted. Broken or indistinct print, colored or poor quality illustrations and photographs, print bleedthrough, substandard margins, and improper alignment can adversely affect reproduction.

In the unlikely event that the author did not send UMI a complete manuscript and there are missing pages, these will be noted. Also, if unauthorized copyright material had to be removed, a note will indicate the deletion.

Oversize materials (e.g., maps, drawings, charts) are reproduced by sectioning the original, beginning at the upper left-hand corner and continuing from left to right in equal sections with small overlaps.

Photographs included in the original manuscript have been reproduced xerographically in this copy. Higher quality 6" x 9" black and white photographic prints are available for any photographs or illustrations appearing in this copy for an additional charge. Contact UMI directly to order.

Bell & Howell Information and Learning
300 North Zeeb Road, Ann Arbor, MI 48106-1346 USA
800-521-0600

Efficient Forward Error Correction Coding Technique for Spread Spectrum Communications

Shafiq Ullah Hashmi

A Thesis

In

The Department

of

Electrical and Computer Engineering

Presented in Partial Fulfillment of the Requirements
For the Degree of Master of Applied Science at
Concordia University
Montreal, Quebec, Canada

June 2000

ABSTRACT

Efficient Forward Error Correction Coding Technique for Spread Spectrum Communications

Shafiq Ullah Hashmi

This thesis presents the study of the coding technique and the simulation results for the Forward Error Correction (FEC) of the wireless data in a highly noisy and severe fading wireless medium, based on standard (IEEE 802.11 Wireless Local Area Network specification) and GPS driven non-standard MAC schemes. The design and testing of this coding scheme is a part of MYMAR, a new Mobile Yellow page Messaging And Retrieval system, which is based on GPS driven slow frequency hopping access.

The main contributions of this thesis are the demonstration of the performance of the coding scheme, which works well in severe fading environments. The coding technique uses simple Reed-Solomon Forward Error Correction mechanisms coupled with a new highly interleaved data table.

The performance of the coding scheme is assessed in Rayleigh fading multipath propagation with additive white Gaussian noise interference coupled with interference due to like user frequency hop overlapping (in non-standard MAC scheme). Simulation results for severe fading channel with burst error models are presented for both standard and non-standard MAC mechanisms. The simulation show very good and satisfactory results for high data rate with good TPDU (Transport Protocol Data Unit) loss probabilities.

This work is dedicated to my

Elders

and

to all those who are involved in

the effort to save the humanity

from the great failure of

hereafter

ACKNOWLEDGMENTS

At the outset I would like to express my most sincere gratitude to my thesis supervisor, Dr. A. K. Elhakeem for being a guiding force necessary for this work and creating a friendly environment during the entire course of this thesis. Without his guidance, support, encouragement this work would not have been possible.

Also on behalf of our whole MYMAR group I would like to thank Communication Research Center (CRC), Ottawa, Canada for their full support and coordination for this project.

My special thanks to the great group of friends I have in Montreal Tanvir, Zia, Shibli, Owais, Masood, Faisal, Najam, Farrukh, Muzaffar, Hussam, Mehdi, little Sauban and many more for their encouragement and support throughout the course of this thesis.

I am indebted to my parents and my brothers for all the encouragement and moral support they have provided me throughout my academic career. No words can express my gratitude to them.

TABLE OF CONTENTS

LIST OF FIGURES

LIST OF TABLES

LIST OF ACRONYMS and SYMBOLS

Acronym	Definition
ACK	Acknowledgement
AP	Access Point
AWGN	Additive White Gaussian Noise
BSS	Basic Service Set
CF	Coordination Function
CSMA/CA	Carrier Sense Multiple Access/Collision Avoidance
CTS	Clear To Send
CW	Contention Window
DCF	Distributed Coordination Function
DIFS	Distributed (Coordination Function) Inter-Frame Space
DS	Distribution System
ESS	Extended Service Set
FEC	Forward Error Correction
DSSS	Direct Sequence Spread Spectrum
GFSK	Gaussion Frequency Shift Key
FH	Frequency Hopping
FHSS	Frequency Hopping Spread Spectrum
IFS	Inter-Frame Space
IR	Infrared (PHY)
ISM	Industrial, Scientific and Medical band

Acronym	Definition
LLC	Logical Link Control
MAC	Medium Access Control
MYMAR	Mobile Yellow page Messaging And Retrieval system
NAV	Network Allocation Vector
PC	Point Coordinator
PCF	Point Coordination Function
PHY	Physical (Layer)
PIFS	Point (Coordination Function) Inter--Frame Size
PSD	Power Spectral Density
RTS	Request To Send
SIFS	Short Inter-Frame Space
TH-SS	Time Hopping Spread Spectrum
TPDU	Transport Protocol Data Unit
STA	Station
WM	Wireless Medium

Symbol	Definition
α	Probability of entering into bad state
A_l	Rayleigh faded signal magnitudes
β	Probability of entering into good state
d_l	User binary data symbols

Symbol	Definition
e	Probability of symbol error in affected hop
E_b/N_0	Signal to Noise Ratio (SNR)
G_p	Processing gain
p	Probability of channel to be in fading
P_e	Probability of Error due to AWGN
P_j	Probability of like user FH overlapping
t	Error correcting capability
T_c	Code time period
T_h	Hop period
T_s	Symbol time period
ω_{if}	FSK IF frequency
z	Signal to Noise Ration (E_b/N_0)

CHAPTER 1

Spread Spectrum Communications

1.1 Introduction

Spread spectrum communication technology has been used extensively in a wide variety of military applications since the 1940's because of its inherent military advantages: immunity to intentional jamming interference, the capability of hiding a spread signal from eavesdroppers, security and high-resolution ranging [Sim 85]. In the last decade, the wire-less communication market experienced significant growth, especially in cellular telephony, personal communications systems (PCS) and wireless local area networks (WLANs). Increasingly, researchers have been interested in the issue of spread spectrum because of its potential technical advantages including higher spectrum utilization and resistance to multipath. Currently, spread spectrum techniques have been used in satellite communications, position location systems and telemetry systems. These techniques are also emerging in personal communications systems and wireless information network applications.

In 1985, the Federal Communications Commission (FCC) released three unregulated ISM bands to encourage the development of spread spectrum technology. The frequencies of these unlicensed spectrum are 902 to 928 MHz, 2400 to 2483.5 MHz and 5725 to 5850 MHz. Part 15.247 of FCC rules governing these frequency bands requires that the transmitters use spread spectrum modulation with a transmitted power less than 1 W and the processing gain of the spread spectrum system be larger than 10 (we will discuss the processing gain in the following sections). The drawback of this unlicensed operation is that one must be able to operate with interference from other users in the same bands.

1.2 Principles of Spread Spectrum Communications

1.2.1 Spread Spectrum and the PN Code

Generally, a spread spectrum signal is generated by modulating a signal so that the resultant transmitted signal has a bandwidth much larger than the original signal bandwidth. This is shown in Figure 1.1. A definition of spread spectrum that adequately reflects the characteristics of this technique is as follows:

> "Spread spectrum is a means of transmission in which the signal occupies a bandwidth in excess of the minimum necessary to send the information; the band spread is accomplished by means of a code which is independent of the data, and a synchronized reception with the code at the receiver is used for despreading and subsequent data recovery." [1]

A number of modulation techniques use a transmission bandwidth much larger than the minimum required for data transmission such as FM and PCM, but are not spread spectrum modulations under the above definition. A key parameter of the spread spectrum system is the bandwidth expansion factor or the processing gain. As we see in Figure 1.1, the transmitted power is spread over a bandwidth N times wider than the information symbol rate. Thus, without changing the signal power, the power spectral density (PSD) of the signal would be N times lower than it would be in non-spread transmission and the signal is less likely to be detected. Obviously, this property makes spread spectrum attractive for military applications in which the signal must be hidden from eavesdroppers.

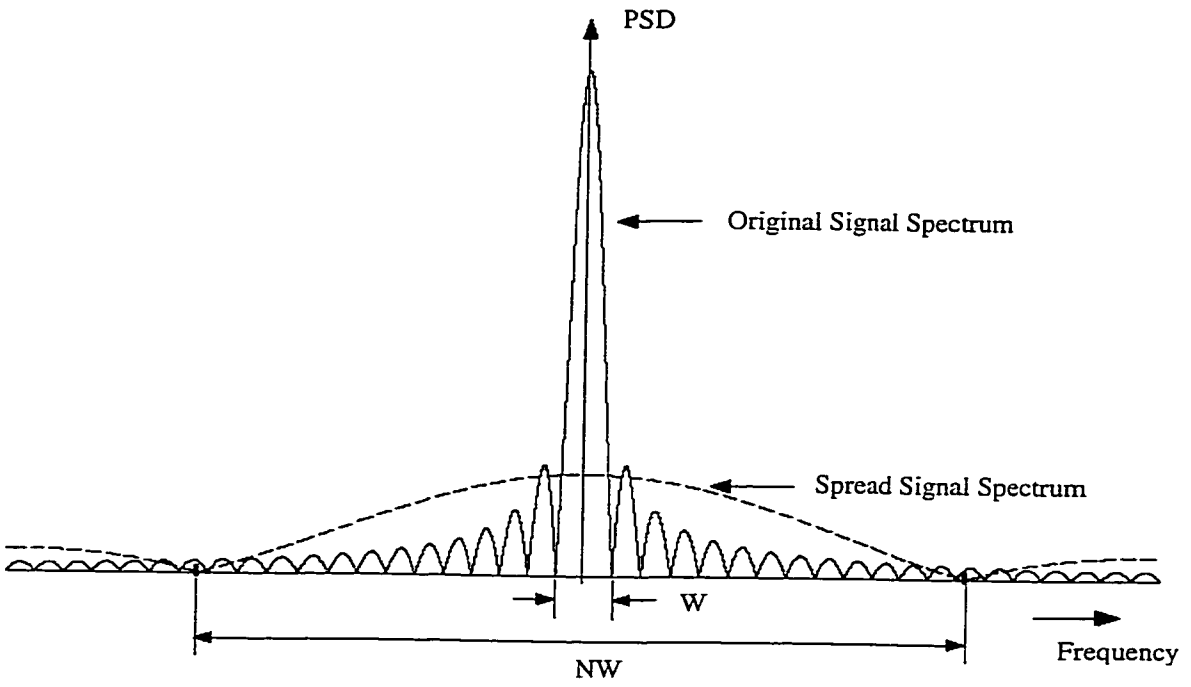

Figure 1.1: Power Spectral Density (PSD) of Spread

The processing gain N is defined by

$$processing\ gain = N = \frac{transmitted\ signal\ bandwidth}{information\ bandwidth} \qquad 1.1$$

which specifies to what extent the original signal is spread. Practically, N is an integer with a typical value of $10log_{10}N = 10$ to $30\ dB$.

The pattern used in the spread spectrum system to spread the information spectrum is called the spreading pattern or spreading code. This spreading code is generated in a deterministic way but should appear to be random or noise-like. Hence, it is usually called the pseudo-random or pseudo-noise (PN) code. In order for the spread spectrum receiver to reliably despread the signal, a common requirement of the PN code is good autocorrelation performance.

Summarizing the salient features of spread spectrum techniques:

- Resistance to intentional and non-intentional interferences;
- The ability to eliminate or alleviate the effect of multipath propagation;
- The ability to share the same frequency band with other users by using noise-like spreading signal;
- Suitability for low-power unlicensed SS radios in the ISM bands: 902-928 MHz, 2.4-2.4835GHz, and 5.725-5.85 GHz;
- Offering a certain degree of privacy, due to the use of pseudo-random spreading codes, making it difficult to intercept the signal;
- High resolution ranging;
- Accurate universal timing.

The means by which the spectrum is spread is crucial. Several of the techniques are:

- Direct Sequence modulation, in which a fast pseudo-randomly generated sequences causes phase transitions in the carrier containing data;
- Frequency Hopping, in which the carrier is caused to shift frequency in a pseudo-random way;
- Time Hopping, wherein bursts of signal are initiated at pseudo-random times;
- Pulsed-FM or chirp modulation, in which a carrier is swept over a wide band during a given pulse interval and is exclusively used in radar;
- Finally Hybrid combinations of the above techniques.

Pseudo-random code is the key to the operation of Spread Spectrum systems, though in chirp modulation it is not employed. Later in this chapter we will discuss only Direct Sequence (DS), Frequency Hopping (FH) and Time Hopping (TH) modulation techniques briefly along with a new Spread Spectrum application, i.e. MYMAR (Mobile Yellow Page Messaging and Retrieval System).

1.2.2 Synchronization Requirement in the Spread Spectrum System

In a spread spectrum system, the generated PN code at the receiver side must be aligned or synchronized to the received PN sequence, otherwise, the PN code misalignment will prevent effective despreading. Synchronization is usually accomplished by two processes: an acquisition of the initial PN code alignment followed by a tracking process to eliminate a possible new phase shift introduced to the received signal during the signal reception process. The synchronization is important in a spread spectrum system. Without synchronization, the spread spectrum will appear as a noise at the receiver an it will be unable to perform despreading. Hence, synchronization performance greatly affects the overall system data reception capability.

1.3 Direct-Sequence Spread Spectrum (DS-SS) Systems

A DS-SS system achieves spectrum spreading by multiplying the source having symbol rate ($1/T_s$) of a +– binary baseband data waveform with a pseudo-random +– binary waveform whose "chip" rate ($1/T_c$) is much faster than the symbol rate ($T_s = NT_c$). The effect of this operation is to spread the instantaneous bandwidth of the waveform by the factor N, which for the same signal power causes the spectral density of the waveform

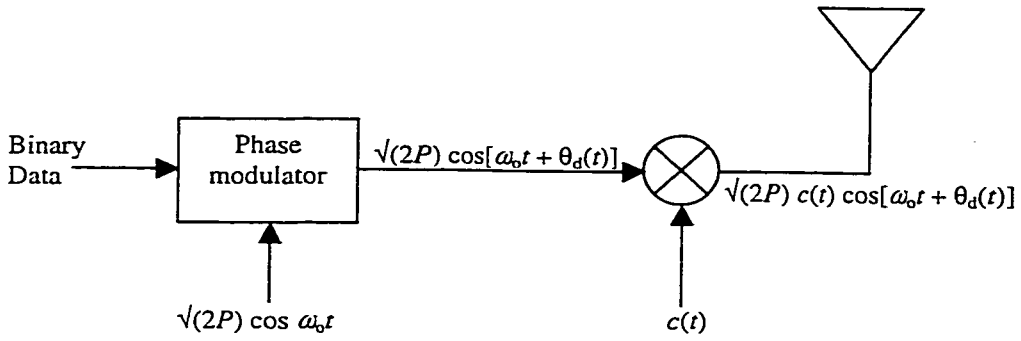

(a) Transmitter

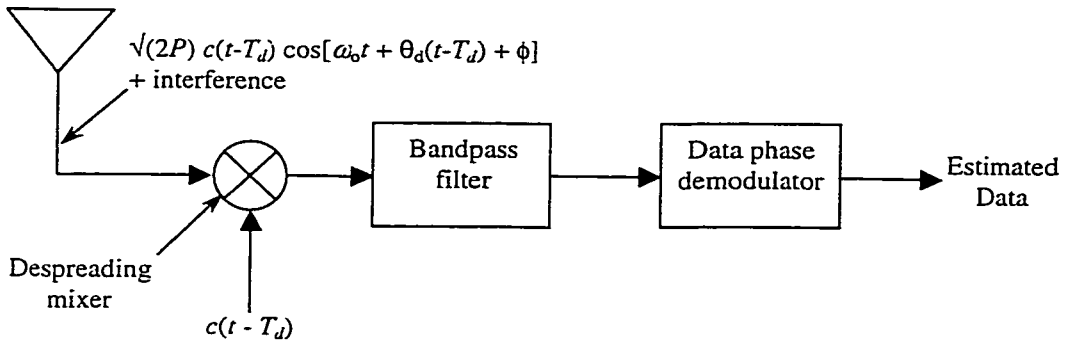

(b) receiver

Figure 1.2: BPSK direct-sequence spread-spectrum transmitter/receiver

to be quite low and "noise-like." At the receiver, despreading (multiplication by the same +– binary waveform as at the transmitter) and removal of the carrier modulation restores

the original baseband data waveform, allowing the receiver to filter out a large part of the wideband interference. The transmitter and receiver of the system are depicted in Figure 1.2. The processing gain of the DS system (processing gain is the performance improvement achieved through use of spread spectrum techniques over techniques without spread spectrum) is equal to the number of chips (pulses of code sequence) in a symbol interval

$$G_p = \frac{T_s}{T_c} \qquad 1.2$$

1.4 Frequency-Hopped Spread Spectrum (FH-SS) Systems

A FH-SS system achieves spectrum spreading by hopping its carrier frequency over a (large) set of frequencies in a pseudo-random pattern. Typically, each carrier frequency is chosen from a set of frequencies which are spaced approximately the width of the data modulation bandwidth apart. The spreading code in this case does not directly modulate the data-modulated carrier but is instead used to control the sequence of carrier frequencies. In the receiver, the frequency hopping is removed by down converting (mixing) with a local oscillator signal which hops synchronously with the received signal, as illustrated in Figure 1.3 [2].

A typical FH waveform is depicted in Figure 1.4 in terms of bandwidth occupancy as a function of time [7]. Within each hop period T_h, there can be more than one modulation symbol, with period T_s. If T_h is a multiple of T_s, with multiple symbols per hop, as is typical for systems employing continuous phase modulation, the system is said to be

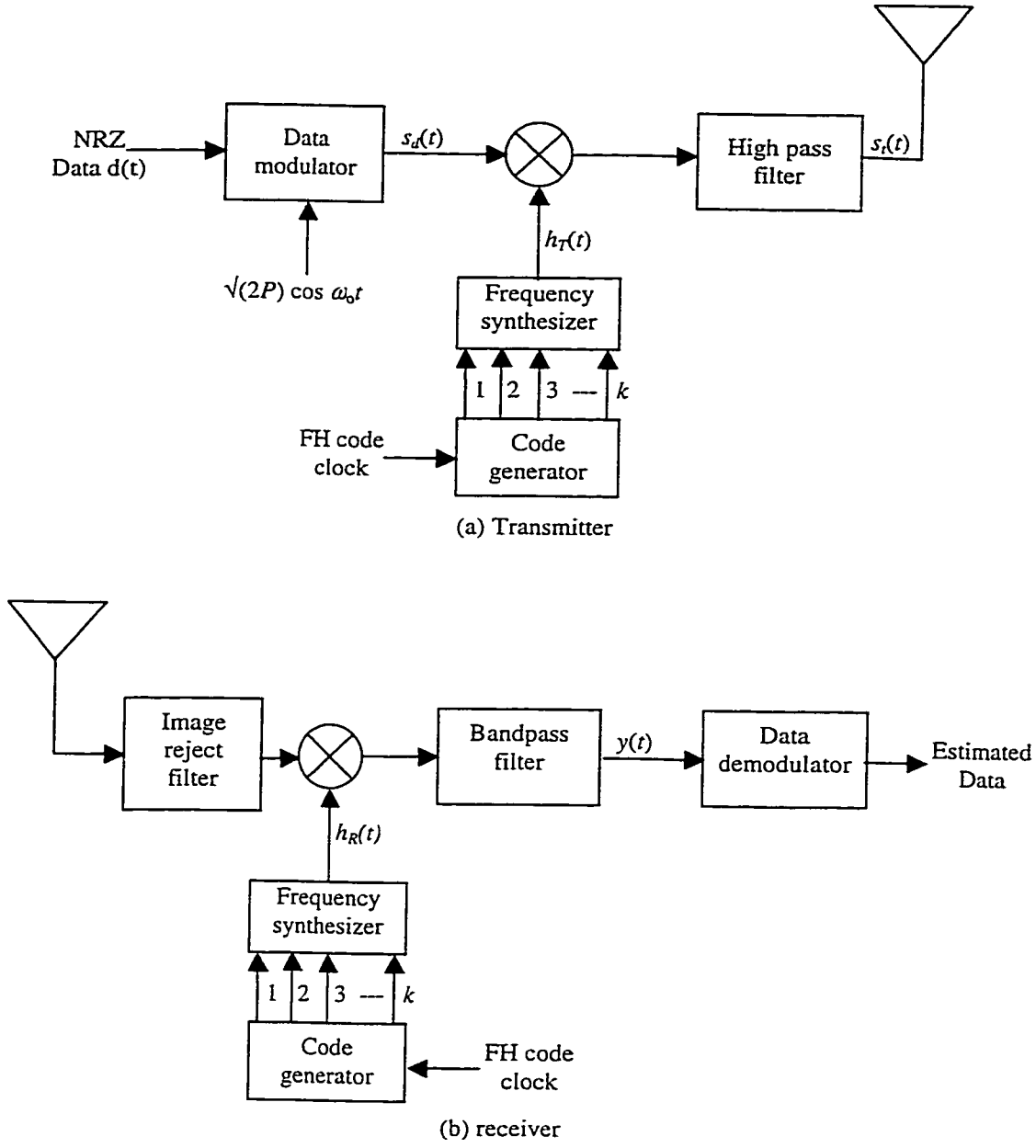

Figure 1.3: Coherent frequency-hop spread-spectrum modem

"slow hopping." If T_h is a submultiple of T_s, with multiple hops per symbol, as is typical for systems employing noncoherent frequency-shift keying, the system is said to be "fast hopping."

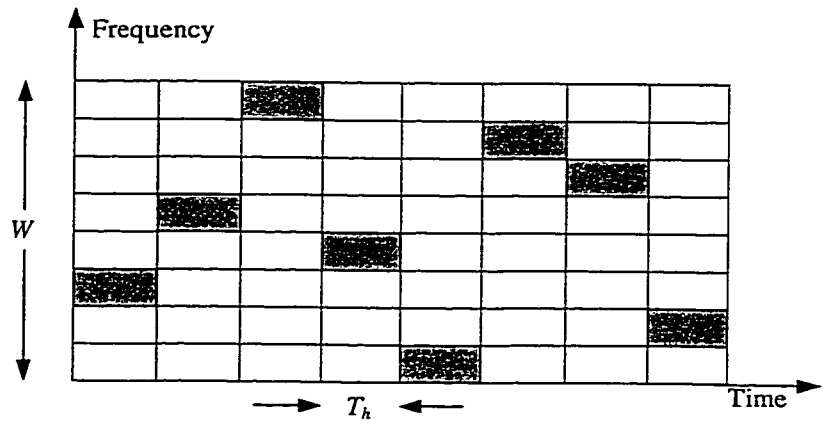

Figure 1.4: Typical frequency-hopping waveform pattern.

1.5 Time-Hopping Spread Spectrum (TH-SS) Systems

In a TH-SS system, a block of data bits is compressed and transmitted in a pseudo-randomly chosen time slot within a frame that consists of a large number of time slots. The code sequence is used to key the transmitter on and off. The transmitters on and off times are therefore pseudo-random. Time hopping may be used to aid in reducing interference between systems in time division multiplexing where stringent timing requirements must be placed on the overall system to ensure minimum overlap between transmitters. One of the primary advantages that offered by this type of spread spectrum communications in interference rejection is the reduced duty cycle; i.e., an interfering transmitter to be really effective would be forced to transmit continuously. Thus the power required by a reduced duty cycle time hopper would be less than that of the interfering transmitter by a factor equal to the signal duty cycle. Time hopping systems are very useful for Ranging, multiple access because of the relative simplicity of generating the transmitted signal. The transmitter and receiver of a Time hopping system is shown in Figure 1.5 [4].

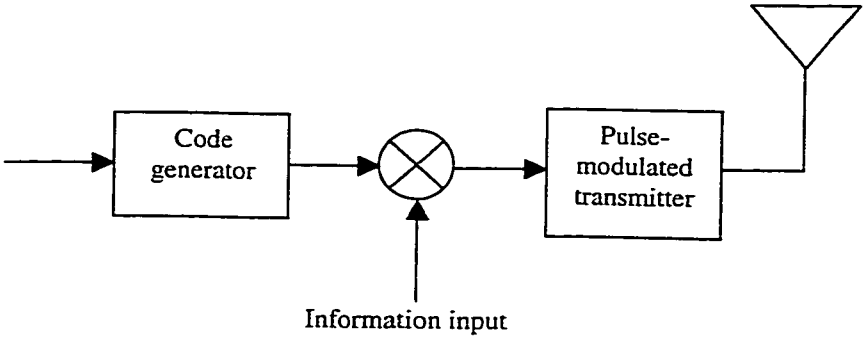

(a) Transmitter

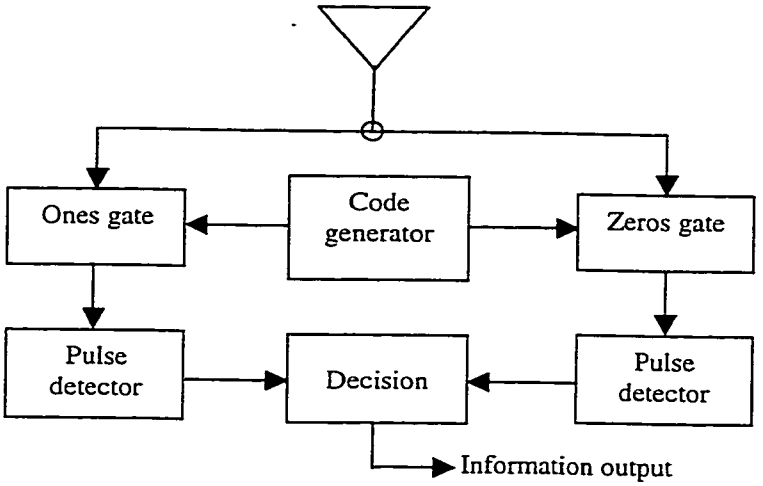

(a) Receiver

Figure 1.5: Simple Time-Hopping (pseudo-random) system.

1.6 MYMAR, a SFH Access to Mobile Yellow Page Messaging and Retrieval System

MYMAR [5][6], is a new idea that exploits the inherent interference rejection capability, high spectral efficiency and multiple access capability of spread spectrum system. Here a new distributed access communications system is envisioned that works without Central Base Stations, Cellular Structure, Backbone PSTN or otherwise, operating in the 2.4 GHz unlicensed bands. In this system Hotels, Restaurants, all kinds of Road Services, hospitals, police, stores, all faces of activities would transmit a short commercial message followed by their GPS location and the region's digital map to travelers, dwellers, etc., to enable them to quickly determine the locations of intended services and easily guide them to destination. A user friendly voice activated software at the Mobile Station (MS) would then enable the mobile user to retrieve all local information, forward voice messages or even access global web through the base station.

In MYMAR system the Base Stations (BS) can be mobile or fixed. All the units operate in same 2.4 GHz band, on the same bandwidth and assume the utilization of SFH access techniques. All BS and MS transmissions in a certain area overlap in time and frequency. Orthogonal FH access provides both fading resistance and like user interference rejection, and increases the system capacity. All BSs have the same functionality and handle the network management and control in a distributed manner. Formation of new zones (cells of old-fashioned cellular system) is totally handled by the BS itself according to specific methodology and strategy.

Some of the major aspects of the SFH based MYMAR [6] are:

- There will be 4 spread spectrum subbands of bandwidth 15.36 MHz in 2.4 GHz range each having a Pilot channel defined by the center of band carrier frequency and a pilot FH pattern.
- Each station in a certain zone share a subset of all available FH Spreading codes on a certain transmission subband.
- Each BS and MS packet is physically identified at any time by its GPS location, a serial identification number and a certain Direct Sequence (DS) code to which its receiver is being matched.
- Full rate BS and MS can transmit at a full rate of 96 Ksps.
- 64 active users can be accommodated per subcarrier per zone, each operating at a respectful data rate of 58.839 bps.
- All FH used by all active users at any time are orthogonal because of GPS standard timing, which is assumed available at all stations.
- All transmissions are point to point transmission, though it increases the total transfer delay but optimizes the bit error performance and system capacity;
- Many zones can overlap in the same geographical area and even can operate very close to each other geographically as shown in the Figure 1.5;
- MS handoff is handled by MS itself and is purely based on quality of reception;
- Due to point to point transmission it needs small transmission powers and distances which guarantees a small number of interference and less power differentials and hence less near far problems.

For the interested readers all the aspects and the complete system are given in [6].

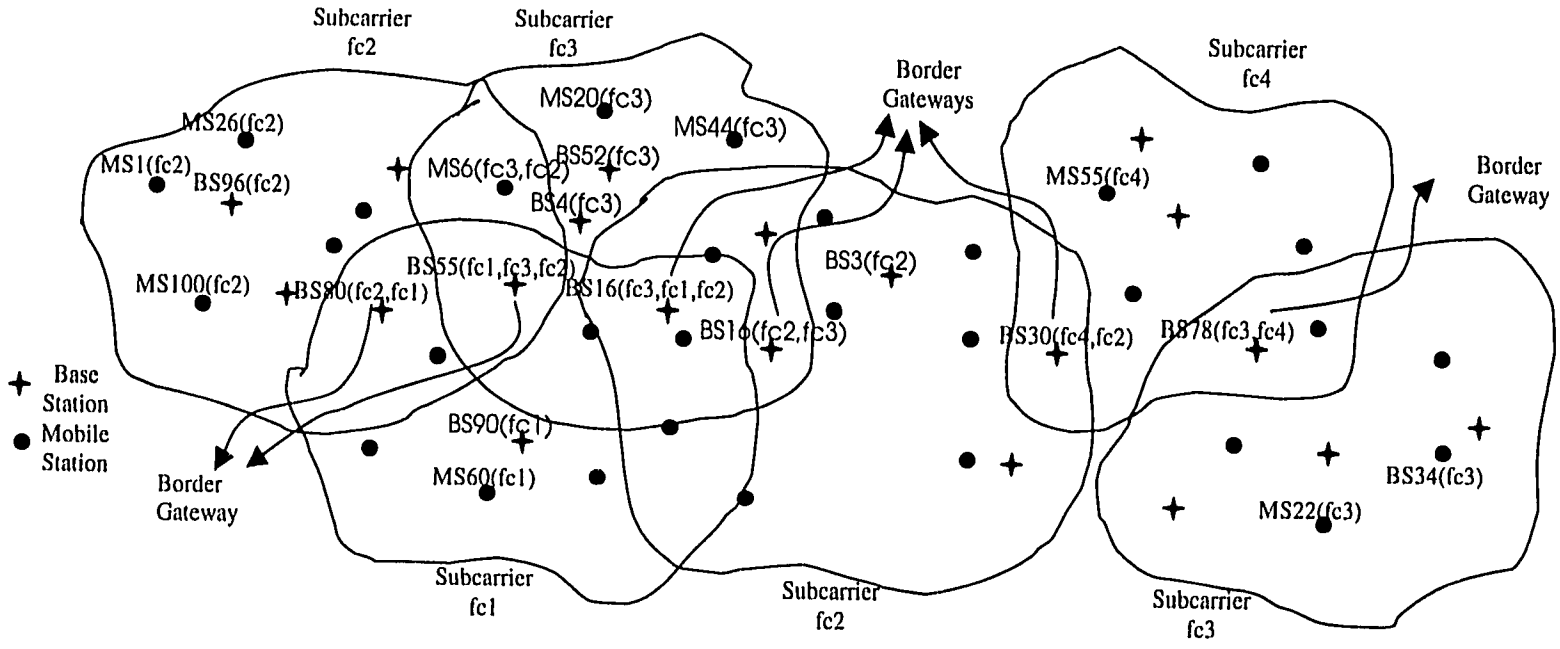

Figure 1.6: Typical Deployment of parts of a certain zone on 4 subcarriers in the MYMAR Internet. Subsets of users on few different subcarriers can exist in same geographical area, no Frequency allocation or planning, etc. necessary, all real time dynamic processes only some not all BS in overlapping areas serve as BG and among these only some would have enough transceivers to handle all traffic of MS, BS of overlapped parts.

1.7 Performance of the Frequency-Hopping Spread Spectrum

In FH-SS systems, several users independently hop their carrier frequencies while using BFSK modulation. If two users are not simultaneously utilizing the same frequency band, the probability of error for BFSK can be given by

$$P_e = \frac{1}{2}\exp\left(-\frac{E_b}{2N_0}\right) \tag{1.3}$$

However, if two users transmit simultaneously in the same frequency band, a collision, or 'hit', occurs. In this case it is reasonable to assume that the probability of error is simply 0.5. Thus the overall probability of bit error can be modeled as

$$P_e = \frac{1}{2}\exp\left(-\frac{E_b}{2N_0}\right)(1-p_h)+\frac{1}{2}p_h \tag{1.4}$$

where p_h is the probability of a hit. It can be determined by assuming if there are M possible hopping channels (called slots), then there is a $1/M$ probability that a given interferer will be present in the desired user's slot. If there are K-1 interfering users, the probability that at least one is present in the desired frequency slot is

$$p_h = 1-\left(1-\frac{1}{M}\right)^{K-1} \approx \frac{K-1}{M} \tag{1.5}$$

assuming M is large. Hence Eq 1.4 becomes

$$P_e = \frac{1}{2}\exp\left(-\frac{E_b}{2N_0}\right)\left(1-\frac{K-1}{M}\right)+\frac{1}{2}\left(\frac{K-1}{M}\right) \tag{1.6}$$

So if $K = 1$, the probability of error reduces to equation 1.3, the standard probability of error for BFSK. If SNR, E_b/N_o approaches infinity,

$$\lim_{\frac{E_b}{N_0}\to\infty}(P_e) = \frac{1}{2}\left[\frac{K-1}{M}\right] \tag{1.7}$$

which illustrates the irreducible error rate due to multiple access interference. This analysis is for the synchronous hopping by all users which is a slotted frequency hopping case. For the asynchronous case, the probability of hit is given by

$$p_h = 1 - \left\{1 - \frac{1}{M}\left(1 + \frac{1}{N_b}\right)\right\}^{K-1} \qquad 1.8$$

where N_b is the number of bits per hop. Hence the probability of error for the asynchronous FH-SS case becomes

$$P_e = \frac{1}{2}\exp\left(-\frac{E_b}{N_0}\right)\left\{1 - \frac{1}{M}\left(1 + \frac{1}{N_b}\right)\right\}^{K-1} + \frac{1}{2}\left[1 - \left\{1 - \frac{1}{M}\left(1 + \frac{1}{N_b}\right)\right\}^{K-1}\right] \qquad 1.9$$

However in this work as will follow shortly, we merely deal with the binary case i.e. FH/FSK.

CHAPTER 2

IEEE 802.11 MAC Protocol for Wireless LAN

2.1 Introduction

Ideally, users of wireless networks want the same services and capabilities that they have commonly experienced with wired networks. However, the wireless community faces certain challenges and constraints such as interference and reliability. In order to adapt user applications to WLANs, an intensive understanding of the medium and the data-link layer of WLANs is critical.

Although WLANs have been available commercially for several years, there was no international standard available until the recent approval of IEEE 802.11 by the IEEE Standards Committees. Due to the fact that a large number of manufacturers announced the introduction of IEEE 802.11-conforming products recently, we expect most of the WLANs to be IEEE 802.11 compatible in the near future. Thus, a thorough understanding of IEEE 802.11 will benefit the future development of user applications for the standard.

Wireless computing is a rapidly emerging technology providing users with network connectivity without their being tethered to a wired network. WLANs are being

developed to provide high bandwidth to users in a limited geographical area. IEEE 802.11 [13, 16] is a proposed IEEE standard for WLAN. This project was initiated in 1990, and approved by the IEEE Standards Committee in 1997. The scope of IEEE 802.11 is to develop a Medium Access Control (MAC) sublayer and Physical Layer (PHY) specification for wireless connectivity for fixed, portable and moving stations within a local area. In the remainder of this chapter, the architecture, PHY, and MAC of the IEEE 802.11 will be described.

2.2 Purpose and the Advantages of IEEE 802.11 Standard

There are two major purposes of the standard:

- To provide wireless connectivity to automatic machinery, equipment, or stations that require rapid deployment, which may be portable, or hand-held or which may be mounted on moving vehicles within a local area.
- To offer a standard for use by regulatory bodies to standardize access to one or more frequency bands for the purpose of local area communication.

The IEEE 802.11 standard describes mandatory support for a 1 Mb/s WLAN with optional support for a 2 Mb/s data transmission rate. It defines 2 Mbps as the maximum data rate between wireless equipments, using Direct Sequence Spread Spectrum (DS-SS). This modulation technique is based on the substitution of each data bit by an equivalent sequence of 11 bits, easily recognized by the receiver, so even if some of the received signal spectrum has been affected by interferences, the receiver will still be able of extract the data information from it.

This IEEE standard also provides fairness among the wireless users by a channel access method based on CSMA/CA (carrier sense multiple access/collision avoidance) scheme. Here all users with data to transmit have an equal chance of accessing the network.

2.3 Architecture

The Basic Service Set (BSS) is the basic building block of the IEEE 802.11 architecture. A BSS is a set of stations controlled by a single coordination function. There are two coordination functions defined in the IEEE 802.11: Distributed Coordination Function (DCF) and Point Coordination Function (PCF), which are described below.

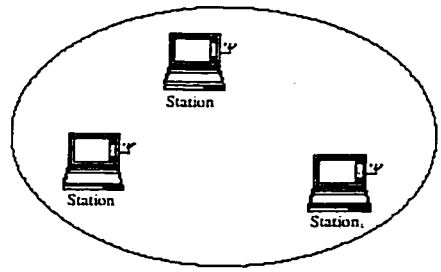

Figure 2.1: Sketch of an IBSS

The independent BSS (IBSS) is the most basic type of IEEE 802.11 instantiation. An IBSS is a BSS in which any station can establish a direct communication session with any other station in the BSS without the aid of an infrastructure network. Figure 2.1 shows an example of an IBSS, which is often referred to as an ad hoc network [13].

In contrast to an IBSS, infrastructure networks are defined to provide coverage area extension and specific services. An infrastructure network is built with multiple BSSs,

which are interconnected by a common Distribution System (DS). Each BSS in an infrastructure network has an Access Point (AP), which provides access to the DS, for all associated stations, via the wireless medium. The DS can be thought of as a backbone to transfer MAC-level packets between different BSSs in an infrastructure network. The DS, as specified by IEEE 802.11, is implementation independent. Therefore, the DS could be any network type such as IEEE 802.3 Ethernet LAN or another IEEE 802.11 WLAN. With the DS, the coverage area can be extended to the limitations of the DS. The

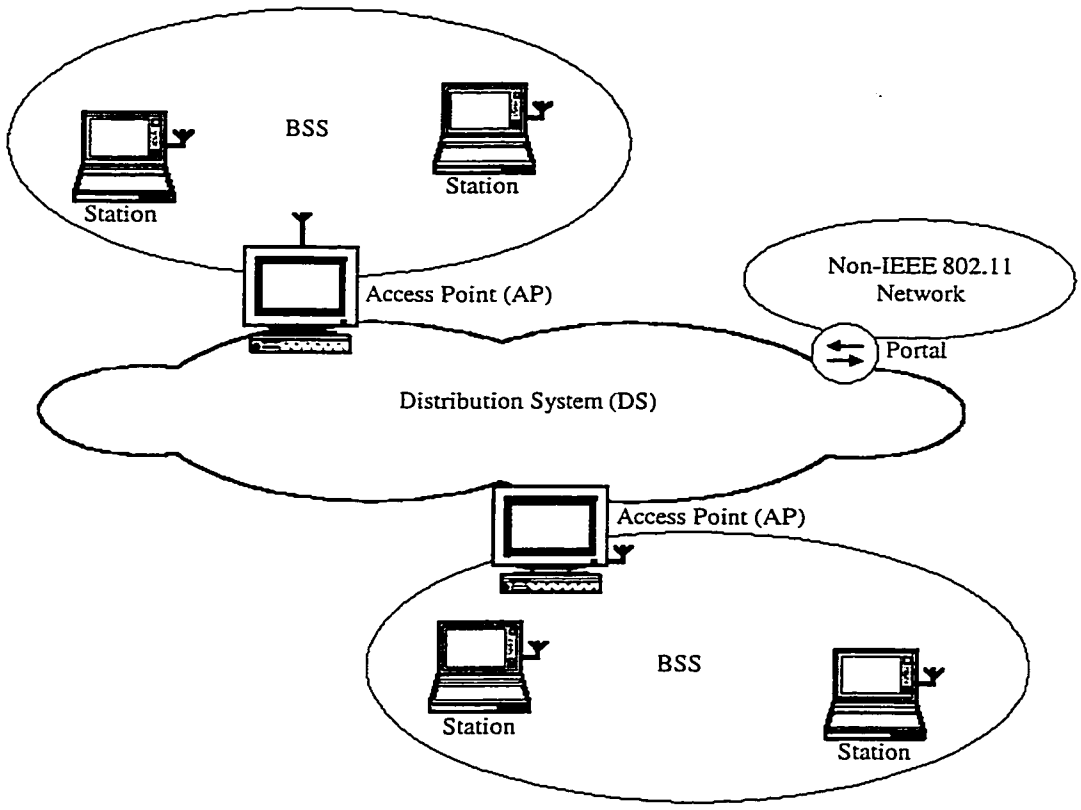

Figure 2.2: Sketch of an infrastructure network

infrastructure architecture can integrate with a wired network to provide specific services such as Internet access. A logical entity, a portal, is specified as the integration point on

the DS where the IEEE 802.11 network integrates with a non-IEEE 802.11 network. Figure 2.2 illustrates an example of an infrastructure network built with two BSSs, a DS, and a portal access to a wired LAN [16].

2.4 Physical Layer (PHY)

The IEEE 802.11 PHY is responsible for mapping the IEEE 802.11 MAC frame unit into a format suitable for sending and receiving via a wireless medium, between two or more stations using one of the following implementations: Frequency-Hopping Spread Spectrum (FH-SS), Direct Sequence Spread Spectrum (DS-SS), or Infrared (IR). The FH-SS utilizes the 2.4 GHz Industrial, Scientific, and Medical (ISM) band (2.4000-2.4835 GHz). The band is divided into frequency channels with 1 MHz bandwidth each. A frequency-hopping sequence consists of a permutation of all frequency channels. Three different hopping sequence sets are defined in the specification, with 26 hopping sequences per set. With the FH-SS implementation, the carrier frequency is hopped with a predefined hop rate according to a hopping sequence. Different hopping sequences enable multiple BSSs to coexist in the same geographical area, which may become important to alleviate congestion and maximize the total throughput in a single BSS. The reason for having three different sets is to avoid prolonged collision periods between different hopping sequences in a set. Two access rates, 1 Mbit/s and 2 Mbit/s, are specified using 2-level Gaussian Frequency Shift Key (GFSK) and 4-level GFSK modulation respectively.

The DS-SS implementation also uses the 2.4 GHz ISM frequency band. The band is similarly divided into frequency channels, but with 11 MHz bandwidth each. The

spreading is done by chipping each data symbol at 11 MHz in one channel with a predefined 11-bit chip sequence. That is, a chip sequence and its one's complement are sent for bit values of 1 and 0 respectively [16]. The DS-SS also provides both 1 Mbit/s and 2 Mbit/s access rates with Differential Binary Phase Shift Keying (DBPSK) and Differential Quadrature Phase Shift Keying (DQPSK) modulation schemes respectively.

The IR implementation uses wavelengths from 850 nm to 950 nm for signaling. It is designed for indoor use only and operates with non-directed transmissions. Two access rates are also specified for IR: 1 Mbit/s and 2 Mbit/s using 16-Pulse Position Modulation (PPM) and 4-PPM respectively [13].

2.5 Medium Access Control (MAC) Sublayer

The IEEE 802.11 MAC sublayer is responsible for frame addressing and formatting, error checking, channel allocation procedures, fragmentation and reassembly.

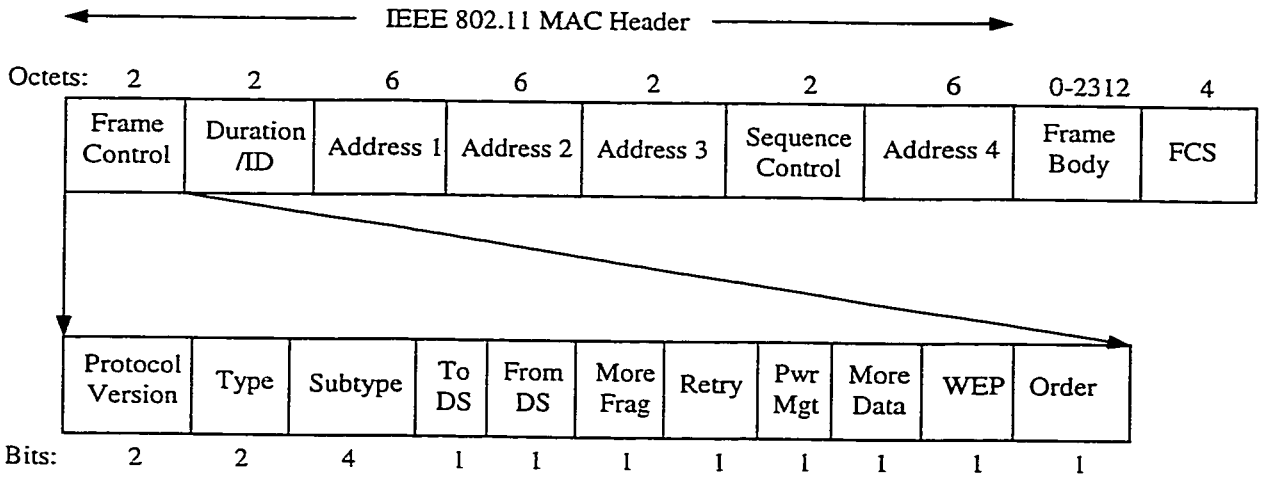

Figure 2.3: IEEE 802.11 MAC frame format

The IEEE 802.11 MAC frame format is illustrated in Figure 2.3. Note that the IEEE standard 48-bit MAC address is used to identify a station. The content of the four address

fields is dependent upon the values of the 'To DS' and 'From DS' bits, and can be either Destination Address (DA), Source Address (SA), Receiver Address (RA), Transmitter Address (TA), or BSS Identifier (BSSID). DA and SA identify the MAC entities that are the final recipient and initiator of the frame respectively. RA identifies the intended immediate recipient on the wireless medium. TA contains the address of the station, which transmitted the frame onto the wireless medium. Note that RA and TA are often the addresses of an AP. BSSID uniquely identifies each BSS, which is the address of the AP in an infrastructure BSS, and a randomly generated address in an IBSS. The 2-bit type field identifies the frame as either control or management or data. The subtype bits further identify the type of the frame, such as a Request To Send (RTS) control frame. A Frame Check Sequence (FCS) contains a 32-bit Cyclic Redundancy Check (CRC) code, which is used for error detection.

Two channel allocation procedures are defined in the IEEE 802.11 MAC architecture: DCF for contention services, and PCF for contention-free services (see Figure 2.4). DCF is similar to traditional legacy packet networks supporting best effort delivery of the data. The DCF is designed for asynchronous data transport, where all users with data to transmit have an equally fair chance of accessing the network. The PCF is primarily designed for the transmission of delay-sensitive traffic.

2.5.1 Distributed Coordination Function (DCF)

The DCF is the fundamental access method, based on a Carrier Sense Multiple Access with Collision Avoidance (CSMA/CA) scheme. As identified in the standard, all stations must support the DCF for use within both IBSS and infrastructure networks.

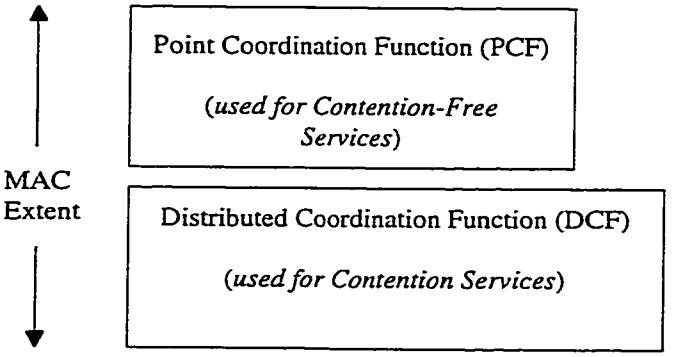

Figure 2.4: IEEE 802.11 MAC architecture

A station wishing to transmit will sense the medium to determine whether another station is transmitting. If the medium is free, the transmission may proceed after ensuring that the medium is idle for a fixed duration, defined as DCF Interframe Space (DIFS). If the medium is determined to be busy, the station will defer until the end of the current transmission plus a DIFS delay. After the deferral, or before attempting to transmit again immediately after a successful transmission, the station will apply a random backoff procedure.

To begin the procedure, the station will select a random backoff interval corresponding to a number of backoff slots. Initially, the station selects one or more backoff slots in the range of 0-7. The station performing the backoff procedure will use the carrier sense mechanism to determine whether the medium is idle during each backoff slot. If the medium is busy at any time during a backoff slot, the backoff procedure is suspended at the beginning of the backoff slot. The backoff procedure is allowed to resume only if the medium is determined to be idle for a DIFS period again. If the

medium is idle for the duration of a particular backoff slot, the station will decrement its backoff interval by one slot. After the backoff procedure is completed, the station transmits its frame immediately. If two or more stations complete their backoff procedure at the same time, a collision will occur, and each station will have to select a new number of backoff slots in the range of 0-15. For each retransmission attempt, the backoff slots range doubles.

Upon receipt of a correct packet, the receiving station waits an interval, the Short Interframe Space (SIFS), and transmits an acknowledgment frame (ACK) back to the source station, indicating that the transmission is successful. If the source station does not receive an ACK within an interval, ACKTimeout, the source station will invoke a backoff procedure for retransmission. All stations except the source station in the BSS use the two duration octets to adjust their Network Allocation Vector (NAV), which indicates the amount of time that must elapse until the end of the current transmission, for deferring access to the channel. Figure 2.5 illustrates an example of some transmissions of data among five stations in one BSS with the DCF access method. The medium operates under the DCF for a time known as Contention Period (CP) in the standard.

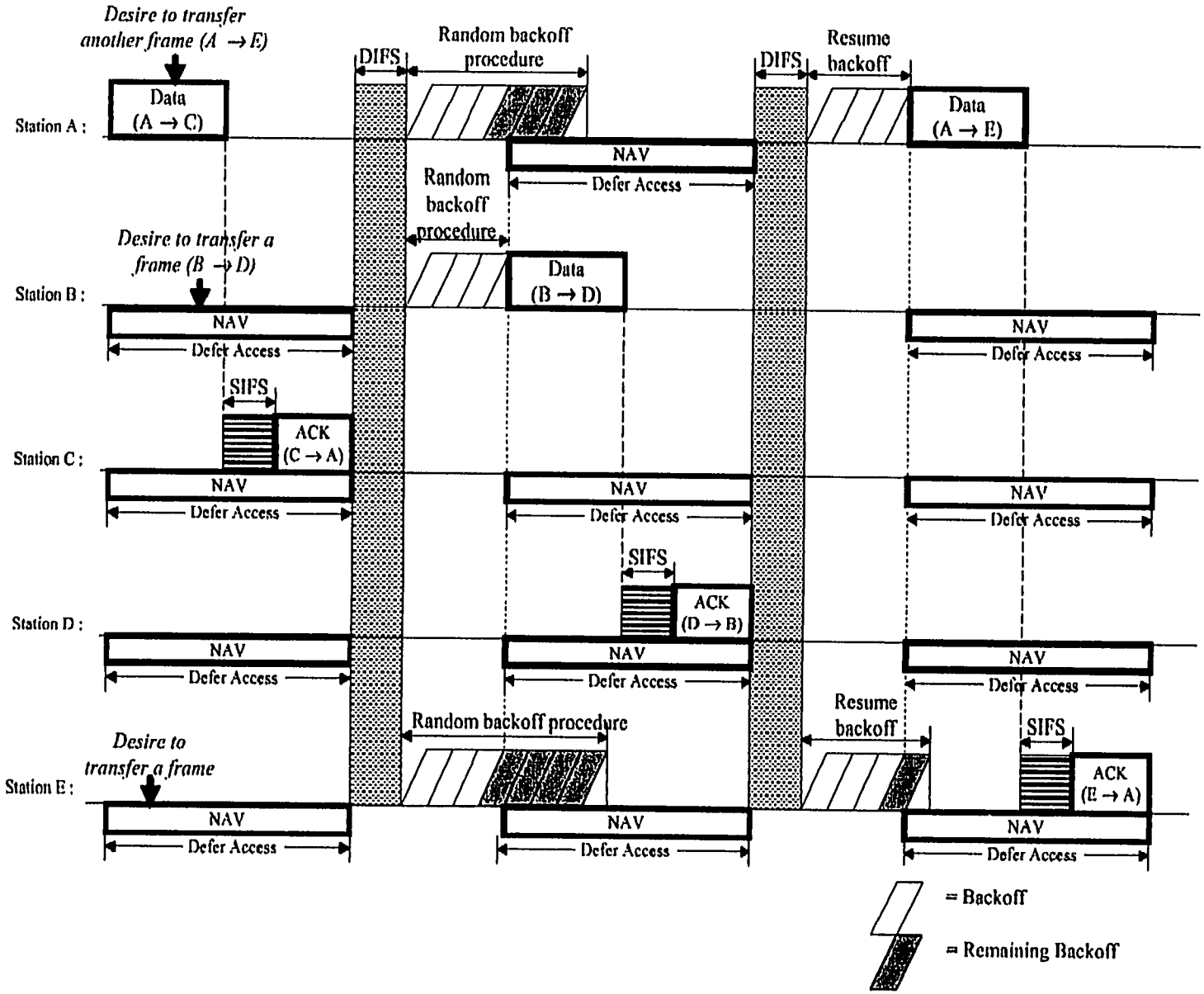

Figure 2.5: An example of some transmissions of data among five stations in one BSS

A refinement of the DCF may be used under various circumstances to further minimize the amount of bandwidth wasted when collisions occur. The refinement is to exchange two short control frames, Request To Send (RTS) and Clear To Send (CTS), between the source and the destination stations prior to data transmission. As in the basic DCF, all stations except the source station in the BSS adjust their NAV using both RTS and CTS to avoid contending for the channel until the end of the current transmission. Figure 2.6 shows the transmission of a data frame with the DCF using RTS/CTS. Since all stations must contend for access to the channel for each transmission, the DCF provides fair access to the channel for all stations.

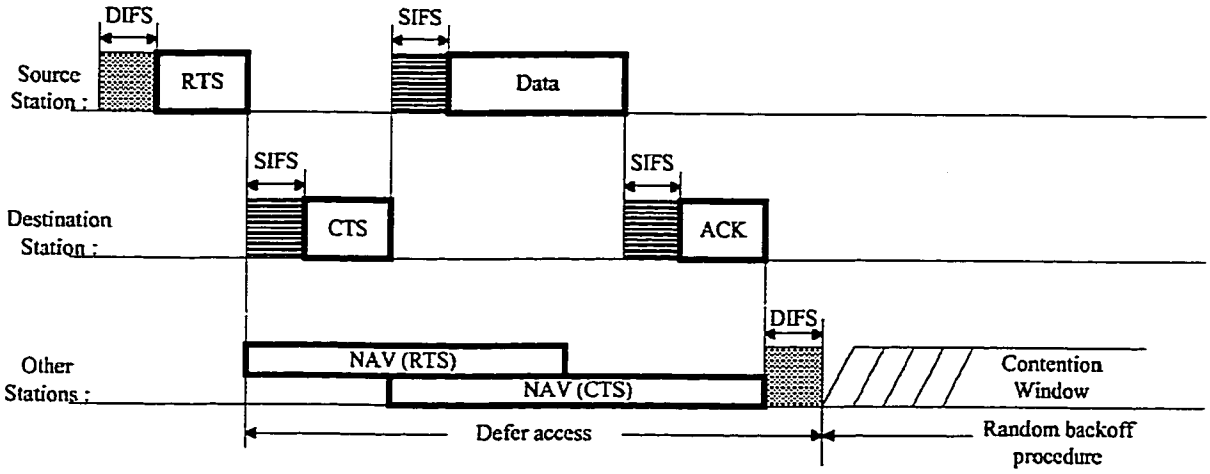

Figure 2.6: A successful transmission of a data frame using the DCF with RTS/CTS

2.5.2 Point Coordination Function (PCF)

The PCF is an optional access method, which is only usable in an infrastructure network. The PCF is required to coexist with the DCF, and logically sits on top of it as shown in Figure 2.4. The PCF relies on the point coordinator, which will operate at the

AP of the BSS, to perform polling and enabling a polled station to transmit without contending for the channel. The period of time when the medium operates under the control of the PCF is known as a Contention-Free Period (CFP). The CFP repetition interval is used to determine the frequency with which the PCF occurs. Within a CFP repetition interval, a portion of the time is allotted to PCF traffic and the remainder is provided to DCF traffic. Figure 2.7 illustrates the coexistence of the PCF and DCF.

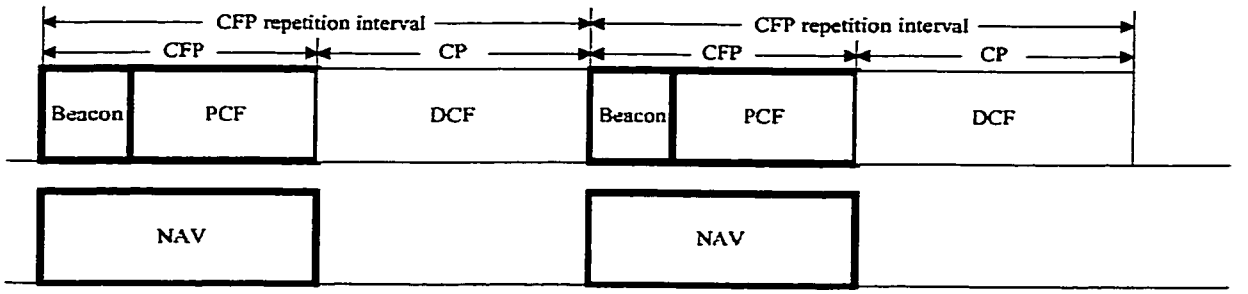

Figure 2.7: Sketch of the coexistence of the PCF and DCF

The CFP repetition interval is initiated by a beacon frame from an AP after the medium remains idle for a PCF Interframe Space (PIFS). The beacon frame contains the parameters for synchronization and the duration of the current CFP. All stations in the BSS will update their NAV to the maximum length of the CFP after receiving the beacon. The AP waits for an interval, SIFS, and transmits a poll frame. The polled station, the only station allowed to respond, can transmit after a SIFS idle period. The AP can terminate the CFP by transmitting a CFP-End frame. Upon receiving the CFP-End frame, all stations will reset their NAV. Figure 2.8 illustrates the transmission of frames between the AP and the polled station using the PCF in a CFP [13, 16].

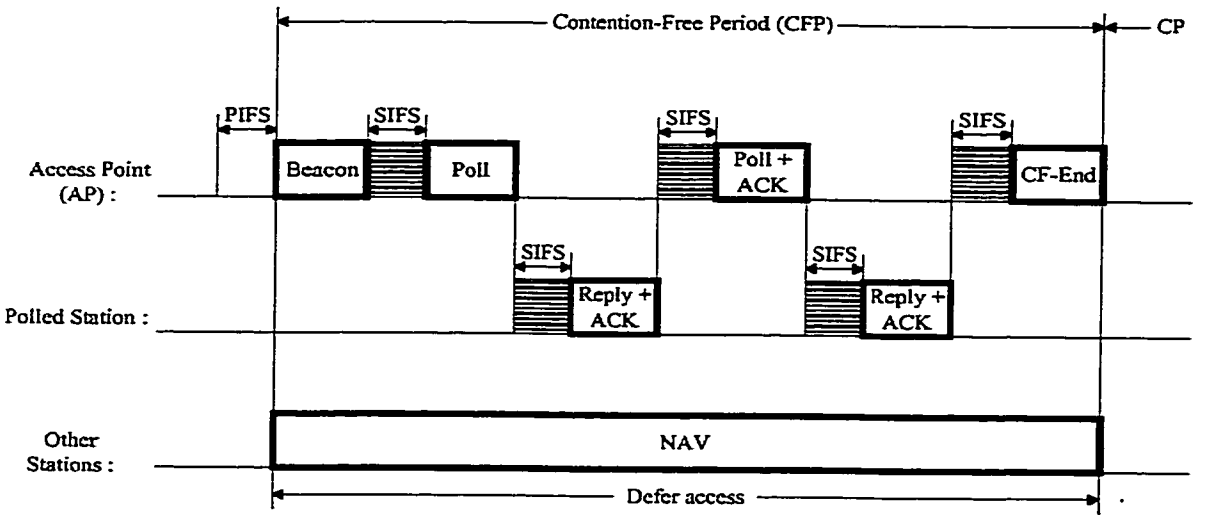

Figure 2.8: A successful transmission of frames using the PCF

Large data frames from an upper protocol layer may require fragmentation to increase transmission reliability. If the size of the data frame exceeds a predefined value, the Fragmentation-Threshold, the frame is broken into multiple fragments with a size of Fragmentation-Threshold, except that the last fragment has a variable size not exceeding Fragmentation-Threshold. When a data frame is fragmented, all fragments are transmitted sequentially. Upon receiving a fragment, the receiving station will send an ACK back to the source station after waiting for a SIFS period. After receiving an ACK, the source station will wait a SIFS period, and transmit the next fragment. The source station will not release the channel until all the fragments are successfully transmitted or the source fails to receive an ACK for a transmitted fragment. When an ACK is not received for a previously transmitted frame, the source station halts the transmission and re-contends for the channel. The source will start transmitting with the first unacknowledged fragment upon gaining access to the channel [13]. The fragments of a data frame can be sent using

either the basic DCF or the DCF with RTS/CTS. Figure 2.9 illustrates the successful transmission of three fragments using the DCF with RTS/CTS [13]. For details of the IEEE 802.11 MAC, refer to [16].

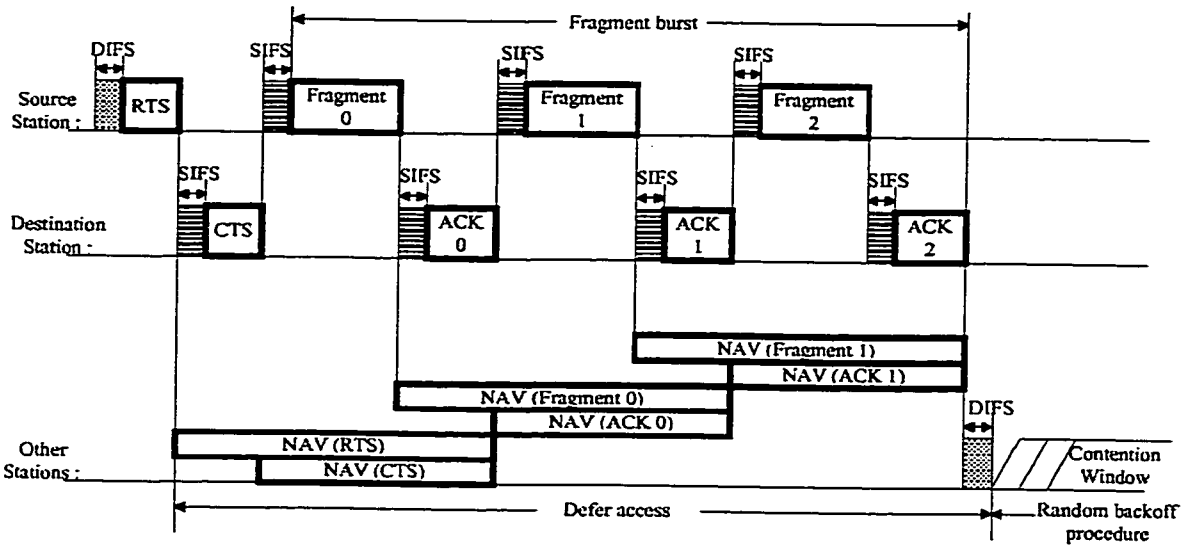

Figure 2.9: A successful transmission of three fragments using the DCF with RTS/CTS.

2.6 Problems in IEEE 802.11 Standard

The IEEE 802.11 standard even though providing a fair chance among users and with fairly high data rate of 1 Mb/s, it does not support any Forward Error Correction technique at MAC sublayer as yet. Since there is no FEC specified at MAC sublayer in the standard, only Automatic Repeat Request (ARQ) at TCP/IP level is adopted on top of 802.11 MAC protocol, thus it results in an inefficiency of the protocol in high noise and severe fading environment. Only a few errors in frames will require frequent ARQ retransmissions.

To overcome this shortcoming and to improve the performance of the IEEE 802.11 standard, in this thesis we applied our hybrid interleaving/FEC technique design (described in the next chapter) on the standard in DCF access mode with RTS and CTS frames and proved that the performance of the standard is improved with the use of FEC technique in the information data.

CHAPTER 3

GPS Driven Coding and Simulation

3.1 Introduction

In this chapter we will present a new and robust interleaving table/RS FEC strategy for our MYMAR system (explained in the first chapter). Same new hybrid FEC/interleaving and packet division technique will be applied to the 802.11 standard, which currently lack this FEC capability. The data loss due to the additive white Gaussian noise, deep Rayleigh fading environment and users overlapping in the same frequency hop are the main concerns while designing and simulating this coding strategy. Though the combined RS/Interleaving tables are well known, the specific interleaving technique herein is of particular application to the error correction problem at hand. The Global Positioning System (GPS) is used here in this system to provide accurate timing and hence to guarantee orthogonal FH and thus to restrict the interference from outside the local cluster. This GPS capability provides minimum end to end probability of TPDU (Transport Protocol Data Unit) loss. Here first we will discuss the coding strategy and then will present the simulation and the results.

3.2 Data Packet

For the MYMAR system the data packet is designed keeping the overall efficiency around 48% (considering overhead, FEC overheads, TCP/IP headers, etc). Figure 3.1 shows a typical data packet of 5225 bits, carrying 3 Transport Protocol data units (TPDU), each 1488 bits long. The Cyclic Redundancy checksum (CRC) for each TPDU is of 16 bits. These CRCs are just to detect the error in the corresponding TPDU. At the receiving end if the TPDU does not give the same CRC then the TPDU will be considered as in error, even if the error is in the received CRC.

The synchronization packet is 280 bits long in order to synchronize the frame at the receiving end with the receiving code. Padding bits are added to make the whole packet exactly 5225 bits long.

The 45-byte header contains all the information about the whole packet. This information is very important as it contains the destination address, number of padding bits, number of TPDUs and their length, GPS time, etc. If there is any error in the header of the packet then the whole packet will be considered in error, as rest of the information will be unreliable.

It is possible to loose only one or two TPDU of a certain packet, this mechanism reduces the frequency of packet loss and ARQ retransmission, since the end users will transmit only those lost TPDUs and not whole packets.

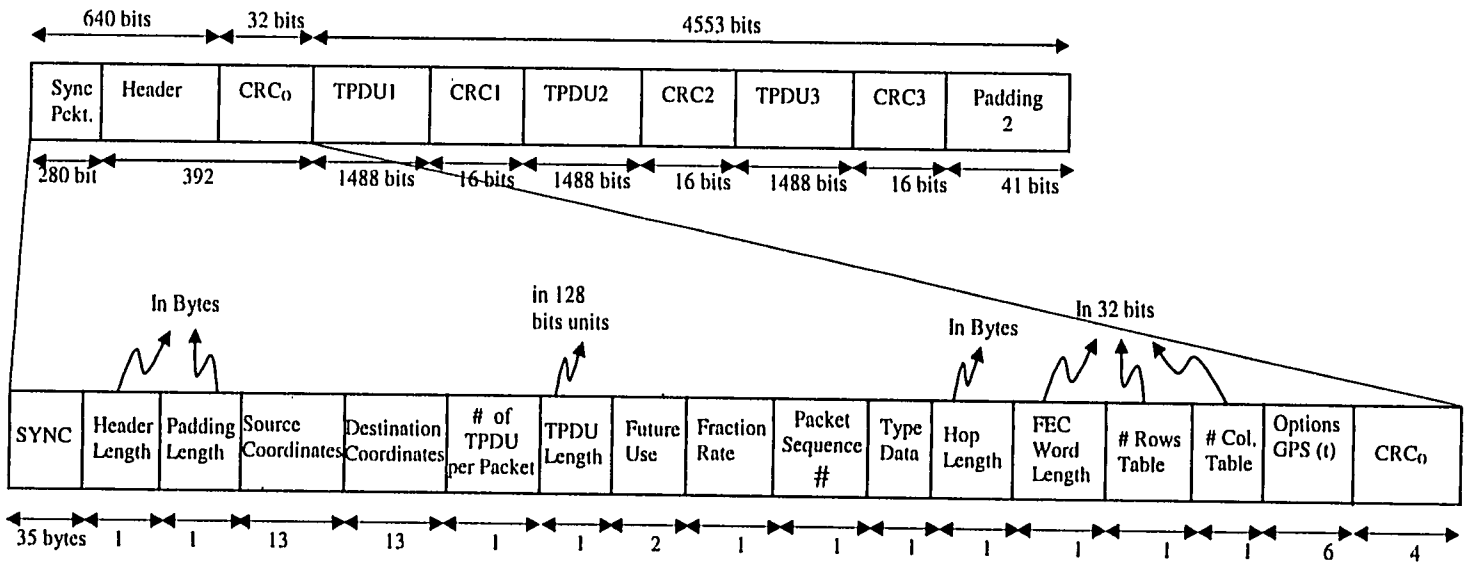

Figure 3.1: A typical data packet of 5225 bits

Padding 1 used, so header will be multiple of 32 bits

Interleaving table parameters used for FEC scalable FEC coding/ Interleaving.

Padding 2= 41 bits, so total packet length will be multiple of FEC Code word length.

Subcarriers in Source and destination coordinate fields are those of immediate neighbours and not of original source or final destination, nor of other intermediate nodes visited by this packet Though other fields of users coordinates refers to final source or destination. Options include GPS time and Time to live of data frame in units of hops. Only two bytes needed for source and destination codes since part of these are already indicated by the fraction rate field.

3.3 Data Encoding

A single data packet is Reed Solomon encoded (RS (31,19)) with a code rate of 19/31 ($n = 31$ and $k = 19$). It is done by first breaking the whole data packet into 55 data words, each of 95 channel symbols. These 55 data words are then input into the Reed Solomon FEC encoder which gives 55 code word, each of 155 channel symbols. The number of correctable symbols 't' is

$$t = \frac{n-k}{2} \qquad 3.1$$

$$t = \frac{31-19}{2} = 6 \text{ code symbols}$$

and

$$6 * 5 = 30 \text{ channel symbols per code word.}$$

Hence the total packet size after coding becomes 5225 * 31/19 = 8525 channel symbols.

3.4 Interleaving Table

The large Block Interleaver is designed to scramble packet symbols and randomize errors so that even a burst fading of long duration producing burst of errors, would not affect the whole TPDU and the employed FEC would recover the lost data. Figure 3.2 shows the encoder output of 55 code words, each 155 symbols long. The Figure 3.3 depicts the block interleaving table of 31 rows and 275 columns. Each table encompasses 55 FEC code words.

All 55 155-symbol code words are fed column by column. The first code word is fed in the first column. After 31 symbols, the 32nd symbol is separated by 55 symbols

from the 1st symbol of the code. Hence the 56th column is filled with symbols 32-62 of the first code word. Similarly 111th column will be fed by symbols 63-93 of the code word and so on. The first 31 symbols of second code word will be fed into the 2nd column and will follow the same strategy. Hence each consecutive 31 symbols of a certain code are spaced by 55 symbols from the following 31 symbols of same code word. So 155 symbols of each code word are spread over 5 columns and these 5 columns are further interleaved to provide further time diversity.

These symbols from the table are then transmitted row by row. Since our MYMAR system utilizes a slow frequency hopped access technique, after every 55 symbols the frequency hop is changed. So each row constitutes 5 hops and each hop carries single channel symbol from each code word. So if fading or any other noise or interference factor affects even 30 hops of a single packet in certain bands, the RS code will recover it back. There are also 2 guard symbols at the start of each hop and 2 symbols at the end. Though in the simulation we did not use it.

With the assumed data rate for our MYMAR system of 96ks/s, the total packet will be transmitted in (55*31*5)/96 k = 88.8 ms.

155 Channel Symbols

Code Word 1	1,1	1,2	.....	1,31	1,32	.....	1,62	1,63	.....			.....		1,124	.....	1,155
Code Word 2	2,1	2,2	.....	2,31	2,32	.....	2,62	2,63	.....			.....		2,124	.....	2,155
Code Word 3	3,1	3,2	.....	3,31	3,32	.....	3,62	3,63	.....			.....		3,124	.....	3,155
Code Word 55	55,1	55,2	.....	55,31	55,32	.....	55,62	55,63	.....			.....		55,124	.....	55,155

Figure 3.2: 55 code words, each 155 channel symbols long after Reed Solomon coding.

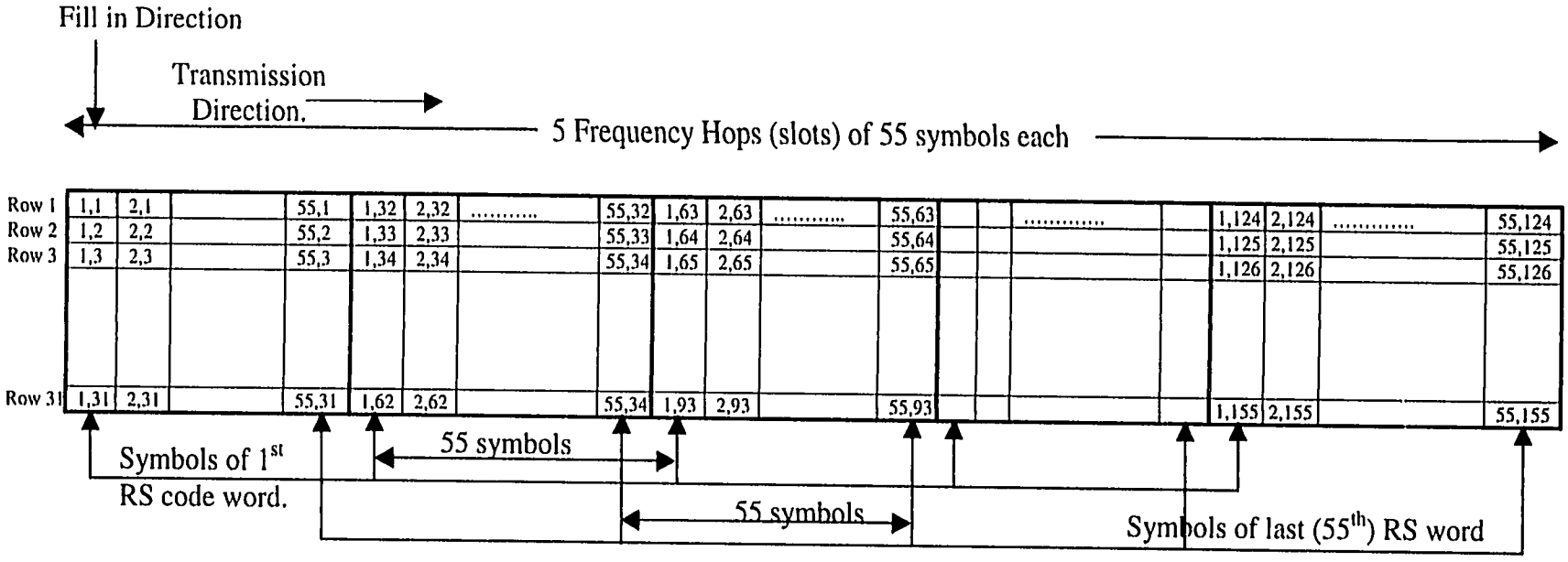

Figure 3.3: The 31 rows x 275 columns interleaving table, symbol of each code word are fed column by column & transmission commences row by row. Each consecutive 31 symbols of a certain code are separated by 55 symbols from the following 31 symbols of same code word.
Supported data rate = 58.8 kbps, 29.42 kbps, ... , 1.84 kbps.
Typical Table Length of Frame = (55*31*5)/96k = 88.8 ms.

3.5 Overhead Efficiency of the Data Payload

Here is the overhead efficiency of the data symbols in the whole packet is calculated.

The total number of data symbols in each interleaving table, (D) = 1488 * 3 TPDUs

(D) = 4464 channel symbols

3 CRCs + Sync Packet + Header + CRC0, (OH1) = 3*16 + 280 + 360 + 32

= 720 symbols

RS code overhead, (OH2) = (31-19)* 5 * 55 = 3300 symbols

Guard bits overhead, (OH3) = 4 * 155 = 620 symbols

Padding, P = 41 symbols

Overhead efficiency, η = D / (D + OH1 + OH2 + OH3 + P) = 4464 / 9145 = 48.8%.

The overall overhead efficiency of 48.8% is not bad with an actual data rate of 54.85 ksps.

3.6 Simulation Parameters

A generic simulation model was developed to verify the end to end error performance of the designed hybrid code of this FH/FSK system. At the receiving end after dehopping, corresponding to a certain hop duration the received signal at the FSK demodulator can be expressed as:

$$r(t) = A_1 \cos(\omega_{if} t + d_1.\Delta\omega\ ) + n(t) \qquad 3.2$$

where A_1, ω_{if}, d_1, $\Delta\omega$, *and* $n(t)$ are respectively the Rayleigh faded signal magnitudes, the FSK IF frequency, the user binary data symbols, the spacing between the FSK Mark and space frequencies/2, the AWGN receiver and other noises of power spectral density No/2. The total number of interference hitting the same FH is assumed zero due to orthogonality of FH.

The intended user (first user) AWGN Signal to noise ratio (SNR) is varied. SNR is given by

$$\text{SNR} = z = A_1^2 T_s / 2N_o \qquad 3.3$$

where $z = E_b/N_0$ and defined from equation 1.3 as

$$z = \frac{E_b}{N_0} = -2\ln(2P_e) \qquad 3.4$$

The unfaded intended signal amplitude was fixed at 1, T_s assumed to be (1/96000) and N_o varied according to the AWGN SNR range assumed. The fast Rayleigh fading was generated by assuming the deep fade duration to follow a uniformly distributed fade duration of average = 55 channel symbols (corresponding to a fade duration of 572 μs which is typical of the severe GHz subject Mobile channel). The number of hops in a certain interleaving table affected by fading is indicated by the parameter: $p = 0.05, 0.1,$

0.2. As an example if $p = 0.1$, this means on average there will be 155*0.1 ≈ 16 frequency hops in the table suffering deep Raleigh fading. Similarly the number of hops suffered by the like user FH overlap is defined by the parameter 'P_j'. If P_j is 0.15, it means 155*0.15 ≈ 23 hops are jammed by the like user FH overlapping. The probability of symbol errors in those hops contaminated by fading or like user FH overlapping is assumed very high (e = 0.2, 0.3, 0.5, 0.7). Another Bernoulli random generator with parameter 'e' is called and if the outcome of the generator is above 'e' the symbol is assumed to be received in error. If the outcome of this generator is less than 'e' or there is neither fading nor FH overlapping to start with in the current FH, then the symbol error is decided upon by the FSK demodulation in AWGN alone.

The values of the four channel parameters that we used in our simulation for two different cases are given in the following table. When one parameter is varied the other three are frozen on these values.

Table 3.1. Simulation Parameters

	SNR, z	**Probability of Rayleigh Fading, p**	**Probability of like user FH overlapping, P_j**	**Probability of Symbol Error, e**
With Low Noise Factor	7.824	0.065	0.155	0.6
With High Noise Factor	5.628	0.09	0.18	0.7

3.7 Simulation Procedure

In each run of the simulations, the data packet of Figure 3.1 is created by randomly generating the individual fields and then filling up in a single frame of size 5225 channel symbols in sequence. The frame is then broken into data words each equal to 95 channel symbols. Then each data word is encoded by RS coding and it makes the code word equal to 155 channel symbols. From here the 55 encoded code words are fed into an interleaving table that constitutes 155 hops, each carrying 55 channel symbols. The interleaving table is shown in Figure 3.3 and filled up as mentioned earlier. It is also possible to add 2 guard symbols at start and end of each hop, which may help in detecting interference and frequency synchronization, but in this simulation we have ignored these guard symbols.

Now the 155 hops in the interleaving table are sent to the channel. The number of hops suffered by Rayleigh fading and like user FH overlapping implied by p and P_j respectively are effectively added together. For example if $p = 0.05$ and $P_j = 0.1$, then it means approximately $\{(0.05 * 155) + (0.1 * 155)\} \approx 24$ hops are in error. Then 24 times the Bernoulli random generator is called and if the result is more than 50% then one hop is picked randomly to be in error, which has not been picked before. Each bit of this contaminated hop is in error depending upon the Symbol Error probability parameter 'e'. Another random generator is called a number of times equal to the number of symbols per hop and if each outcome is more than 'e' then the symbol is changed otherwise it is contaminated with the AWGN probability P_e, which is a function of the SNR 'z'.

When symbols of the whole table are transmitted through the channel, the decoder then retrieves back the 55 code words in the reverse order (table deinterleaving). The

words are corrected if the number of errors is not more than the error correcting capability of RS code per code word defined by t in section 3.3.

Now there is a counter recording the TPDU losses in each run. When there are one or more decoding bit errors in the packet header, it results in the three TPDUs loss constituting the whole packet and the TPDU loss counter is incremented by 3. Also the CRCs of three TPDUs and the three TPDUs themselves are individually checked, and the TPDU loss counter above is incremented only once for each loss of a TPDU and/or the CRC of a certain TPDU. The total number of lost TPDUs are added and divided by the total number of TPDU in each simulation run thus giving the probability of TPDU loss in each AWGN and fading environment. Similarly we computed the probability of overhead loss and CRC errors.

This whole process goes on 1000 times per simulation run to get the average result.

3.8 Results

Figures 3.4 to 3.23 are the results using the simulation parameters with low noise factor in table 3.1. While varying the parameters, ten different performance criteria (responses) have been obtained. The number of errors received by different fields of the packet after deinterleaving and decoding, gives the distribution of errors and loss probabilities. The ten different criteria results for each case (simulation run) are the total TPDU loss probability (in the whole simulation), total errors corrected by our FEC/interleaving design, header loss probability and probability of error in its CRC, 3 TPDU loss probabilities and 3 CRCs error probabilities.

3.8.1 Varying AWGN

In Figure 3.4, the probability of a FH in fading was set at $p = 0.065$, the probability of symbol error for those FH in fading or FH overlap was set at $e = 0.6$, and the probability of FH hit by like user interference (mostly from fractional rate users and users from outside the network) was set at $P_j = 0.155$. If the applicable symbol of the interleaving table was not in error due to any of the imperils above, an AWGN symbol error in the varying amounts 'P_e' in the Figure was generated. The Total average TPDU loss Probability (average of the loss probability of the three TPDUs in any packet as previously indicated) was computed. Reasonable results are noticed from Figure 3.4, e.g. at $P_e = 0.02$, TPDU loss Probability ≈ 0.4 which means on the average, a number of transmission = 1/(1-0.4) $\approx$ 1.7 till final TPDU success (not very bad given the severe environments above and that this is a final data delivery at the end user). It also shows that with zero AWGN, less than 10% of the TPDUs were in loss due to fading and like user FH overlapping factor.

Figure 3.5 represents the errors corrected by our coding strategy. It shows that the 2% P_e, more than 90% of the errors were corrected successfully though 40% of the TPDUs were still lost as indicated in Figure 3.4.

In Figure 3.6, the header loss probability given by solid line, shows that at P_e = 0.02, 20% of the packet headers were lost which constitutes half of the total TPDU loss in Figure 3.4 at P_e = 0.02. The rest of the loss in Figure 3.4 at P_e = 0.02 is due to the individual data unit loss. In the same Figure the dotted line is representing the packet header CRC loss probability. Its share for the destruction of the whole packet is obviously less due to its smaller length.

Figure 3.7 shows the response of the three individual TPDU loss probabilities. All almost take the same trend. This loss also includes the loss when packet header was lost. Figure 3.8 represents the three CRC loss probabilities. Here again all the three curves go the same way. Hence the errors produced are equally distributed due to interleaving/deinterleaving.

3.8.2 Varying Like User FH Overlap

In Figure 3.9 to Figure 3.13 the values of the parameters p, e, and the SNR z were all fixed and P_j is varied as shown. Figure 3.9 represents the total TPDU probability. We notice the resilience of the FEC/ interleaving table to all kinds of errors, for example, we get almost perfect TPDU transmission (TPDU Loss Probability = 0) even when $P_j = 0.1$, $z = 7.824$, $p = 0.065$, $e = 0.6$ (all in Figure 3.9).

Figure 3.10 representing the errors corrected by the code also gives the same behavior. Even with 12% of jamming probability and the other parameters as mentioned above, it does provide a 100% recovery of the data.

In Figure 3.11 the packet header loss and its CRC loss are shown. Figure 3.12 and Figure 3.13 show the individual TPDU loss and their CRC loss probabilities. All these results reflect the strength and the resistance of the proposed hybrid FEC/interleaving against the AWGN and other errors.

3.8.3 Varying Rayleigh Fading Probability

Figure 3.14 to Figure 3.18 shows the results obtained by changing p while fixing the remaining parameters. In Figure 3.14 with AWGN probabilities of errors $P_e = 0.01$ ($z = 7.824$), $e = 0.6$ and $P_j = 15.5$, the end to end performance of the system shows a 50% TPDU loss probability at 9% fading probability p. While there were almost zero TPDU loss till p reaches 4%.

In Figure 3.15 the total number of errors corrected by the decoder is shown. When $p = 6\%$, more than 98% of the channel symbol errors were corrected but as in Figure 3.14, these 2% of uncorrectable errors caused around 10% TPDU loss.

The packet header loss is represented in Figure 3.16. The slight bump at $p = 0.09$, was the cause to raise the TPDU loss to 50% in Figure 3.14. A single decoding error in packet header causes a damage of the whole packet i.e. 3 TPDUs. Figure 3.17 and Figure 3.18 are the individual TPDU loss probabilities and individual CRC loss probabilities respectively. In both figures the results show the equal and same distribution of errors in the whole packet.

3.8.4 Varying Symbol Error Probability

Figures 3.19 to 3.23 are the results when we varied the Symbol Error probabilities e, in the affected hops. With 6.5% of fading probability p and 15.5% of the jamming probability P_j, which translates into 34 hops in error, even if the symbol error $e = 0.75$,

only a 60% TPDU loss results, which means 1/(1-06) = 2.5 times transmission trials on average for each TPDU, which is not bad in these sever channel impairments.

Figure 3.20 shows the error corrected after decoding the received data. Here again the decoder corrected almost 98% of channel symbol errors at $e = 60\%$ but still nearly 20% of the TPDUs were lost (in Figure 3.19).

Figure 3.21 represents the packet header and its CRC loss probabilities. At e = 75%, packet header loss accounts for 45% of the 60% TPDU loss (in Figure 3.19). Packet header loss increases sharply with the increase in symbol errors.

Figure 3.22 represents the individual TPDU losses. All the three TPDU loss probabilities are almost the same at the values of symbol errors. Same case is with the CRC loss probabilities in Figure 3.23.

3.9 Comparisons

Here total TPDU loss is compared for two different sets of values of the simulation parameters. The two sets of values are given in Table 3.1. Figure 3.24 to Figure 3.27 show the results.

In Figure 3.24a, the probability of a FH in fading was set at $p = 0.065$, the probability of symbol error was set at $e = 0.6$, the probability of FH hit by like user interference was set at $P_j = 0.155$, and AWGN symbol error is varied. The Total average TPDU loss Probability was computed. Results from Figure 3.24a shows that at $P_e = 0.02$, TPDU loss Probability = 0.4 which means on the average, a number of transmission = 1/(1-0.4) = 1.7 till final TPDU success as discussed above. The average TPDU loss probability increases in Figure 3.24b due to increasing the values of p, e, P_j as indicated.

In Figure 3.25 the values of the parameters p, e, and the SNR z were all fixed and P_j is varied as shown. Figure 3.25a is the same as the one in Figure 3.9. Here it is compared with the case when we increased the noise probabilities. The result of Figure 3.25b is slightly worse due to increasing the AWGN level (less SNR z); it is not only FH overlaps, or fading that causes decoding errors!

Figure 3.26 shows the results obtained by changing p while fixing the remaining parameters. Here again the Figure 3.26a is the same as in Figure 3.14 and discussed in the previous section. Here it is compared when the channel situation became worse. With low AWGN probabilities of error (SNR, $z = 7.824$), $e = 0.6$ (i.e. 60% of the symbols of the affected hop are in error) and $p = 0.09$ (i.e. 9% of the total 155 hops are faded), the end to end performance of the system shows a 50% TPDU loss probability at 15.5% jamming probability (P_j), all in Figure 3.26a. While the same TPDU loss is obtained at $z = 5.628$, $e = 0.7$ and $p = 0.01$ while having 18% jamming probability in Figure 3.26b.

In Figure 3.27a, probability of Symbol Error per affected hop (e) is varied. The TPDU loss, slowly rises as a function of e at low probabilities of Fast Raleigh Fading (p) and Frequency Hop overlap (P_j), all in Figure 3.27a. However in Figure 3.27b the TPDU loss probability shoots up with high probability of AWGN error. Even in this worst case, combined FEC/Interleaving provided TPDU loss of 0.6 (i.e. 2.5 transmissions on average for each TPDU) at $e = 0.5$, $z = 5.628$, $P_j = 0.18$, $p = 0.09$.

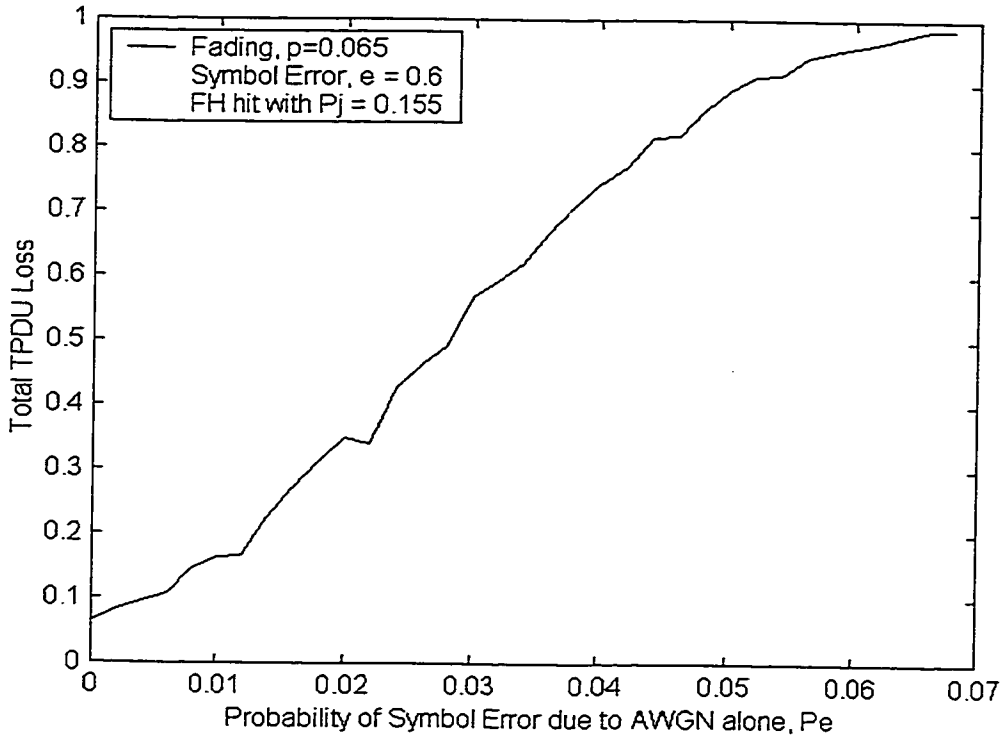

Figure 3.4: Total TPDU loss encountered due to variation in AWGN error, P_e.

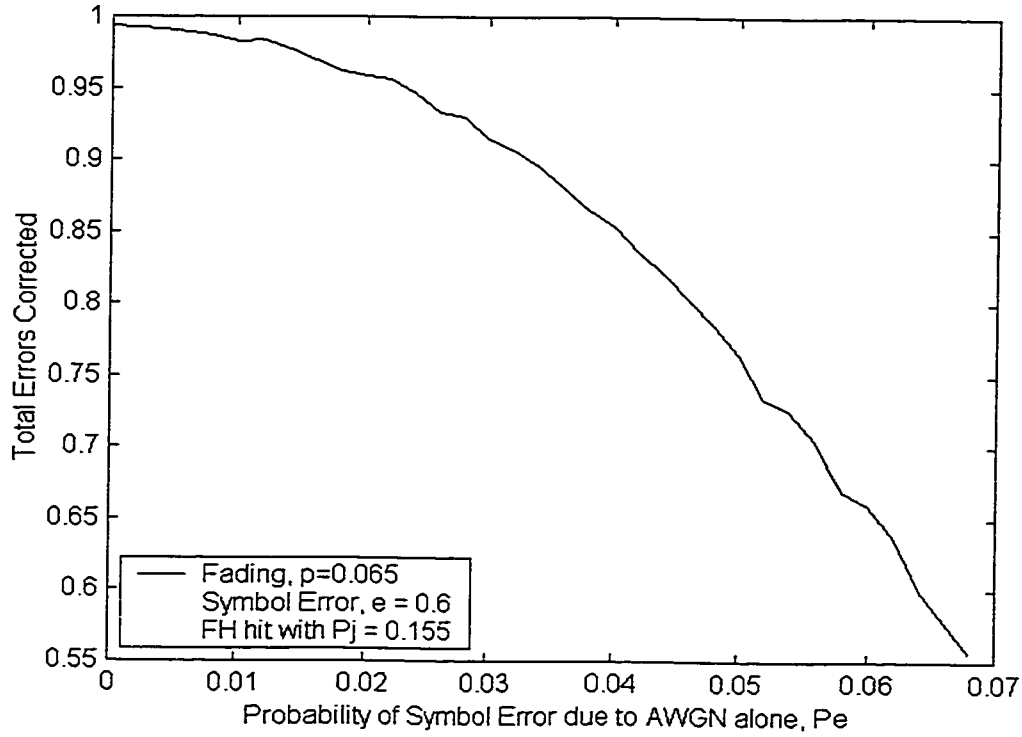

Figure 3.5: Total errors corrected by the designed interleaving/FEC while varying AWGN error, P_e.

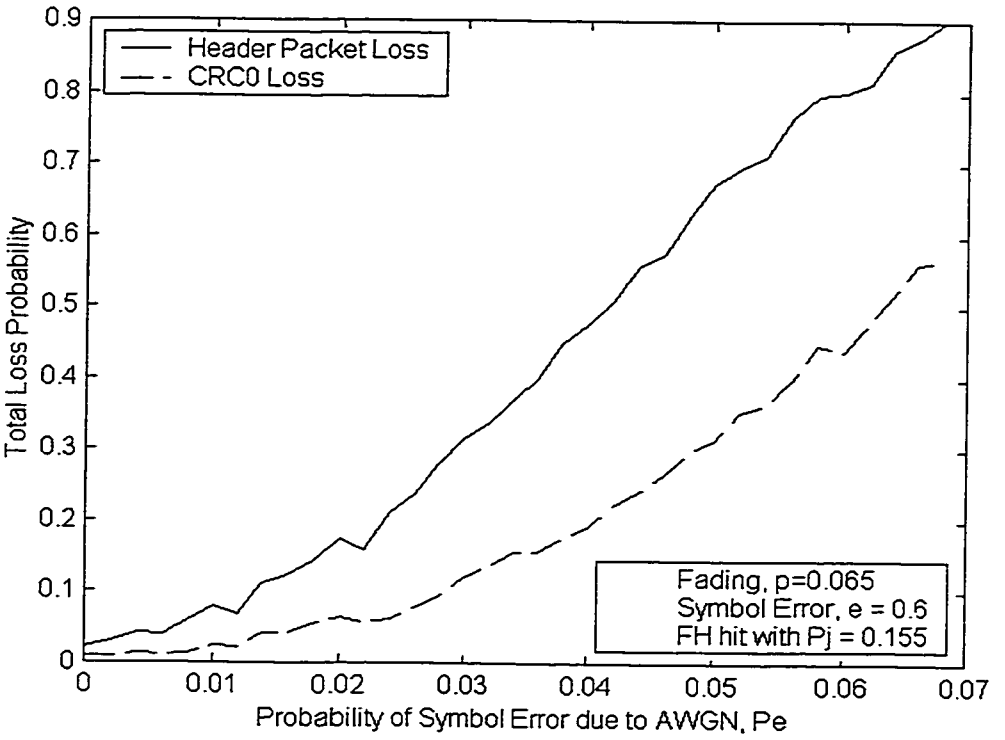

Figure 3.6: Total Header and CRC loss encountered while varying AWGN error, P_e.

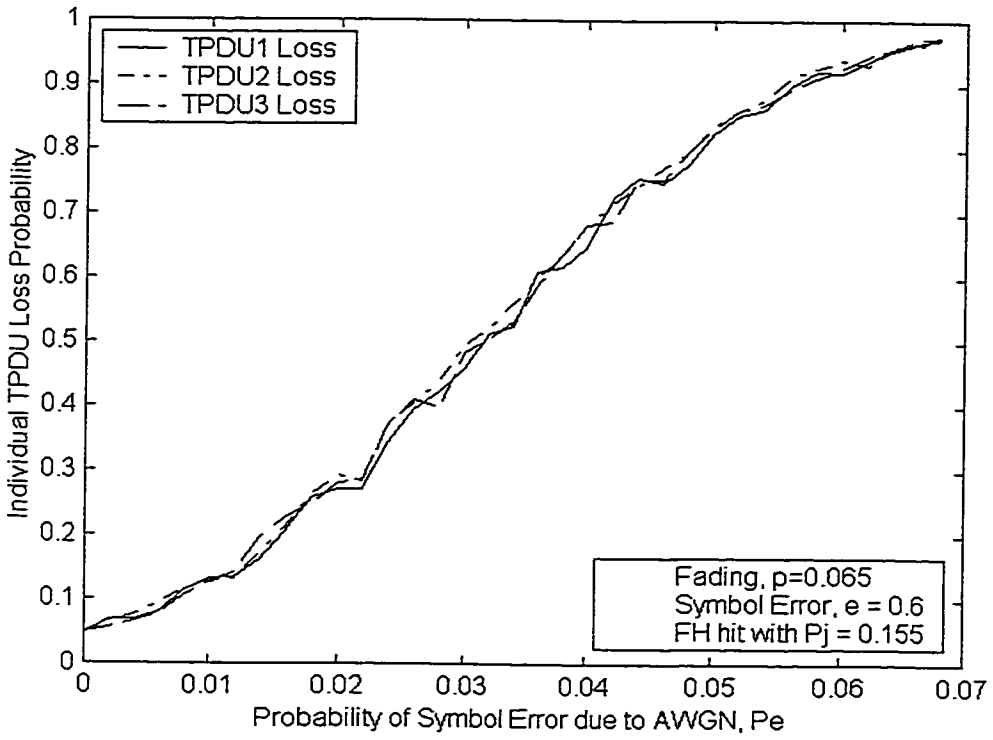

Figure 3.7: Total individual TPDU losses encountered while varying AWGN error, P_e.

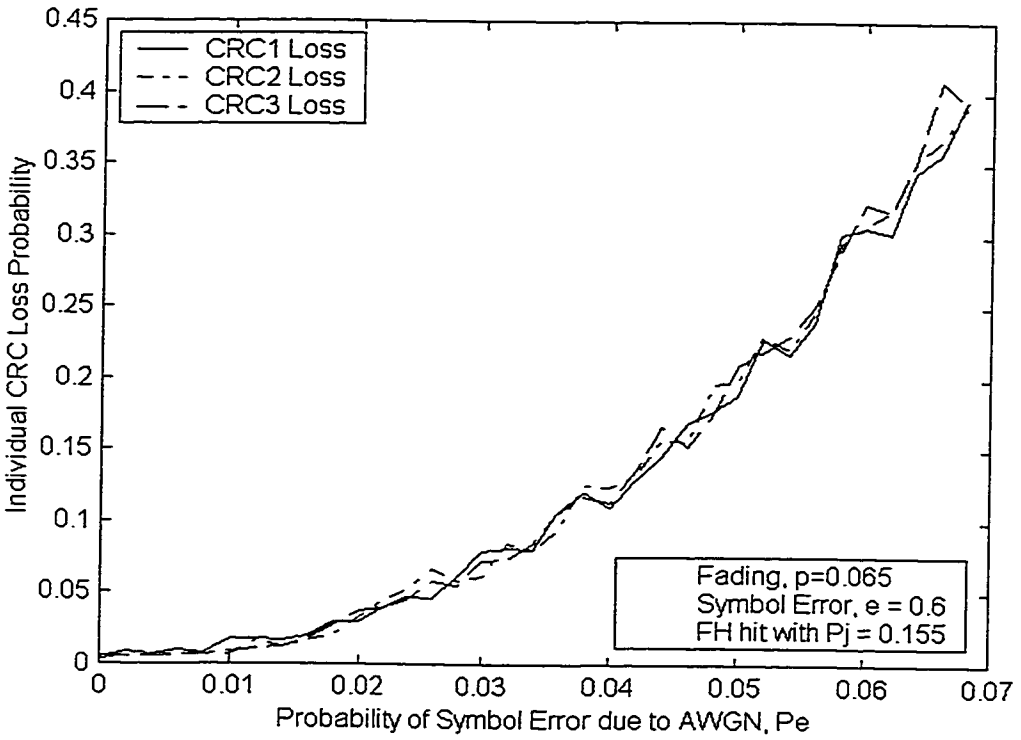

Figure 3.8: Total individual CRC losses encountered while varying AWGN error, P_e.

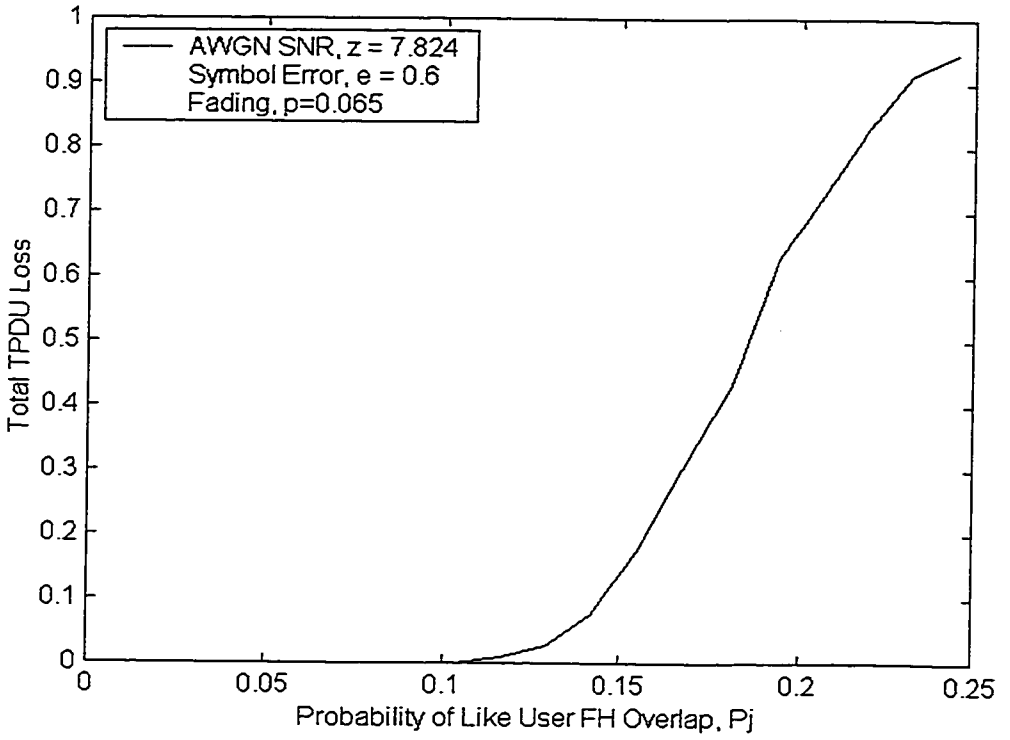

Figure 3.9: Total TPDU loss encountered due to variation in like user FH overlapping, P_j.

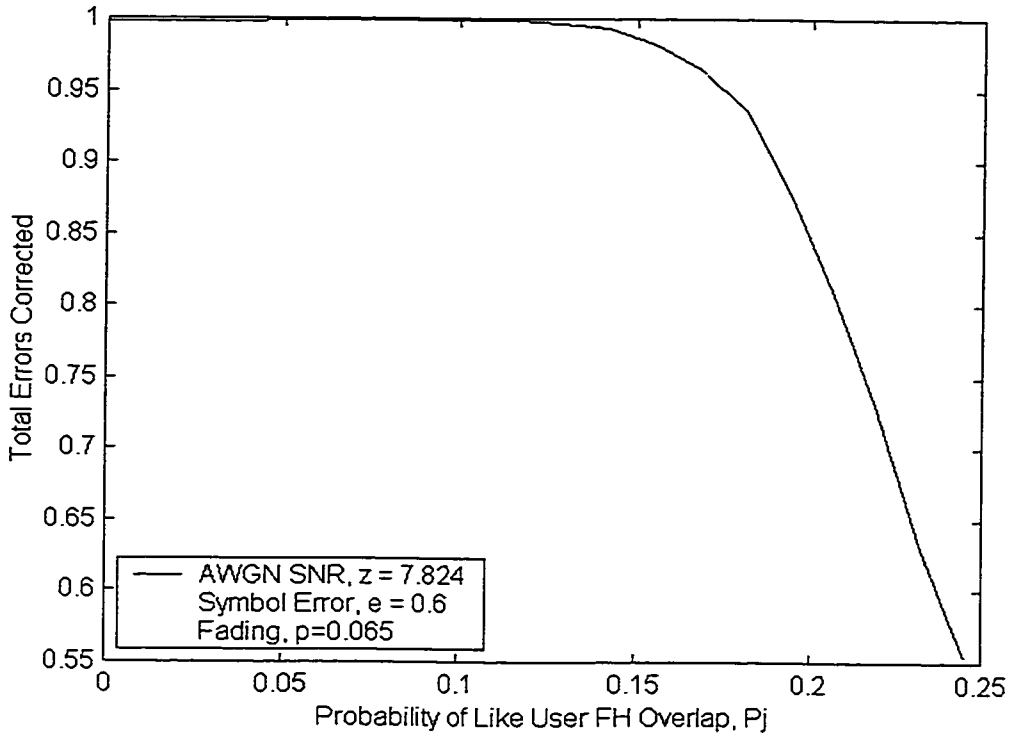

Figure 3.10: Total errors corrected by the designed interleaving/FEC while varying like user FH overlapping, P_j.

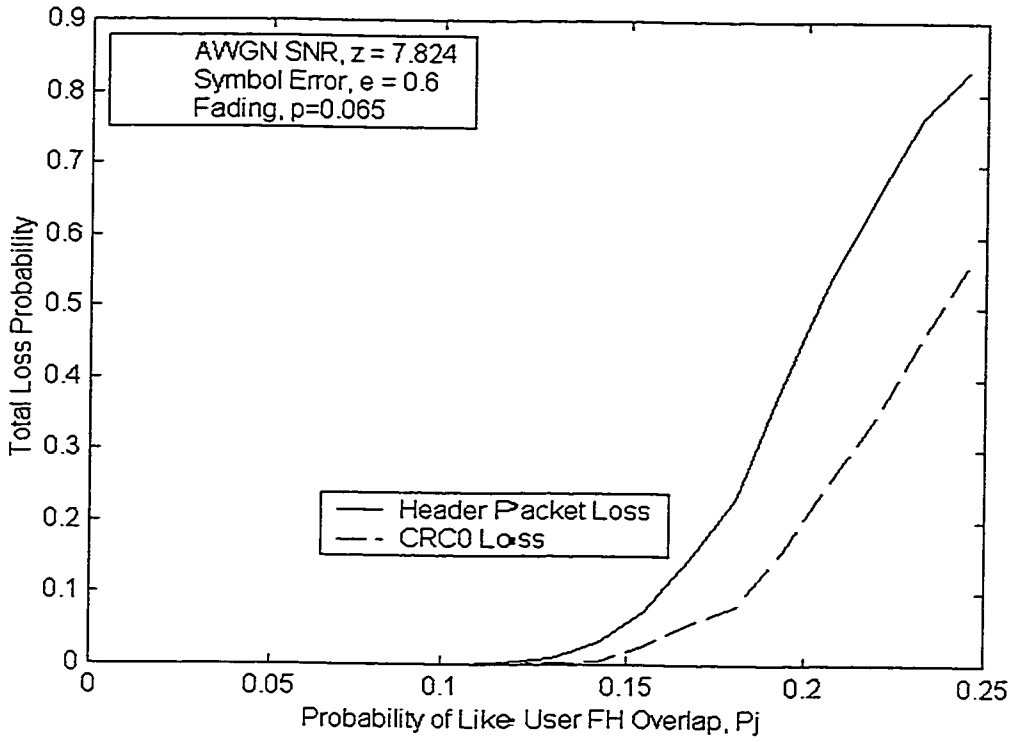

Figure 3.11: Total Header and CRC loss encountered while varying like user FH overlapping, P_j.

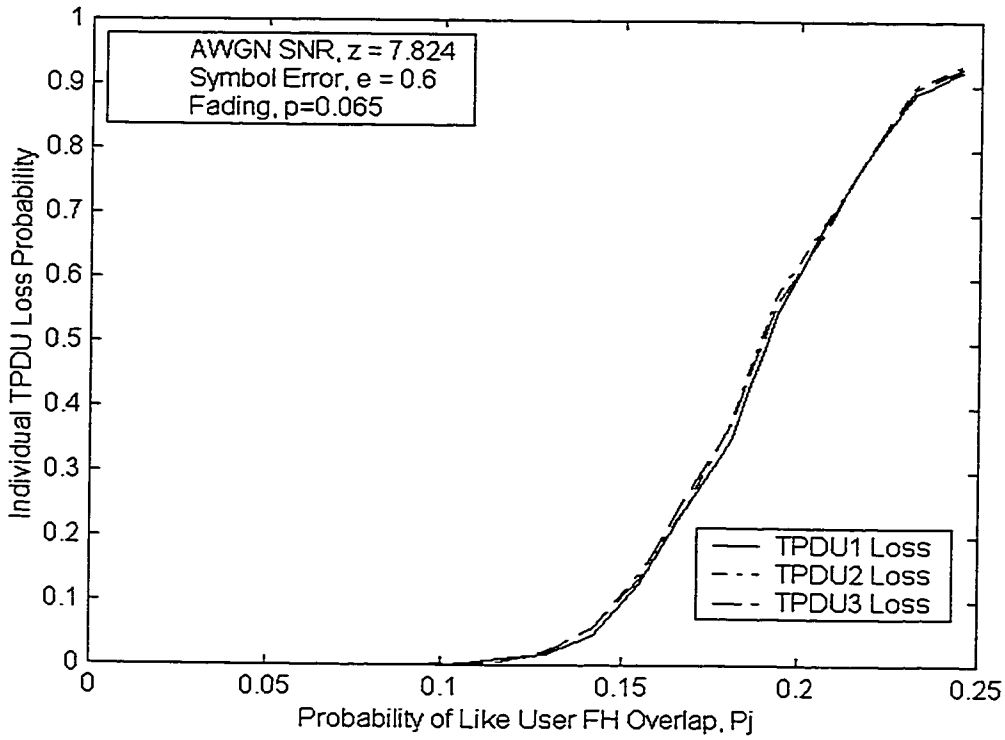

Figure 3.12: Total individual TPDU losses encountered while varying like user FH overlapping, P_j.

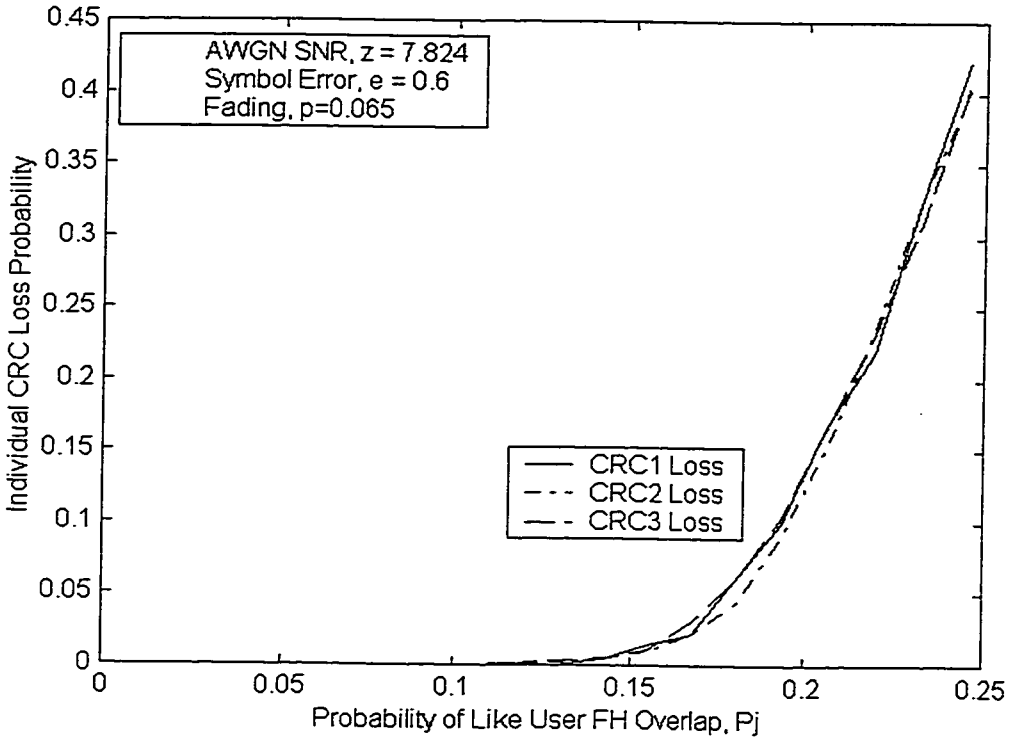

Figure 3.13: Total individual CRC losses encountered while varying like user FH overlapping, P_j.

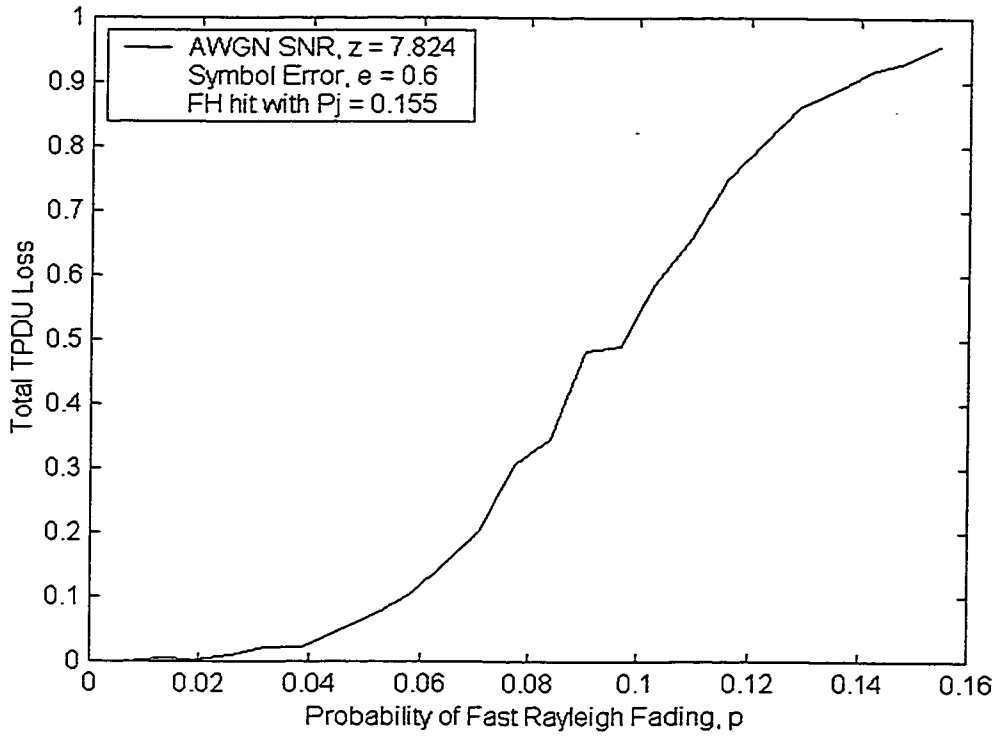

Figure 3.14: Total TPDU loss encountered due to variation in Rayleigh Fading, *p*.

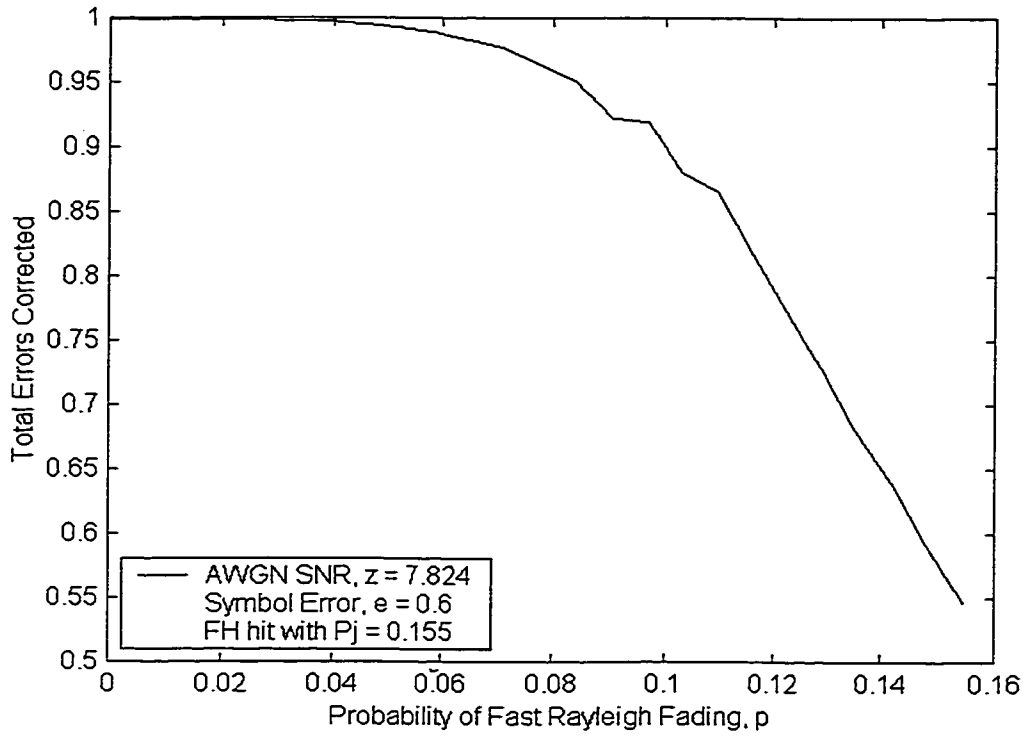

Figure 3.15: Total errors corrected by the designed interleaving/FEC while varying Rayleigh Fading, p.

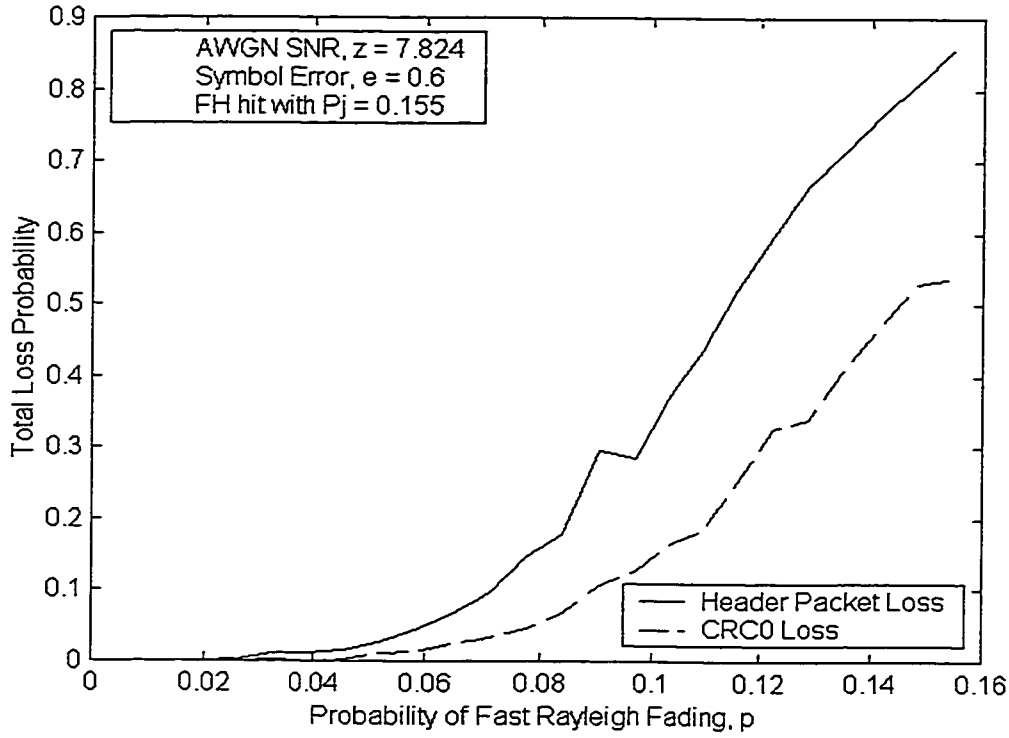

Figure 3.16: Total Header and CRC loss encountered while varying Rayleigh Fading, *p*.

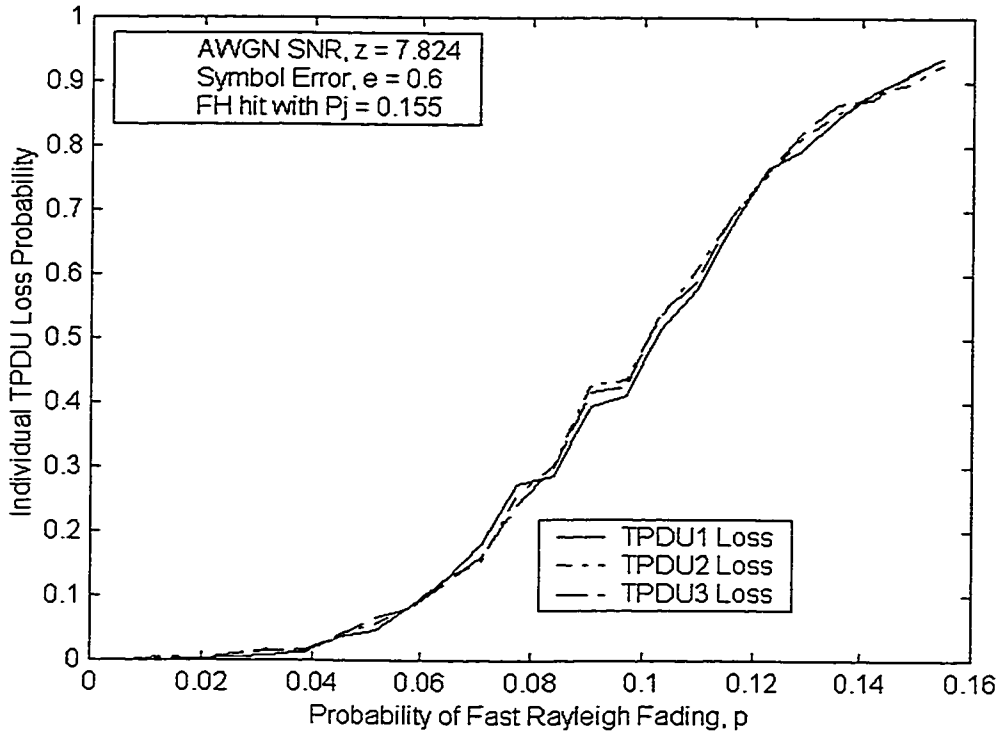

Figure 3.17: Total individual TPDU losses encountered while varying Rayleigh Fading, p.

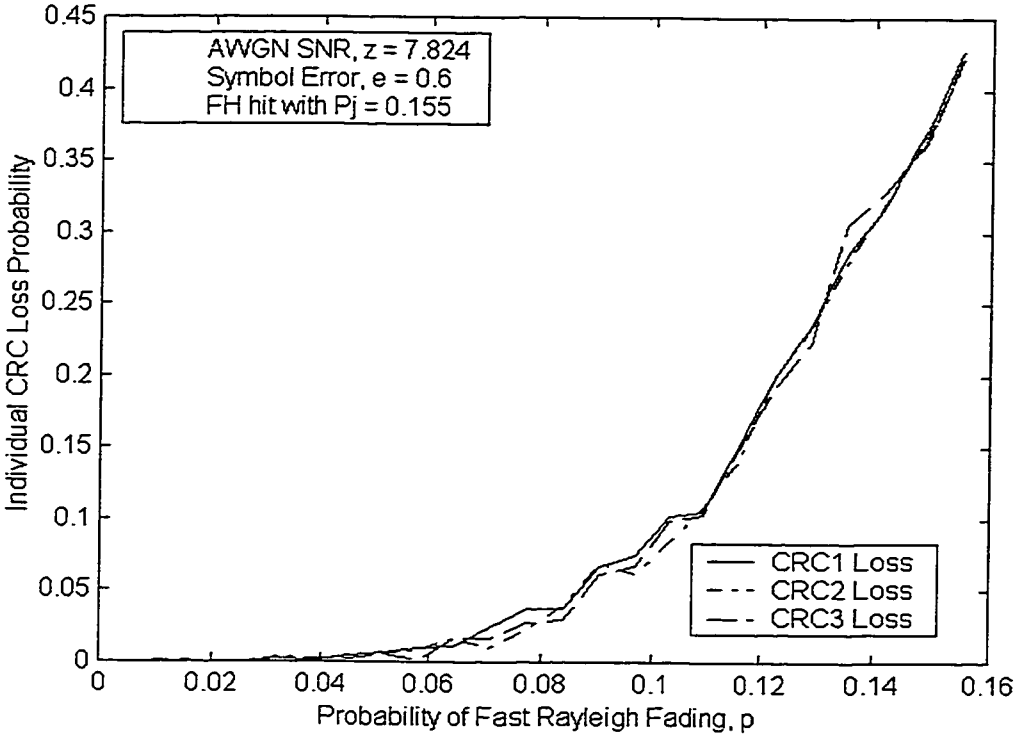

Figure 3.18: Total individual CRC losses encountered while varying Rayleigh Fading, *p*.

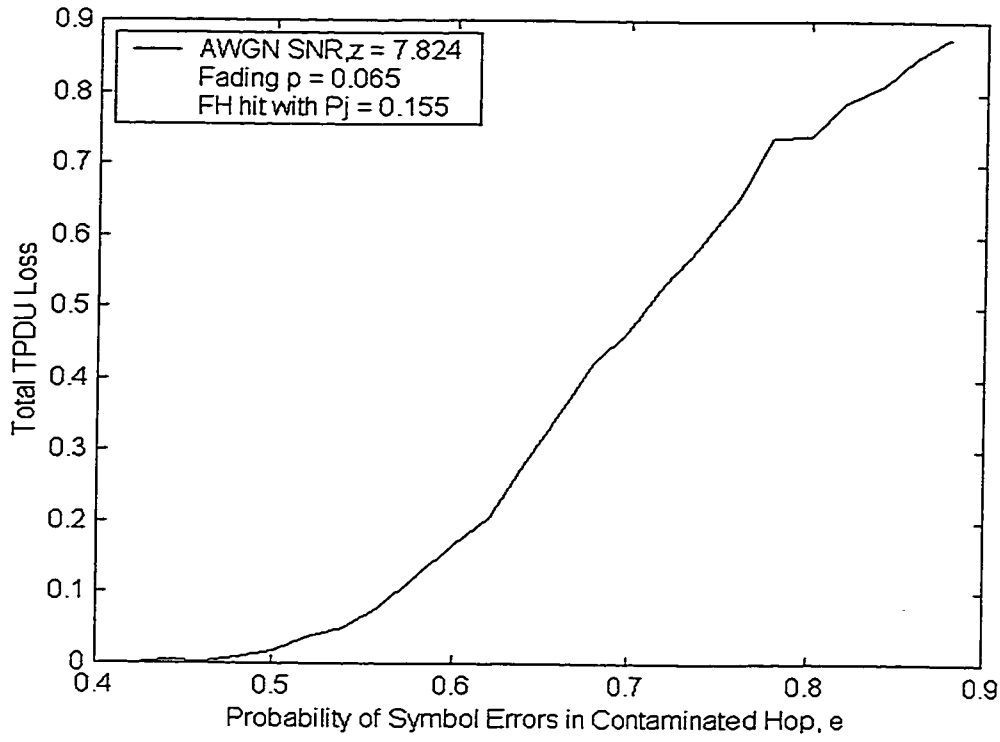

Figure 3.19: Total TPDU loss encountered due to variation in probability of Symbol Error '*e*' in contaminated hops.

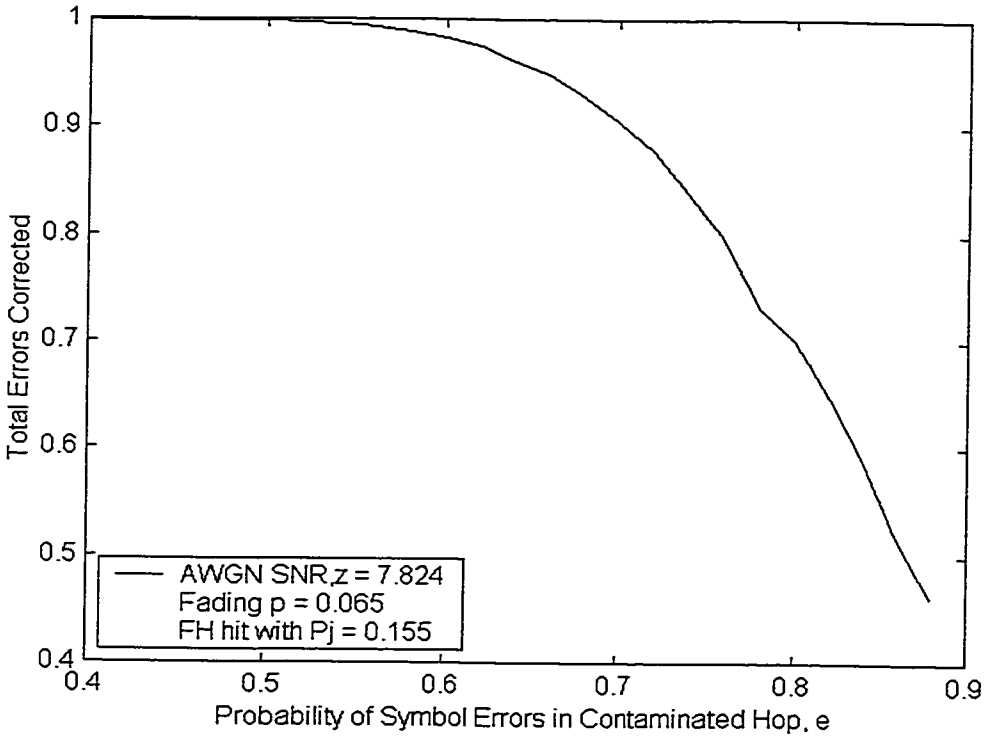

Figure 3.20: Total errors corrected by the designed interleaving/FEC while varying the probability of Symbol Error '*e*' in contaminated hops.

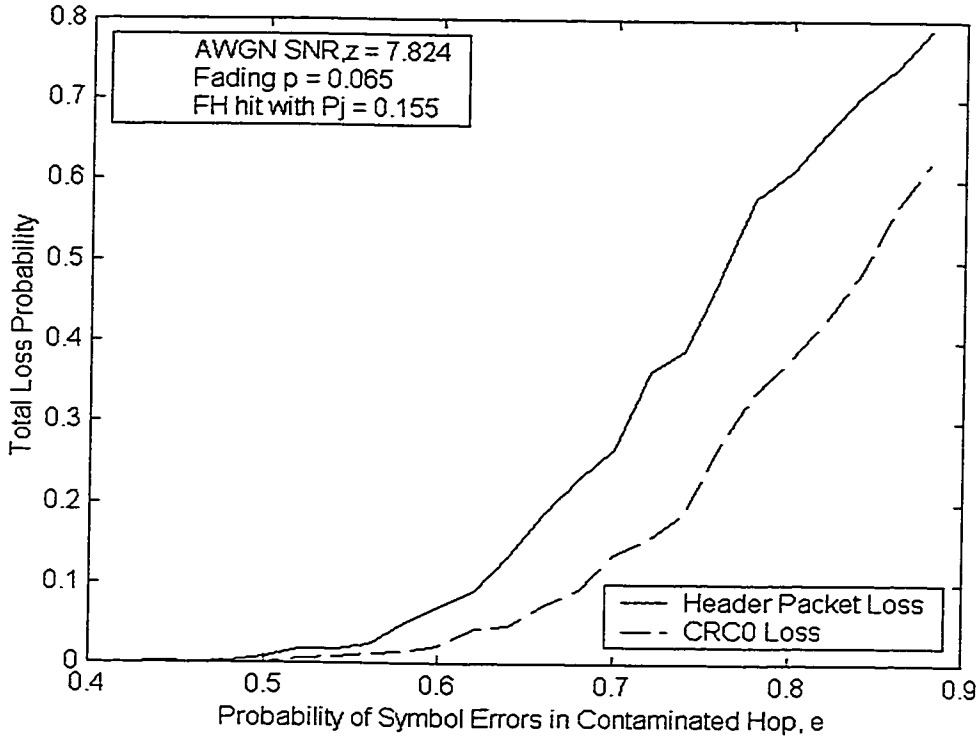

Figure 3.21: Total Header and CRC loss encountered while varying the probability of Symbol Error '*e*' in contaminated hops.

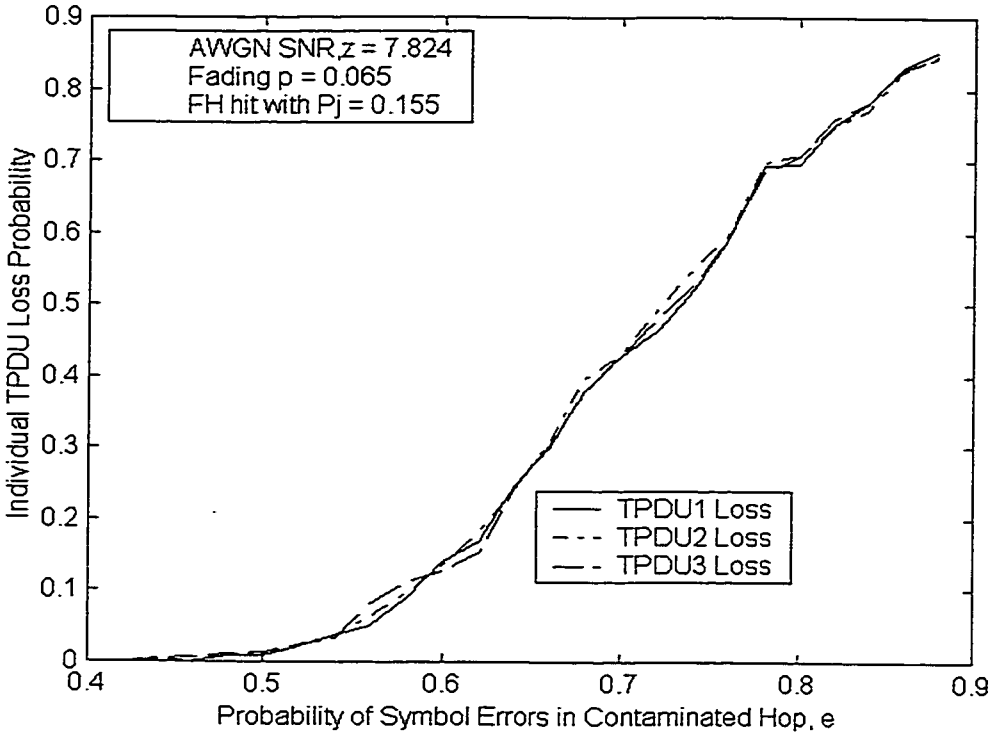

Figure 3.22: Total individual TPDU losses encountered while varying the probability of Symbol Error '*e*' in contaminated hops.

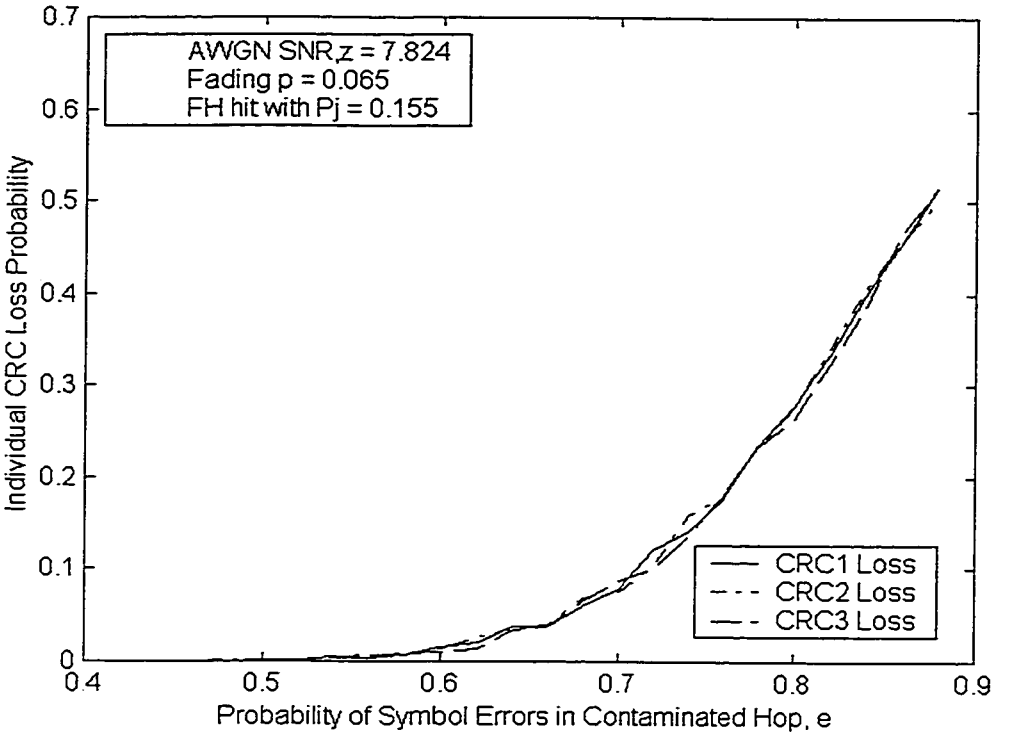

Figure 3.23: Total individual CRC losses encountered while varying the probability of Symbol Error '*e*' in contaminated hops.

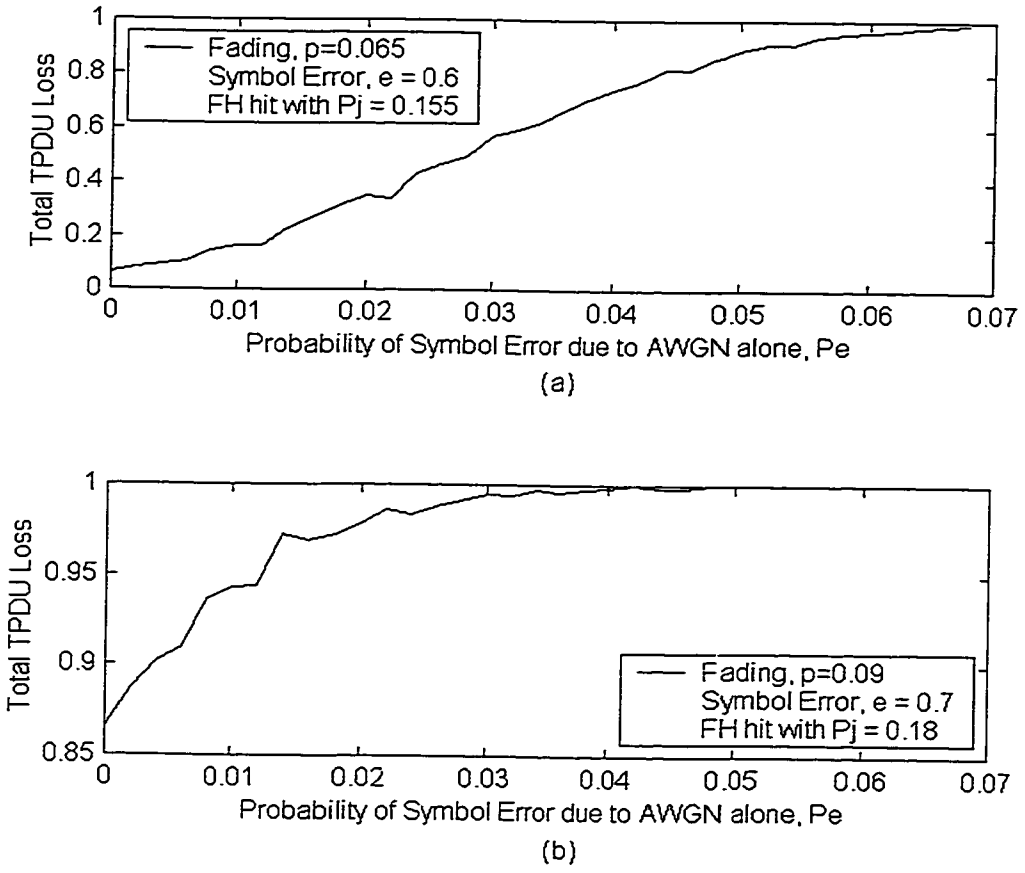

Figure 3.24: Comparing the total TPDU loss encountered due to variation in AWGN error, P_e with two different sets of parameters.

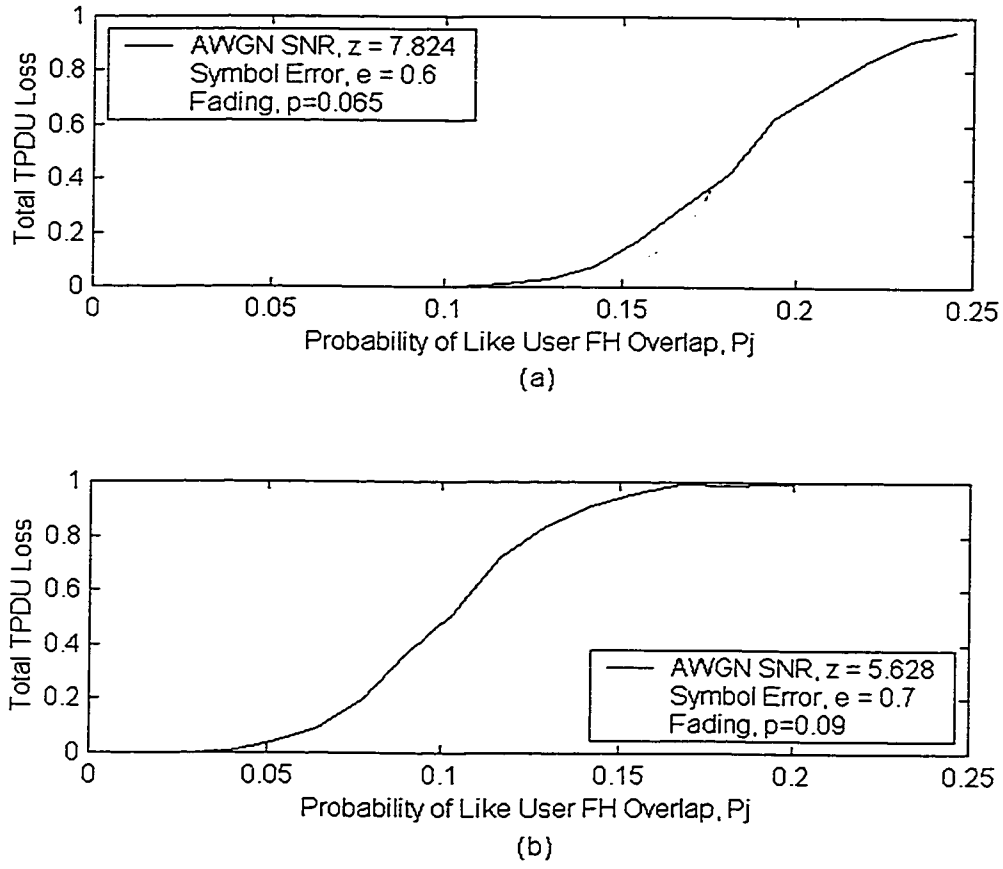

Figure 3.25: Comparing the total TPDU loss encountered due to variation in like user FH overlapping, P_j with two different sets of parameters.

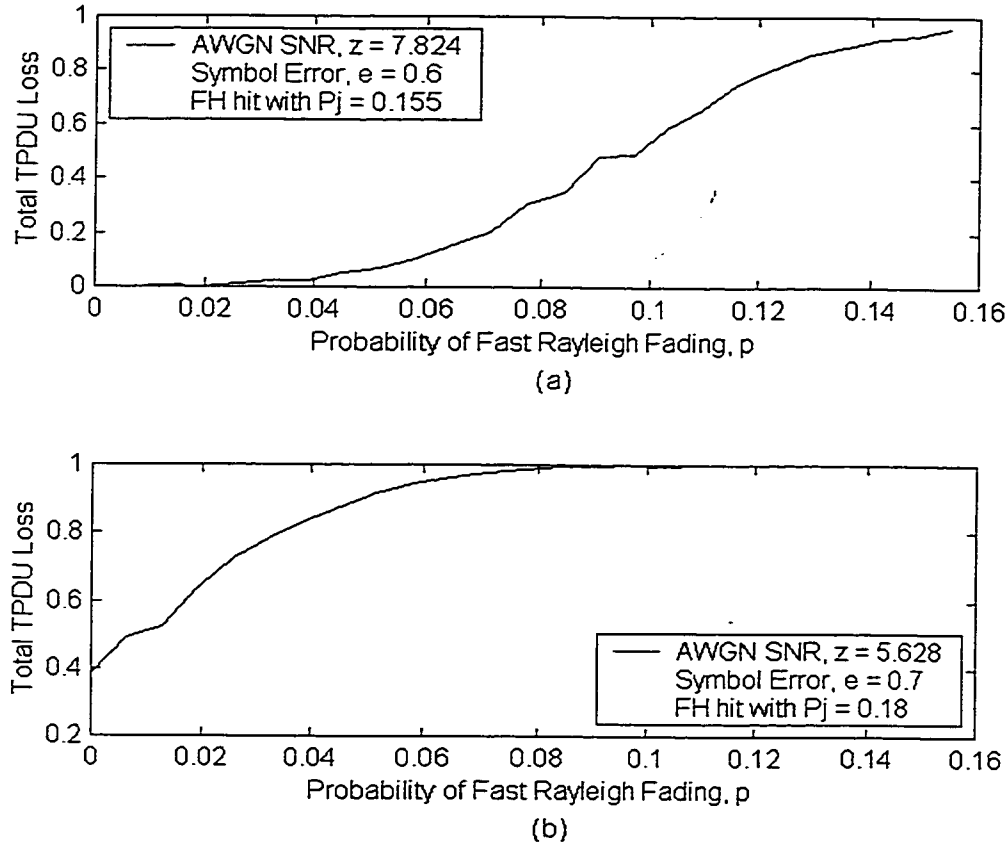

Figure 3.26: Comparing the total TPDU loss encountered due to variation in Rayleigh Fading, p with two different sets of parameters.

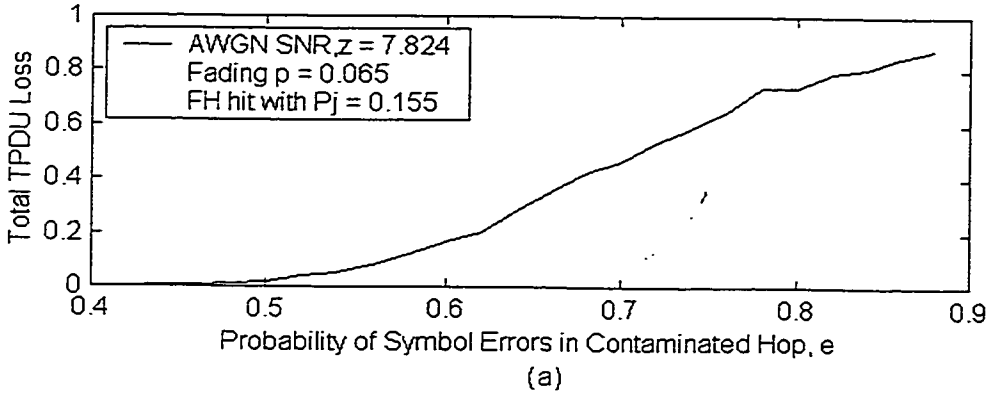

Figure 3.27: Comparing the total TPDU loss encountered due to variation in probability of Symbol Error '*e*' in contaminated hops with two different sets of parameters.

3.10 Conclusion

A new efficient and simple interleaving/RS coding scheme has been introduced and explained and simulation results obtained. The results show that the robust coding technique is highly resilient to noise, interference, fading and jamming environments. It gave a very good TPDU loss probabilities in the assumed severe fading and frequency hops overlapping. Between normal to high noise and fading channels, the ARQ retransmission required was 1.5 to 2.5 times till final TPDU successful transmission.

Also after doing all the simulation for the GPS driven system at hand we may proceed to claim that such results equally apply to the wireless LANs adapting the IEEE 802.11 standard with the following modification.

- Hopping rate will become between 20k to 25k depending on the number of symbols per hop. The product of the hop rate times the number of symbols per hop should come approximately to 1 MHz.
- The processing gain, i.e. the number of data bands equals 64 thus approximating the 78 in the IEEE 802.11 standard.
- Also we can relate our results to the practical scenario of the IEEE standard, as we may compare the results for example, 18% jamming probability in our GPS driven case to the claimed 4 FH overlaps out of each 26 in the standard.

CHAPTER 4

IEEE 802.11 Standard Driven Coding and Simulation

4.1 Introduction

The performance of Spread Spectrum communications improves with the use of Forward Error Correction techniques. The effect of worst-case jamming, highly interference affected channel and severe fading environment can be mitigated using FEC. The IEEE 802.11 standard used in the wireless network employs no FEC for voice /data communication. This would badly hit with the affected environment. The performance of the same network with the use of FEC shows a far better result as compared to the network using no FEC. In this chapter we have tried to prove the same. Here we employed the same hybrid FEC/interleaving technique, introduced in chapter 3, in a system using IEEE 802.11 standard MAC sublayer protocol and simulated the two cases, one when data is transmitted with FEC and the other one when data is transmitted without FEC.

In this simulation we used the DCF (Distributed Coordination Function) access method with RTS and CTS frames, as discussed in chapter 2, section 2.4.1. Figure 2.6

illustrates the example of this access method. Channel environment is kept the same for both the cases and additive white Gaussian noise, Signal to Noise Ratio is kept 3 dB below in the FEC case as compared to without FEC data. It is because in an additive white Gaussian noise interference environment, FEC decoders using reliability information typically require 1 to 2 dB less transmitter power than decoders not using this information [2].

Also we are going to consider errors in the important parts of messages in the 802.11 standard such as RTS, CTS and the data payload as illustrated in Figure 2.6, chapter 2. Here we have not considered any like frequency user overlapping or frequency jamming from within the same wireless LAN because we simulated contention protocol based on CSMA/CA (Carrier Sense Multiple Access and Collision Avoidance). However interference may arise from users in nearby wireless LANs. With all these assumption the performance of the two systems is assessed.

4.2 Fading Channel Simulation Model

Here a generic simulation model is described for the suggested coding technique in a highly interference environment, for which a burst error model is introduced to characterize fading in the communications channel. A two-state continuous-time Markov chain is used to represent the burst error model. State G represents the channel in a "good" state. This indicates that the channel is operating with a very low bit error rate (denoted be BERgood). State B indicates the channel is operating in a fading condition with a higher error rate, denoted by BERbad. The probability of going from state G to state B is denoted by 'α', while the probability of going from state B to state G is denoted

by 'β' as shown in the Figure 4.1. A frame is considered to be corrupt if it contains one or more bit errors.

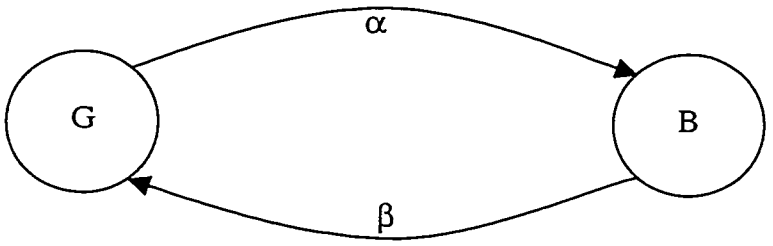

Figure 4.1: State Diagram of two state continuous time Markov chain

The simulation model uses the error model above to determine whether each transmitted frame was transmitted successfully. When the frame is transmitted, a portion of the frame can be sent over the communications medium when the channel is in state G, and a portion can be transmitted when the channel is in state B.

The assumption of α and β are done by assuming the number of bits in Good state and Bad state. For example with 200 symbols in bad state the probability of going into good state, β is calculated as

$$\text{Average fade duration} = \quad 1/\beta \quad = 200 \text{ symbols}$$

$$\beta \quad = 1/200 = 0.005$$

and with 800 symbols in good state the probability of going into bad state, α is calculated as

$$\text{Average duration in Good state} = \quad 1/\alpha \quad = 800 \text{ symbols}$$

$$\alpha = 1/800 = 0.00125$$

The simulation is done with different probabilities of α and β. Also we simulated the results while keeping the channel subject to change its state with the assumed probabilities of α and β.

4.3 Simulation Parameters

In this research, we considered four different parameters that affect the channel behavior, probability of error due to additive white Gaussian noise 'P_e', probability of entering into bad state (fading channel) 'α', probability of entering into good state (unfaded channel) 'β' and probability of symbol error 'e' in burst fading region. As we have discussed before, we have simulated contention protocol based on CSMA/CA (Carrier Sense Multiple Access and Collision Avoidance), so there will be no like frequency user overlapping or frequency jamming from within the same wireless LAN, however interference may arise from users in nearby wireless LANs.

The AWGN Signal to noise ratio (SNR) is defined as

$$\text{SNR} = z = A_t^2 T_s / 2N_o \qquad 4.1$$

where $z = E_b/N_0$ and defined from equation 1.3, using the AWGN error probability P_e,

$$z = \frac{E_b}{N_0} = -2\ln(2P_e) \qquad 4.2$$

In the whole simulation these parameters are varied individually within a certain range while the other parameters are frozen. In a single simulation run, with one value of a parameter in a defined range, 1000 frames are transmitted, each having 6 TPDUs (explained later in simulation procedure). For each packet frame, RTS and CTS are transmitted. The channel's fading state for one packet frame with its RTS and CTS,

remains same and follows the fading channel model. For every new packet frame the channel state is then start over.

4.4 Code Specifications

Throughout this simulation, we assumed the data rate (R_b) of 96ksymbols/s with a spread bandwidth of W_{ss} = 15.36MHz. Frequency Shift Keying (FSK) has a bandwidth of = 2.5* R_b = 240KHz. This means a spreading gain of

$$PG = \frac{15.39MHz}{240KHz}$$

$$= 64$$

The Reed Solomon FEC coding rate that we used here is 19/31. Hence the net date rate is 96k * 19/31 = 58838.71 bps. The number of FSK bands in the total band of 15.36MHz is 64. In the whole of this simulation we use the number of symbols per hop equal to 55. So the hopping rate is 1Meg/55 = 18181.82 hops/s.

The error correcting capability 't' of the code is

$$t = (31\text{-}19)/2 \ = 6 \text{ RS symbols}$$

which means 6 * 5 = 30 channel symbols.

4.5 Simulation Procedure

4.5.1 Data Frame with FEC

The number of data symbols in a single frame with all coding overhead is 8525. The distribution of header, CRCs and the three TPDU sizes are given in Figure 3.1 that accounts 5225 information bits. The difference between 8525 and 5225 is due to the use of RS FEC encoding of rate 19/31 as mentioned earlier.

All symbols of the frame fields of Figure 3.1 are randomly generated and then filled up in a single frame of size 5225 information bits in sequence. The frame is then broken into data words each equal to 95 bits. Then each data word is encoded by RS coding and it makes the code word equal to 155 channel symbols. From here the 55 encoded code words are fed into the interleaving table that constitutes 155 hops, each carrying 55 channel symbols. The interleaving is done the same way as mentioned in chapter 3. It is also possible to add 2 guard symbols at start and end of each hop (as was mentioned before), but in this simulation we have ignored the guard symbols.

The maximum frame size in the IEEE 802.11 standard is 2346 octets (18768 symbols). So we combined the two interleaving tables of size 8525 symbols to make it 17056 symbols (6 symbols are padding bits). Hence each frame has carried 6 TPDUs.

Before sending these 310 hops, the request to send (RTS) and clear to send (CTS) frames (see Figure 2.6 in chapter 2) are sent to reserve the channel for the transmission of data and to avoid the collision. These are also randomly generated frames. The size of the RTS and CTS frames is set to 155 channel symbols, which is equal to one code word. This is done to keep the size close to IEEE 802.11 standard in which RTS is 20 octets and CTS is 14 octets. No FEC is employed on these frames. These frames are passed through the channel. At the end the two frames are checked with the original one. If there is any error then the data hops is not sent and the loop is started from the beginning. But this elapsed time is counted and later on used to get the overall time efficiency.

If there is no error in both of RTS and CTS frames, then symbols of the interleaving table representing the actual data (see Figure 3.3 in chapter 3) are sent to the same channel environment. Each symbol of the table is subjected to undergo with the current

channel environment. Every 50 symbols, the channel is subjected to change its state with probability α and β. If the channel is in deep Rayleigh fading state then again a Bernoulli random generator with parameter '*e*' is called. If the outcome of the generator is 1 the symbol is assumed to have error. If the outcome is '0' or if the channel is in good state then the symbol error is decided upon by the FSK demodulation in AWGN alone.

When symbols of the whole table have been transmitted through the channel, the decoder then retrieves back the 110 code words in the reverse order. The words are assumed corrected if the number of errors is not more than the error correcting capability of RS code per code word. The errors in TPDUs are checked the same way as mentioned in Chapter 3 and the TPDU loss is recorded. This whole process goes on 1000 times to get the average result (corresponding to one simulation run).

4.5.2 Data Frame without FEC

The big interleaving table is formed the same way as in the case that includes FEC. The procedure to transmit symbols through the channel is also the same. The difference here is at the data correction phase. Since here is no FEC (symbols which are added because of FEC, are treated here as mere data symbols), so there is no need to correct the errors. The rest of the process is the same.

4.6 Average TPDU loss calculation

The average TPDU loss is obtained by dividing the total TPDUs received with errors by the total number of transmitted TPDUs. Each final interleaving table has 6 TPDUs. So in each run 6 TPDUs is being transmitted here. The number of simulation

runs, in which either of RTS or CTS is lost, is not counted for averaging TPDU loss, since no data will be transmitted in these cases (see chapter 2).

4.7 Efficiency Calculation

The total time efficiency is calculated by dividing the time required by the total number of successful TPDUs in 1000 transmissions with the total time through one whole simulation i.e. 1000 transmissions.

$$\textit{time efficiency} = \frac{\textit{\# of total successful TPDUs * length of each TPDU in seconds}}{\textit{total time elapsed through whole of one simulation}}$$

The time of each TPDU is approximated by dividing the number of symbols in the TPDU by data rate (96ks/s). The total time elapsed includes all the RTS and CTS times, SIFs and DIFs times as mentioned in chapter 2 and the frame packets which were transmitted.

4.8 Results and Comparisons

4.8.1 Varying AWGN

In Figure 4.2 the two cases (with and without FEC) are compared while varying the probability of additive white Gaussian noise. Figure 4.2a is the result for the case when there was no FEC used in the data packet. Here the probability of Symbol Error in Bad state is set to 50%. The Average duration in bad state is set to 20 bits by keeping the probability of going into good state $\beta = 0.05$ and the average duration in good state is set to 500 bits by keeping probability of going into bad state $\alpha = 0.002$. The result shows that the TPDU loss gradually increases as the Probability of additive white Gaussian noise (AWGN) increases. We see that when $P_e = 0$, the 20% of the TPDUs are loss due to burst fading effect. As soon as P_e reaches 0.06%, the TPDU loss goes beyond 80%. Whereas in Figure 4.2b when FEC is used, for the same parameters the TPDU loss probability is extremely low. Even at 0.1% of P_e, the TPDU loss probability is less than 3%. It means that on the average, the number of transmission required is 1/(1-0.03) = 1.03 for TPDU success, which is an excellent performance.

In Figure 4.3 Time Efficiency is compared when the white Gaussian noise is varied. Figure 4.3a is for the case when no FEC is used. Again at $P_e = 0$, the efficiency comes down to 40% due to the burst fading environment. As the probability of bit error due to white Gaussian noise alone increases the efficiency reduces and goes below 10% when $P_e > 0.06\%$. In Figure 4.3b the total time efficiency remains above 48%, which reflects the coding efficiency alone.

4.8.2 Varying α

Figure 4.4 and Figure 4.5 are the comparisons between the two cases when the probability of going into bad state, i.e. α is varied. The rest of the parameters are kept constant. Probability of going into good state is the same $\beta = 0.05$. The probability of Symbol Error in the bad state is 50%. Signal to noise ratio is kept at $z = 17.03$ dB for no FEC case while 14 dB for the case when FEC is used. The reason for this difference is already mentioned earlier. In Figure 4.4a where no FEC is used α is varied from 0.0 to 0.005, i.e. the average duration of channel to be in good state is reduced from infinity to 200 bits. From Figure 4.4a we observe that even at $\alpha = 0$, 20% of the data TPDU are lost because of the additive white Gaussian noise. This loss increases smoothly with the increase in the value of α. Where as Figure 4.4b is the case when we used the FEC, here α is varied from 0 to 0.02 which corresponds to reduction from infinity to 50 bits respectively in good state. Here even at lower signal to noise ratio there is no error at $\alpha =$ 0 and is below 8% at $\alpha = 0.005$. The TPDU loss reaches only 40% at $\alpha = 0.02$ which is far better performance as compared to former case.

In Figure 4.5 Time Efficiency performance is compared. In Figure 4.5a where no FEC is used, at $\alpha = 0$, efficiency is 40% and gradually decreases to 22% when α becomes 0.005. While in the other case given in Figure 4.5b the efficiency starting with 49%, remains above 45% till $\alpha = 0.005$.

4.8.3 Varying β

Figure 4.6 and Figure 4.7 are the results when average duration of the channel in bad state is varied by varying the probability of going into good state, β. It is varied from 0 to 0.01, which corresponds to average duration in bad state. Here again the Symbol

Error 'e' in the bad state is 50%. α is kept at 0.002 while signal to noise ratio 'z' is frozen at 17dB and 14dB for the non-FEC and FEC case respectively. Figure 4.6a reflects a betterment in TPDU loss as β increases but since no FEC is used so the TPDU loss could not improved beyond 35% even at β = 10%. Whereas Figure 4.6b shows that with the use of FEC, TPDU loss almost gets zero as 'probability of going into good state' increases to 6%.

Figure 4.7a is the Time Efficiency curve with the variation in β when FEC is not used. Here again the efficiency increases initially as β increases but averages around 33% later on. While Figure 4.7b reflects the excellent performance as β reaches 6% where efficiency becomes 49%.

4.8.4 Varying Symbol Error Probability

Figure 4.8 and Figure 4.9 are the results when probability of Symbol Error 'e' is increased from 0 to 60% for the no FEC case and 0 to 94% for the data with FEC. α is fixed at 0.2% and β at 5%, i.e. average duration of bits in good state is 500 while average fade duration is 20. In Figure 4.8a where SNR is 17dB, when $e = 0$ the TPDU loss is 20% due to the additive white Gaussian noise alone. Later on as we increase e, it does not affect much to TPDU loss probability as the effect of α and β are dominant here. In Figure 4.8b where the SNR is 14dB, the TPDU loss probability increases with the increase in e, but this loss is so small that it is negligible.

In Figure 4.9a the Time Efficiency curve is plotted for the no FEC case which also shows a constant behavior at 32% because of the dominance of α and β. Figure 4.9b reflects the decrement in efficiency but due to the use of FEC with data this decrement is negligible.

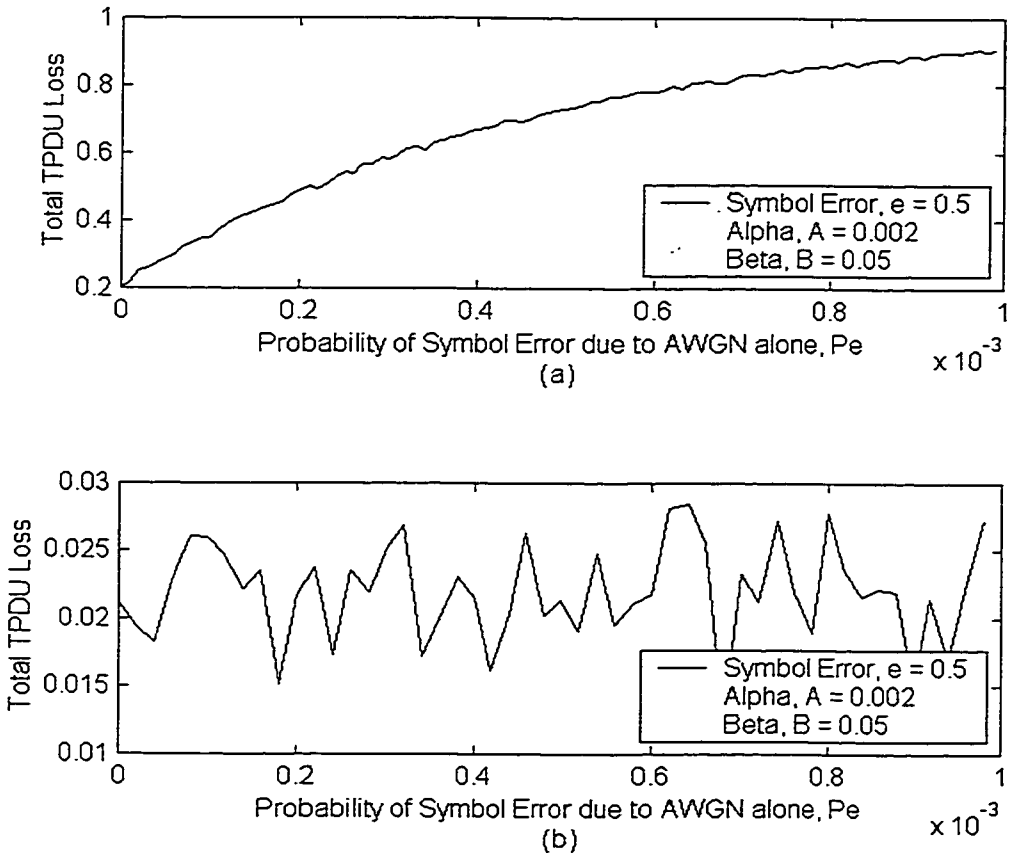

Figure 4.2: TPDU loss probability is plotted against the varying AWGN, P_e. a) without FEC b) with FEC

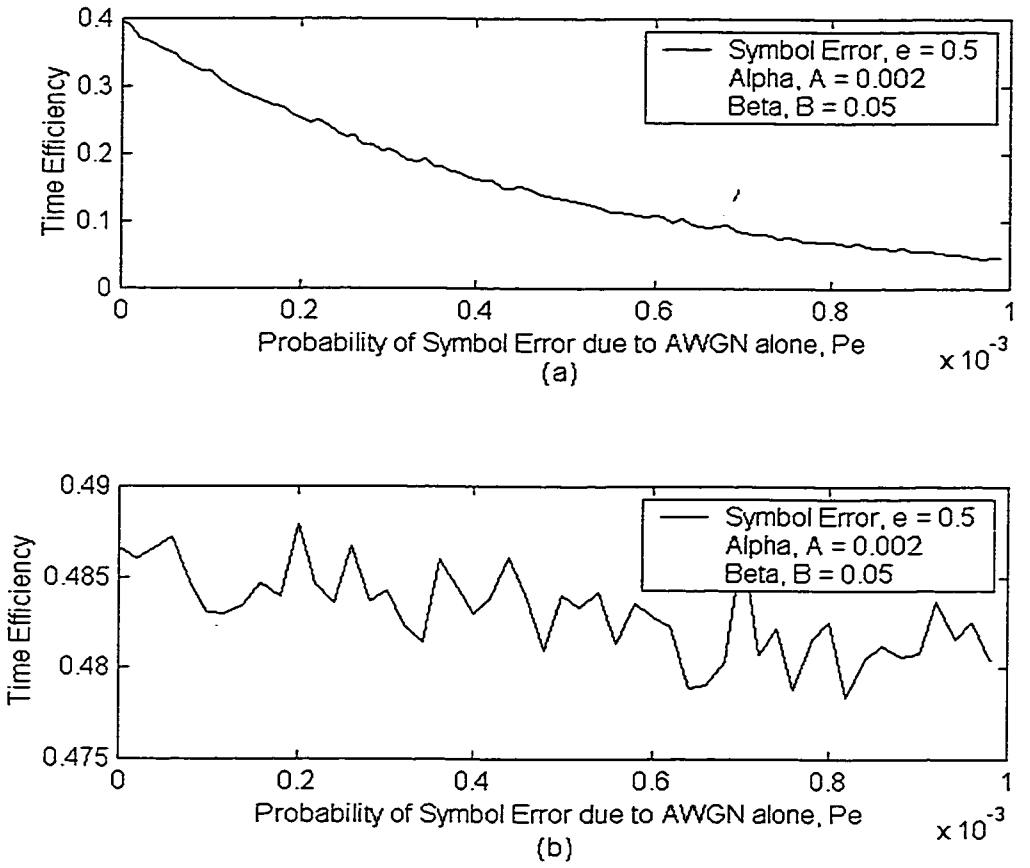

Figure 4.3: Time Efficiency is plotted against the varying AWGN, P_e. a) without FEC b) with FEC

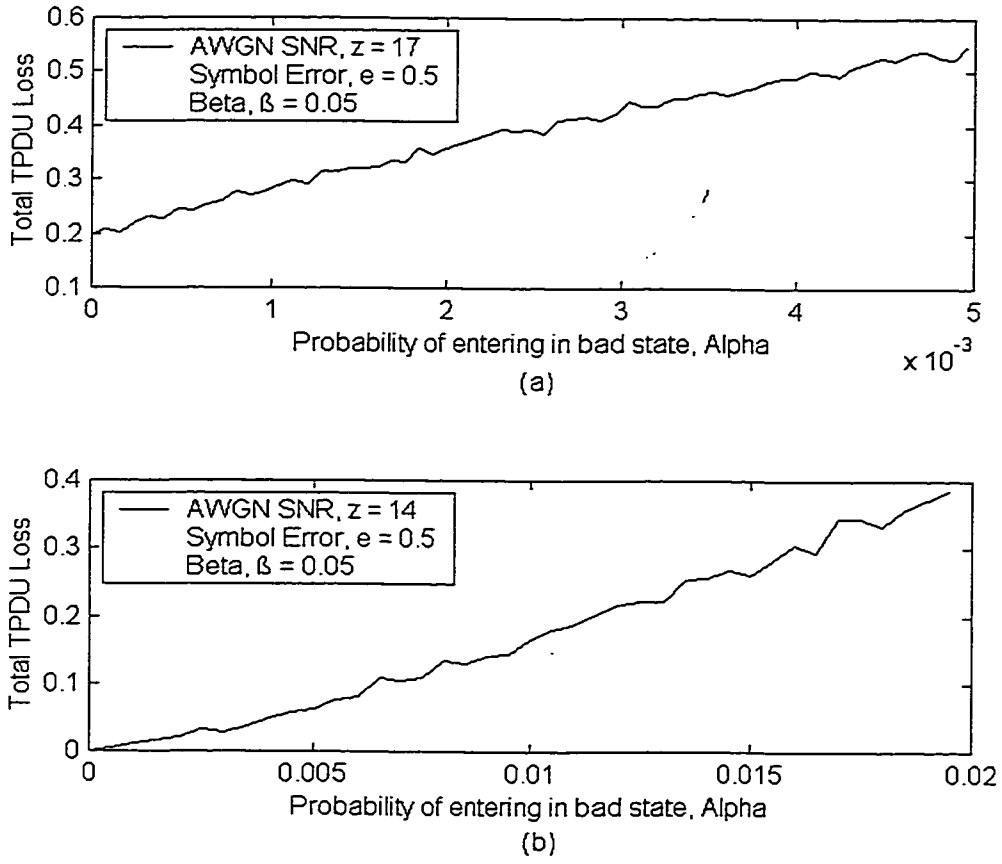

Figure 4.4: Here TPDU loss probability is plotted against α. a) without FEC b) with FEC

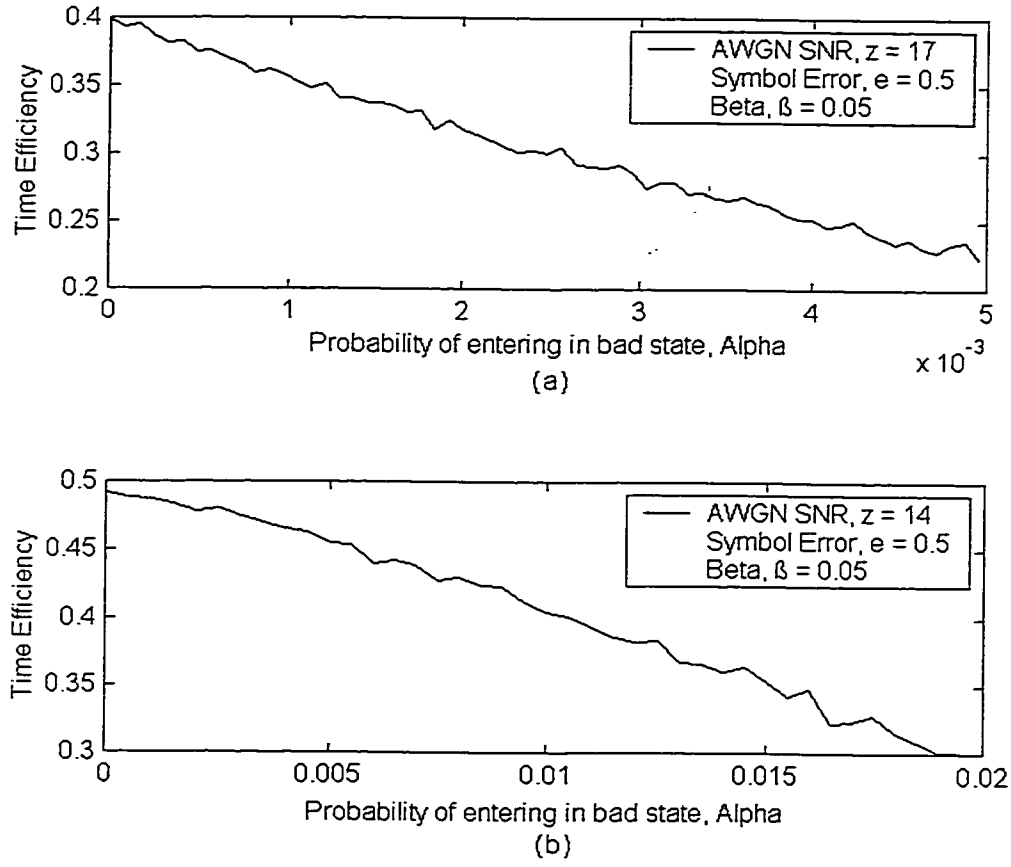

Figure 4.5: Here time efficiency is plotted against α. a) without FEC b) with FEC

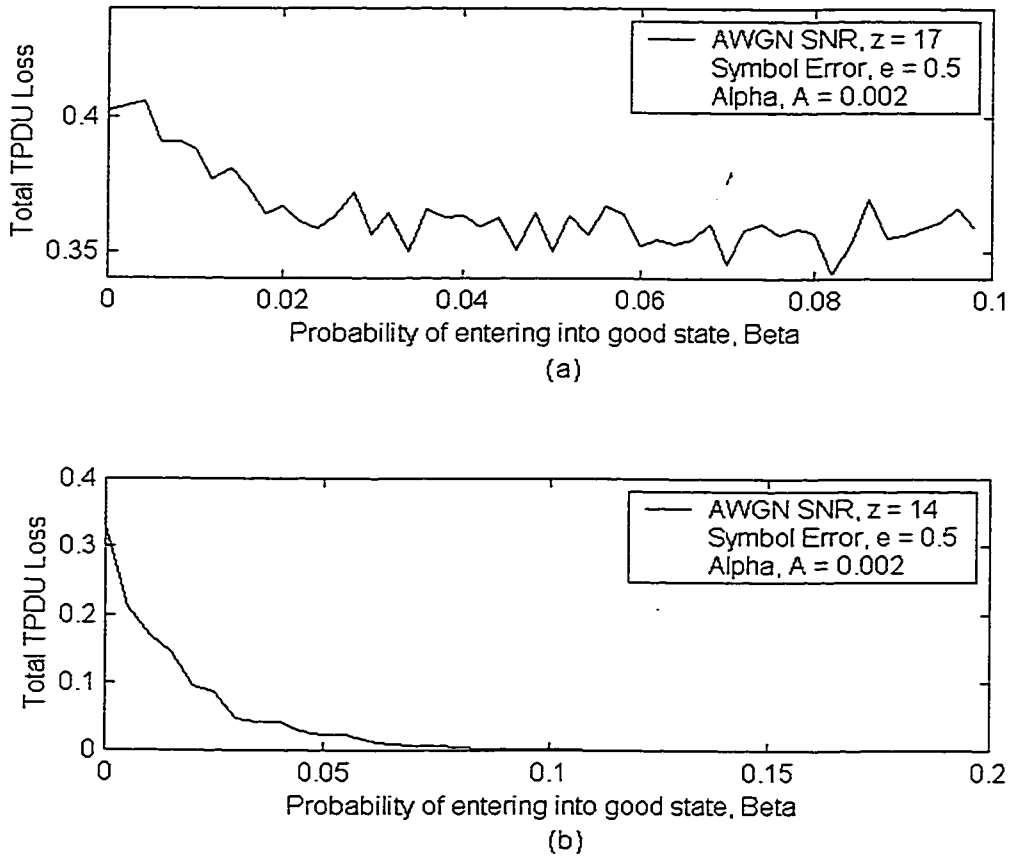

Figure 4.6: Here TPDU loss probability is plotted against β. a) without FEC b) with FEC

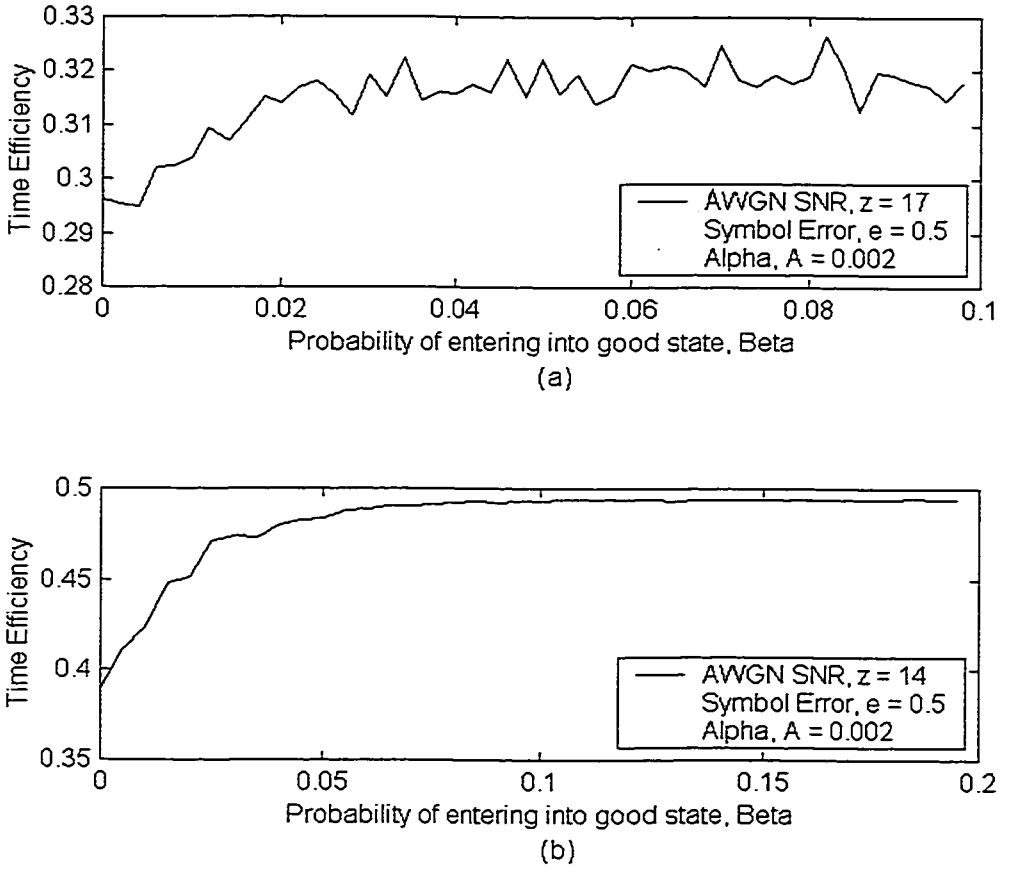

Figure 4.7: Here time efficiency is plotted against β. a) without FEC b) with FEC

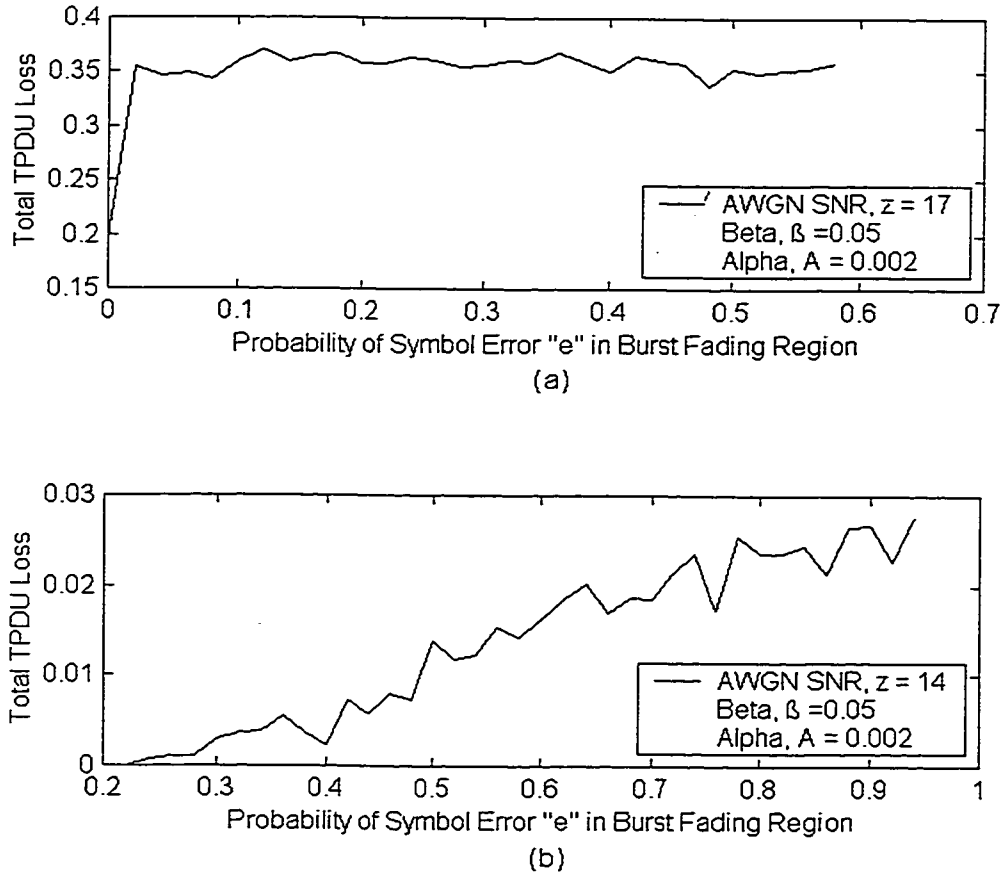

Figure 4.8: Here TPDU loss probability is plotted against probability of Symbol Error '*e*' in fading region.. a) without FEC b) with FEC

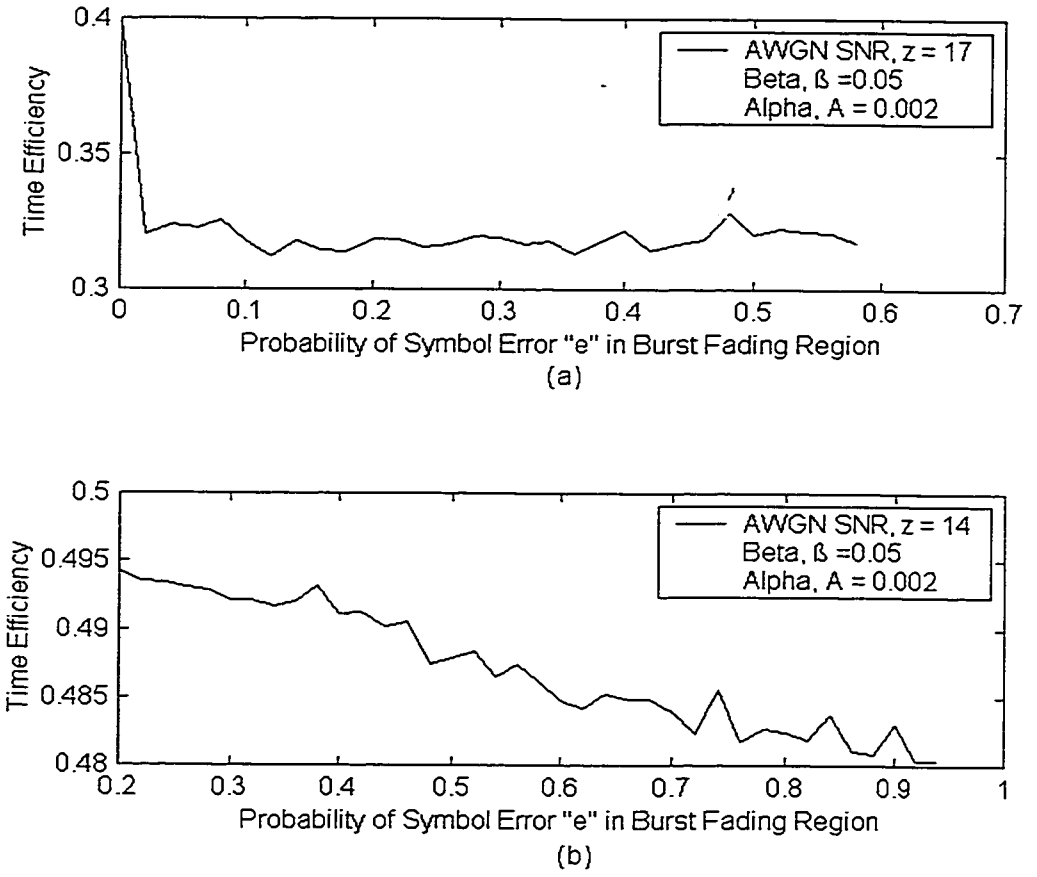

Figure 4.9: Here time efficiency is plotted against probability of Symbol Error '*e*' in fading region.. a) without FEC b) with FEC

4.9 Comparing results with some related works

Here we have compared some of our results with the result of the researchers who have done some simulations using the same channel model. Though the parameters of the channel might be changed but the results may be compared with some assumptions. For example, Figure 4.10, borrowed from [14], represents the effect of load with data length of TPDU (= 1600 bits), on the data throughput. In this result no FEC is employed. Here we can observe that as the load increases the data throughput increases and after some point it saturates and remains constant even when offered load goes beyond 100%. If we more increase the load that is not shown here then the data throughput will definitely go down.

Figure 4.11, which represents the effect of load on our GPS driven system and simulated with the TPDU length (= 1488 bits), shows the effect beyond the full load. All through our simulations, we assumed the full load i.e. all the 64 users were being catered by the system. As shown in the figure, at full load the data throughput is 100%, but as we increase the load the performance degrades and results in less throughput.

Figure 4.12 represents the effect of load on data throughput when we used FEC in IEEE 802.11 standard driven system. Here again it starts with the full load giving 100% throughput and shows degradation as the load increases. Though here we are comparing apple with oranges as in Figure 4.10 no FEC is used while the results from our simulation use FEC that gives 100% data throughput at full load. But for the comparison purposes it may give us some idea of the performance keeping the differences in mind.

Since there are not many work on the wireless LAN standard using FEC in the MAC sublayer, so to compare our results in the Rayleigh fading channel with FEC we considered Figure 4.13, borrowed from [35]. This result uses rate ½ binary convolutional codes with soft-decision decoding and constraint length = 5 and shows the data throughput against SNR. Here it shows that the data throughput shoots up as the SNR gets more than 11 dB. Figure 4.14 shows the response of our hybrid FEC/interleaving with hard-decision decoding. Though the hard-decision decoding cannot give better performance than soft-decision decoding, even then the performance of this system is better than the previous one and by 9dB SNR, the data throughput reaches 90%.

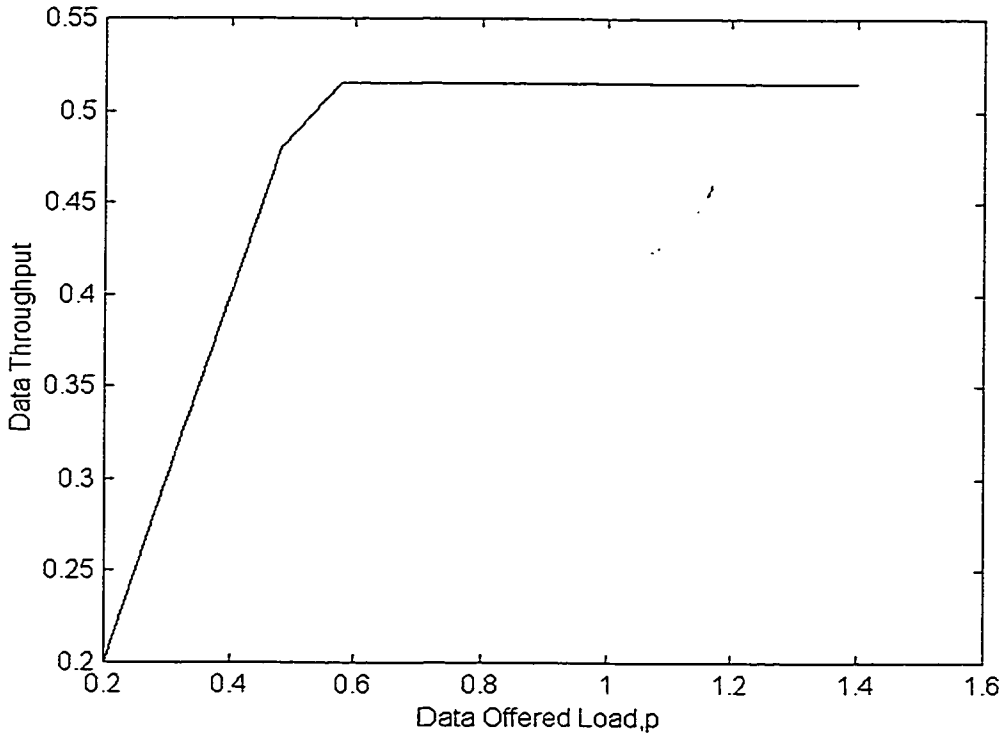

Figure 4.10: Effect of Load with data length of TPDU (= 1600 bits) on data throughput [13].

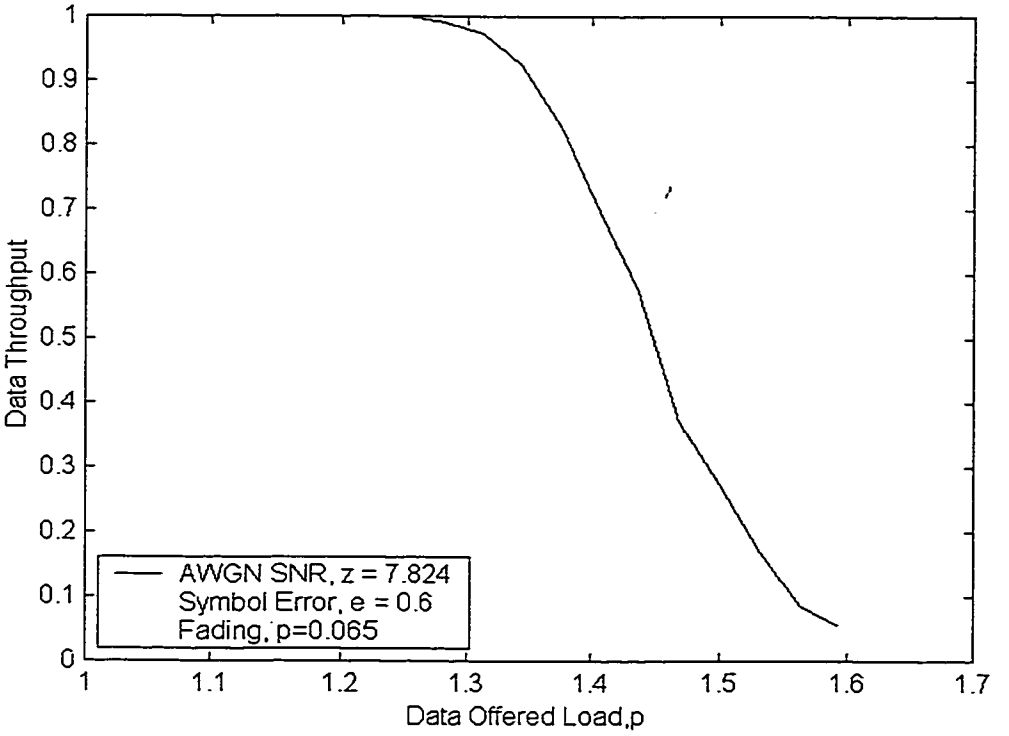

Figure 4.11: Effect of Load with data length of TPDU (= 1488 bits) on data throughput in the GPS driven coding system

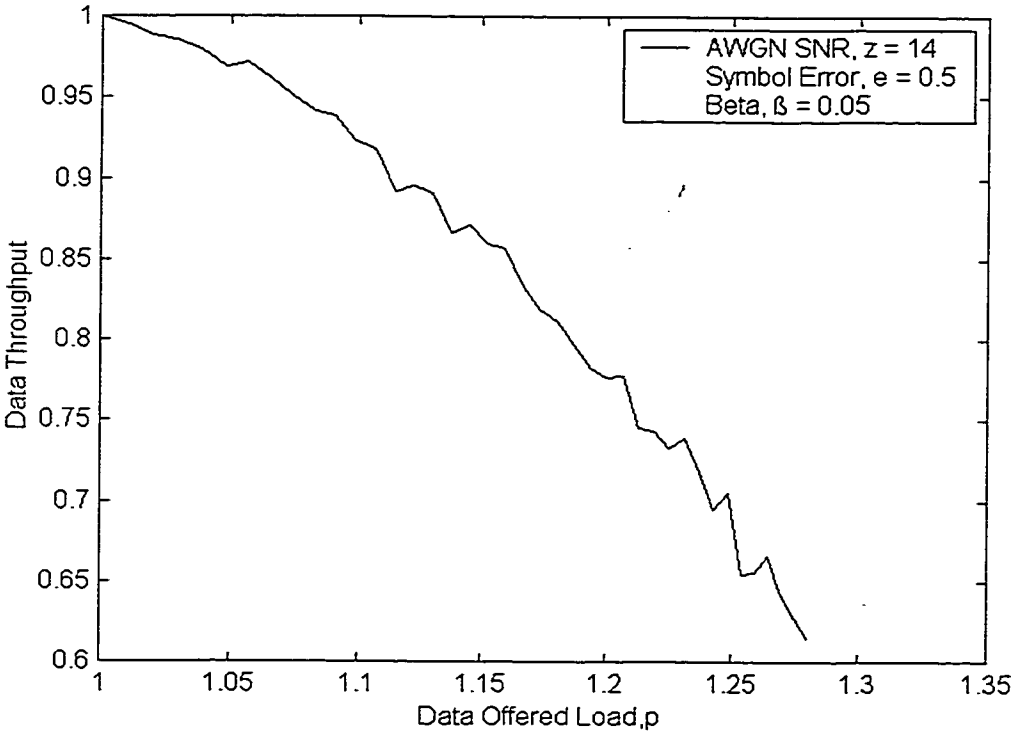

Figure 4.12: Effect of Load with data length of TPDU (= 1488 bits) on data throughput in the IEEE 802.11 Standard driven system

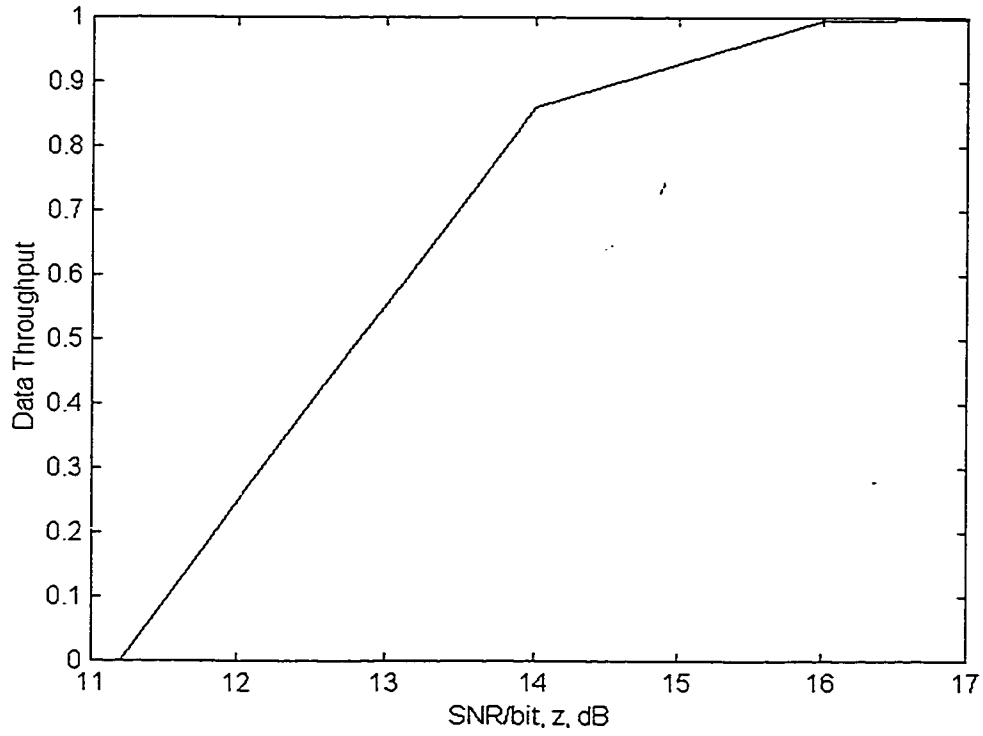

Figure 4.13: Performance of ½ binary convolutional codes with soft-decision decoding and constraint length (= 5) in Rayleigh fading channel

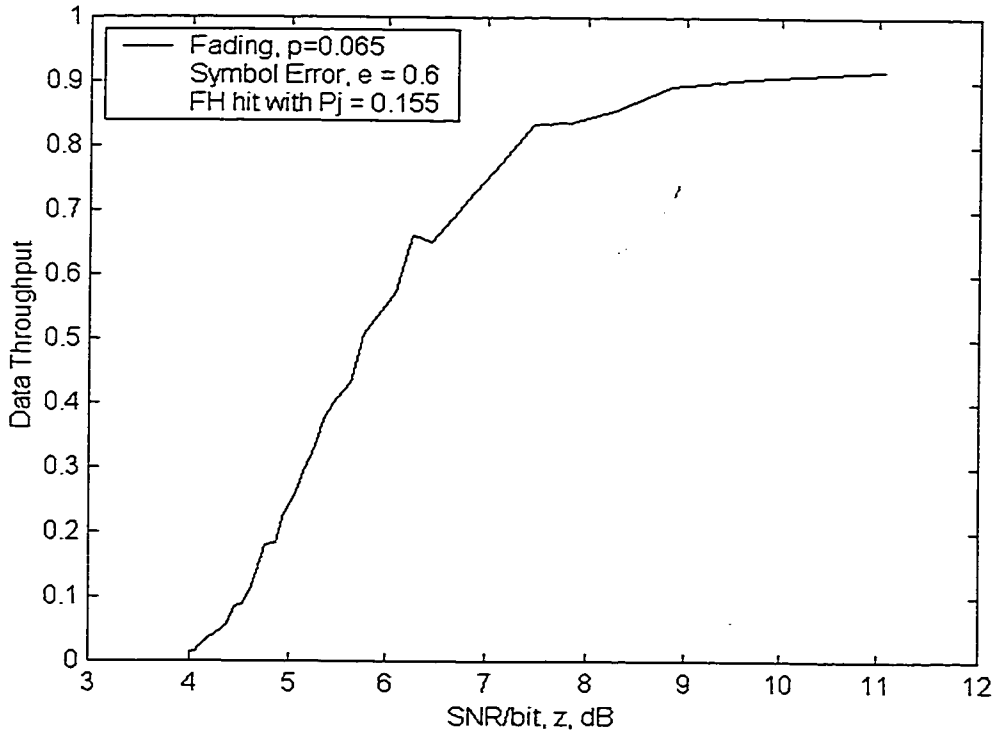

Figure 4.14: Performance of hybrid RS FEC/interleaving with hard-decision decoding in Rayleigh fading channel

4.10 Conclusion

The designed simple interleaving/RS coding technique is applied on a system based on IEEE 802.11 standard protocol and its performance is compared with the current standard specification in which no FEC is used. While varying the different parameters, the TPDU loss probability and total time efficiency is observed. With 0.1% P_e due to AWGN, 1.03 transmissions are required for the data with FEC whereas for without FEC data it needed 10 transmissions for the same P_e. Also for the same P_e, the time efficiency for FEC data is 48% while in without FEC it showed less than 10% efficiency.

While varying α we observed that at $\alpha = 0.005$, TPDU loss is 20% when used without FEC and 8% when data is sent with FEC. Similarly the time efficiency dropped down to 22% for non-FEC case as compared to 45% with FEC data at same α. When β is varied, the performance of the system should get better but we observed that even at $\beta =$ 0.1, time efficiency for without FEC data could not go beyond 32% while for data with FEC it reaches its maximum 49% when β is not even 0.07.

With symbol error probability variation, the degradation of the performance is noticed. Though for non-FEC data the effect of probability of entering and leaving the good state i.e. α and β were dominant. However the decrement in efficiency noticed for the data with FEC was negligible.

In all cases, from every aspect the performance of the system using FEC in the data is better than the system using no FEC. So in the standard IEEE 802.11 MAC sublayer protocol, the efficient use of any FEC technique will improve the performance.

CHAPTER 5

Contribution

Finally we would like to mention the main contributions of this thesis that are listed below.

5.1 GPS aided access

In this work we used the GPS (Global Positioning System) aided access to provide accurate timing and hence to guarantee orthogonal FH and to restrict the interference from outside the local cluster. This GPS capability provides minimum end-to-end probability of TPDU (Transport Protocol Data Unit) loss.

5.2 New Interleaving Table Structure

Here we introduced a new interleaving structure, which provides high time diversity. The table with 31 rows by 275 columns distributes the symbols of the 155 code words in such a manner that each transmitted hop of 155 hops carries only one symbol of the code. So if there is burst fading in the channel or probability of hit, this interleaving will break the burst and will distribute all the errors into 55 code words.

5.3 Introduction of Standard within Standard

There is no FEC specified at MAC sublayer in the standard as yet, only Automatic Repeat Request (ARQ) at TCP/IP level is adopted on top of 802.11 MAC protocol, thus it results in an inefficiency of the protocol in high noise and severe fading environment. Only a few errors in frames will require frequent ARQ retransmissions. So in this thesis we suggested to use the FEC at the MAC sublayer in the IEEE 802.11 standard and proved the improvement in performance by the use of FEC.

5.4 Use of 3 TPDUs in a single packet

In the design of our data packet, we used 3 TPDUs in the whole packet. So whenever a part of the data packet is in error due to burst fading or like user FH overlapping, it will affect 1 TPDU or 2 TPDUs not all, thus only these 1 or 2 TPDUs will be required to be retransmitted and hence saving the time. However if the packet header is in error or all the 3 TPDUs are in error due to severe noisy channel, then all 3 TPDUs will be retransmitted.

CHAPTER 6

Conclusion

6.1 Thesis Summary

In chapter 1, we presented a brief overview of Spread Spectrum Communications along with the principles of Spread Spectrum Communications. Then we briefly discussed the important and the most famous ways of spreading the spectrum. Afterwards we briefly described a new spread spectrum application; MYMAR, a new Mobile Yellow page Messaging and Retrieval system, for which this new hybrid interleaving/FEC code, the subject of this thesis is designed. Finally, the performance of Frequency Hopping in Spread Spectrum Communications with multiple user environment is discussed.

In chapter 2, we discussed the IEEE 802.11 standard, a MAC protocol for Wireless LAN. After the brief introduction we discussed the general architecture of the Wireless LANs, the ad hoc network and the infrastructure network. Then we discussed the three different physical-layer implementations specified by IEEE 802.11 standard. Then we addressed the MAC sublayer protocols and the access methods namely Distributed Coordination Function (DCF) and Point Coordination Function (PCF).

We presented our robust interleaving/RS FEC technique in chapter 3. This technique utilizes the Global Positioning System (GPS) capability to provide minimum

end to end probability of TPDU loss. We described the frame format and its coding and the design of the interleaving system. At the end of this chapter, the simulation procedure to observe the performance of the coding technique and its results are presented.

Chapter 4 shows the performance of the coding scheme applied on a system based on IEEE 802.11 standard protocols and compared the performance of the two systems, one using FEC and the other using no FEC. Here we basically emphasized on the use of FEC scheme in IEEE 802.11 standard for the betterment of its performance. Initially we mentioned the simulation model for the fading channel that we used for our simulations. Then described the simulation procedure and then compared the results of the two systems.

6.2 Conclusions

This thesis addressed a new efficient and simple interleaving/RS coding scheme which may be applied in our MYMAR system. This specific interleaving technique herein is of particular application to the error correction problem. Here it has been introduced, explained and the simulation results have been obtained.

In the GPS driven system, presented in chapter 3, the results show that the robust coding technique is highly resilient to noise, interference, fading and jamming environments. We simulated the channel and considered four different channel parameters namely: SNR, z, Probability of Rayleigh Fading, p, Probability of like user FH overlapping, P_j, Probability of Symbol Error, e. By varying one parameter and fixing the others we observed the performance of the system. It gave a very good TPDU loss probabilities in the assumed severe fading and frequency hops overlapping. Between

normal to high noise and fading channels, the hybrid FEC/interleaving technique was able to correct most of the errors, and the required ARQ retransmission did not exceed 3 times till final TPDU successful transmission. The resistance to errors of our encoding technique was also reflected when we observed the effect of like user FH overlap, P_j. The number of retransmissions required for the successful transmission of a TPDU was less than 2 even when 18% of the transmitted hops were jammed plus with 7% hops in fading.

At the end of this simulation we claimed that these results could be equally applied to the wireless LANs adapting the IEEE 802.11 standard with some modifications as mentioned in the conclusion of chapter 3.

In chapter 4 the same design of simple interleaving/RS coding technique is applied to the IEEE 802.11 standard in the contention protocol mode and simulated the bursty fading channel environment. The performance of the system using above mentioned IEEE standard, with FEC and without FEC, is compared. Due to simulating the contention protocol, there was no like user FH overlapping so no 'P_j' is used as a parameter. Instead here α and β were used to simulate the probability of entering and leaving the fading state of channel, respectively.

While varying the different parameters, the TPDU loss probability and total time efficiency is observed. In all the cases the results show a better result with the use of FEC. For example, with the same probability of error due to AWGN, P_e = 0.001, 1.03 transmissions are required for the data with FEC and 10 transmissions required for without FEC data. Also for the same P_e, the time efficiency for FEC data is 48% while in without FEC it showed less than 10% efficiency.

Similarly with the variation of α its effect is observed and it also showed a better result with FEC. At $\alpha = 0.005$, TPDU loss is 20% when used without FEC and 8% when data is sent with FEC. When β is varied, the performance of the system should get better but we observed that even at $\beta = 0.1$, time efficiency for without FEC data could not go beyond 32% while for data with FEC it reaches its maximum 49% when β is not even 0.07.

Hence all through the simulations and a close look over the results, it reveals that from every aspect the performance of the system using FEC in data is better than the system using no FEC. So we may strongly suggest that in the standard IEEE 802.11 MAC sublayer protocol, the efficient use of any FEC technique will improve the performance.

6.3 Suggestions for Future Work

The response of the proposed hybrid interleaving/RS FEC technique for our particular MYMAR system may be improved by using concatenated RS/Convolutional coding scheme along with the use of deep interleaving table.

Also packet frame designed for the system is for non-real time data traffic. For the real time traffic the packet size should be small thus the interleaving table can be divided into smaller tables. So smaller table means less fading and error sensitive and less time diversity.

References

[1] R. L. Pickholtz, D. L. Schilling, "Theory of Spread-Spectrum Communications – A Tutorial," *IEEE Transactions on Communications*, Vol. COM-30, NO. 5, May 1982.

[2] Roger L. Peterson, Rodger E. Ziemer, David E. Borth, "*Introduction to Spread Spectrum Communications*," (Englewood Cliffs, New Jersey: Prentice Hall, 1995).

[3] R. C. Dixon, Editor, "*Spread Spectrum Techniques*," (IEEE Press, 1976).

[4] R. C. Dixon, "*Spread Spectrum Systems*," Wiley-Interscience publication: 1984.

[5] A.K. Elhakeem, "MYMAR, A new Mobile Yellow Page Messaging and Retrieval, The Advent of the local Wireless Internet," *Presented at the Canadian Conference of ECE, 2000*, Halifax, Canada, May 2000.

[6] A.K. Elhakeem, S. U. Hashmi, "SFH Access to Mobile Yellow Page Messaging and Retrieval, The Advent of the local Wireless Internet," *To be presented at the IIIS conference on EE*, Florida, USA, July 2000.

[7] J. S. Lee, L. E. Miller, "*CDMA Systems Engineering Handbook*," (J.S. Lee Associates, 1998).

[8] R. Skaug, J. F. Hjelmstad, "*Spread Spectrum in Communication*," (Peter Peregrinus, 1985).

[9] M. K. Simon, J. K. Omura, R. A. Scholtz, B. K. Levitt, " *Spread Spectrum Communications*," (Rockville, Maryland: Computer Science Press, 1985).

[10] I. A. Getting, "The Global Positioning System," *IEEE Spectrum*, pp. 36-47, December 1983.

[11] R. A. Scholtz, " The Origins of Spread-Spectrum Communications," *IEEE Transactions on Communications*, Vol. COM-30, pp. 822-854, May 1982.

[12] C. E. Cook, F. W. Ellersick, L. B. Milstein, and D.L. Schilling, Editors, "*Spread-Spectrum Communications*," (IEEE Press, 1983).

[13] Brian P.Crow, Indra Widjaja, G. Jeong, P. T. Sakai, "IEEE 802.11 Wireless Local Area Networks," *IEEE*, 0-8186-7780-5/97: pp. 126-133.

[14] Brian P.Crow, Indra Widjaja, J. G. Kim, P. Sakai, "Investigation of the IEEE 802.11 Medium Access Control (MAC) Sublayer Functions," *IEEE Communications Magazine*, vol. 35, No.9: pp. 116-126, September 1997.

[15] R. V. Nee, G. Awater, M. Morikura, H. Takanashi, "New High-Rate WirelessLAN standards," *IEEE Transactions on Communications*, Vol. COM-37, NO. 12, pp.82-88, December 1999.

[16] T. S. Rappaport, "*Wireless Communications: Principles and Practices*," (New Jersey: Prentice Hall, 1996).

[17] IEEE P802.11, Working Group for Wireless Local Area Networks. "Wireless LAN Medium Access Control (MAC) and Physical Layer (PHY) Specifications" *IEEE Approved Draft Standard*, P802.11D6.1, May 1997.

[18] Lucent Technologies Inc. *WaveLAN Air Interface Data Manual.* Issue B, July 1997.

[19] D.L. Lough, T. K. Blankenship, K. J. Krizman, "*A Short Tutorial on Wireless LANs and IEEE 802.11*," The Bradley Dept.of ece at Virginia Polytechnic Institute and State University.

URL: http://computer.org/students/looking/summer97/ieee802.htm

[20] H. S. Chhaya, "*Performance Evaluation of the IEEE 802.11 MAC Protocol for Wireless LANs*," Master's thesis, Department of Elec. and Comp. Eng., Illinois Institute of Technology, May 1996.

[21] V. Doradla, "*A new Hybrid Acquisition Scheme for CDMA Systems Emplying Short Concatenated Codes*," Master's thesis, Department of Elec. and Computer Eng., Concordia University, June 1997.

[22] S. W. Kim, W. Stark, "Optimum Rate Reed-Solomon Codes for Frequency-Hopped Spread-Spectrum Multiple-Access Communication Systems," *IEEE Transactions on Communications*, VOL. 37, No. 2, February 1989.

[23] U. Cheng, M. K. Simon, A. Polydoros, B. K. Levitt, "Statistical Models for Evaluating the Performance of Coherent Slow Frequency-Hopped M-FSK Intercept Receivers," *IEEE Transactions on Communications*, VOL. 42, No. 2/3/4, February/March/April 1994.

[24] E. A. Geraniotis, M. B. Pursley, " Error Probabilities for Slow-Frequency-Hopped Spread-Spectrum Multiple-Access Communications Over Fading Channels," *IEEE Transactions on Communications*, VOL. COM-30, No. 5, May 1982.

[25] Kenny K. Fok, "*A simulator for Wireless Local Area Networks*," Master's thesis, University of Waterloo, Ontario, Canada, July 1998.

[26] G. Li, "*Physical Layer Design for a Spread Spectrum Wireless LAN*," Master's thesis, Virginia Polytechnic Institute and State University, September 1996.

[27] L. W. Couch, "*Digital and Analog Communication System*," (Macmillan Publishing Company, 1990).

[28] Braden, R. *RFC1122: Requirements for Internet Hosts -Communication Layers*. Internet Engineering Task Force, October 1989.

[29] Cáceres, Ramón, and Liviu Iftode. "The Effects of Mobility on Reliable Transport Protocols" *14th IEEE International Conference on Distributed Computing Systems*, Poznan, Poland, June 1994, pages 12-20.

[30] DeSimone, Antonio, Mooi Choo Chuah, and On-Ching Yue. "Throughput Performance of Transport-Layer over Wireless LANs" *IEEE Globecom: Global Telecommunications Conference*, vol. 1, pages 542-549, Houston, TX, USA, 1993.

[31] IEEE Standard. "*Local and Metropolitan Area Networks, Overview and Architecture*" IEEE 802-1990, pages 1-3.

[32] "*The Spread Spectrum Handbook*," Third Edition, Standford Telecommunications, Inc., September, 1994.

[33] D. Bertsekas and R. Gallager, "*Data Networks - Second Edition*," (Upper Saddle River, New Jersey: Prentice Hall, Inc., 1992).

[34] Tanenbaum, Andrew S., "*Computer Networks - Third Edition*," (Upper Saddle River, New Jersey: Prentice Hall PTR, 1996).

[35] Proakis, John G., "*Digital Communications - Third Edition*," (McGraw Hill Series in Electrical and Communication Engineering, March 1995).